

LIBRARY  
Michigan State  
University

This is to certify that the  
dissertation entitled


INVOLVEMENT OF SATURATED FATTY ACIDS IN  
CAUSING PATHOPHYSIOLOGICAL AND METABOLIC  
CHANGES ASSOCIATED WITH  
ALZHEIMER'S DISEASE

presented by

SACHIN PATIL

has been accepted towards fulfillment  
of the requirements for the

Ph.D. degree in Chemical Engineering



Major Professor's Signature

8/23/07

Date

**PLACE IN RETURN BOX** to remove this checkout from your record.  
**TO AVOID FINES** return on or before date due.  
**MAY BE RECALLED** with earlier due date if requested.

DATE DUE	DATE DUE	DATE DUE
JAN 28 2009		
NOV 23 2009		

**INVOLVEMENT OF SATURATED FATTY ACIDS  
IN CAUSING PATHOPHYSIOLOGICAL AND METABOLIC CHANGES  
ASSOCIATED WITH ALZHEIMER'S DISEASE**

By

SACHIN PATIL

A DISSERTATION

Submitted to  
Michigan State University  
in partial fulfillment of the requirements  
for the degree of

DOCTOR OF PHILOSOPHY

Department of Chemical Engineering and Materials Science

2007



## **ABSTRACT**

### **INVOLVEMENT OF SATURATED FATTY ACIDS IN CAUSING PATHOPHYSIOLOGICAL AND METABOLIC CHANGES ASSOCIATED WITH ALZHEIMER'S DISEASE**

By

SACHIN PATIL

Alzheimer's disease (AD) is a very complex, age-related neurodegenerative disorder. Pathologically, AD brain is characterized by extracellular deposits of amyloid beta ( $A\beta$ ) protein and intracellular accumulation of neurofibrillary tangles (NFTs) composed of hyperphosphorylated tau protein. The present studies were undertaken to investigate the possible causal role of saturated free fatty acids (FFAs) in the pathogenesis of AD with the primary focus on establishing the underlying mechanism, which may prove vital in developing novel therapeutic strategies for AD.

We found that saturated FFAs had no direct effect on primary rat cortical neurons in terms of causing both the pathophysiological ( $A\beta$  production and tau hyperphosphorylation) as well as metabolic (glucose metabolism) abnormalities. In contrast, saturated FFAs significantly increased  $A\beta$  production and tau hyperphosphorylation in neurons through astroglial mediation. The conditioned media from FFA-treated astroglia induced increased production of reactive oxygen species (ROS) in neurons and co-treatment of neurons with N-acetyl cysteine, an anti-oxidant, inhibited FFA-astroglia-induced  $A\beta$  production and tau hyperphosphorylation, suggesting a central role of astroglia-mediated oxidative stress in the FFA-induced

pathophysiological abnormalities in neurons. Furthermore, saturated FFAs significantly decreased the level of astroglial glucose transporter (GLUT1) and downregulated glucose uptake and lactate release by astroglia. By using a powerful mathematical technique, metabolic flux analysis (MFA), we found that *de novo* synthesis of ceramide in PA-treated astroglia was significantly higher as compared to controls. The treatment of astroglia with L-cycloserine inhibited FFA-induced *de novo* synthesis of ceramide in astroglia and in turn, ROS production, A $\beta$  production and tau hyperphosphorylation in neurons. The data suggest that astroglial ceramide may play a central role in FFA-induced, AD-associated pathophysiological changes in neurons.

To conclude, our results establish an underlying mechanism by which saturated FFAs induce AD-associated pathophysiological as well as metabolic changes, placing “astroglial FFA metabolism” at the center of the pathological cascade of AD. Further understanding of astroglial FFA metabolism, both *in vitro* and *in vivo*, may help in uncovering new aspects of AD pathogenesis that may be translated into potential targets for therapeutic intervention in AD.

© COPYRIGHT

SACHIN PATIL

2007

**DEDICATED TO MY FAMILY**

## ACKNOWLEDGMENTS

*No Matter How Hard You Work, You have Only One Brain and Two Hands,  
Great Work Demands Such Numerous Ones, Which You Find In Your Friends.*

At this juncture of successful completion of my dissertation, I wish to convey my deepest sense of gratitude towards those colleagues and friends who have helped me to achieve my goal. First and foremost, I would like to thank my advisor Dr. Christina Chan, for her guidance, constant inspiration and complete intellectual freedom throughout my research tenure. I am also thankful to all the members of my Ph.D. advisory committee-Dr. Bill Atchison, Dr. Worden and Dr. Walton. Their support and interest in my work, together with the critical evaluation of the work, helped me tremendously to improve the quality of the present dissertation. Words fall short to express my heartfelt feelings and gratitude towards these great personalities. I am proud that I got a chance to work with them.

I would also like to thank my M.S. advisor, my GURU, Professor G. D. Yadav (UICT, Mumbai, India). His inspiring guidance has carved a niche in my heart. He imbibed in me the qualities of confidence, perseverance and unwavering commitment towards one's work, which I am sure would definitely help me throughout my life.

If "a friend in need is a true friend indeed", then all my colleagues are my friends, in true sense. I wouldn't be able to justify my thankful feelings by mere words towards my labmates (from Drs. Chan and Walton labs) who have always been there whenever I needed their help. My special thanks my senior colleague, Dr. Shireesh Srivastava who

helped me throughout my tenure in the lab with constant encouragement and valuable suggestions. The mathematical work (MFA) that I performed for dissertation wouldn't have been possible without his kind help. I am also thankful to my friends for their constant, unwavering encouragement- Dr. Mehul (Netherlands) and his wife, Dr. Sameer (Netherlands), Dr. Lek (Scotland) and his wife Heena, Dr. Ambareesh (Texas), Dr. Navin (MSU), Dr. Zheng Li (Boston), Dr. Srivatsan (Harvard), Sachin Injal (Lawyer), Dhanu, Adam, Nandu, Priti, Lufang, Chisa, Tanmay, Susan, Katie, Dana, Tao, Alison, Bahareh, John, Ketan, Hemant, Joe, Mike, Shengnan, Linxia, Deebika and Xureui. My special thanks also to Shirley Owens, for her help in terms of confocal microscopy. I was also very fortunate to have hard-working, sincere undergraduates assisting me- Alexis (Shell), Robert (U of M) and Joe. Their youthful exuberance was pleasantly encouraging.

I would also like to thank the Department of Chemical Engineering and Materials Science, the College of Engineering, Quantitative and Biological Modeling Initiative (QBMI) at MSU, the office of international student and scholars, council of graduate studies (COGS) and the graduate school for the financial support in the form of Food, Nutrition and Chronic Disease Fellowship and travel fellowships. Their contributions helped me present my research at the national and international scientific meetings.

Also, my apartment at Student living Center (SLC) was my home-away-from-home and my roomies made it that way with whom I will always share the deepest friendship- Sarfaraz (India), Arda (Turkey), Jorge (Peru), Kensuke (Japan), Qiang (China) and Paul (USA). It was truly an international experience. I have learned so many things from them

that I cannot repay them in any way. Here, I would also like to express my gratitude towards all my ward mates at SLC for their true friendship- Stephanie, Tiffany, Kelly, Kerry, Emily, Conrad, Justin, Don, Dan, Ben, Josh, Gary. My special thanks to Cindy, Vern, Nicole and President Hinkle. Also thanks to the Elders who taught me how to tie a double knot.

My sincere thanks to Amit and his wife Deboleena, for inviting me over for countless lunches and dinners. But, obviously it's much more than food that is and will be keeping us in the bond of friendship!

Last but not the least, it was the confidence laid in me by my Mom, Dad, my sisters and brother-in-laws, which enabled me to reach this pinnacle of success. I owe a debt of gratitude for their constant encouragement for higher education and unflinching, altruistic help during this work.

## TABLE OF CONTENTS

<b>LIST OF TABLES.....</b>	<b>xii</b>
<b>LIST OF FIGURES.....</b>	<b>xiii</b>
<b>LIST OF ABBREVIATIONS .....</b>	<b>xviii</b>
<b>CHAPTER 1. INTRODUCTION .....</b>	<b>1</b>
1.1 ALZHEIMER'S DISEASE.....	1
1.2 THE CURRENT HYPOTHESES OF AD.....	4
1.2.1 The Amyloid Cascade Hypothesis.....	4
1.2.2 The Cholesterol Metabolism and AD .....	6
1.2.3 Oxidative Stress and AD .....	7
1.2.4 The Cholnergic Hypothesis of AD .....	8
1.2.5 Homocysteine and AD .....	9
1.2.6 The Pathogen Hypothesis of AD .....	10
1.3 POTENTIAL INVOLVEMENT OF SATURATED FATTY ACIDS IN THE PATHOGENESIS OF AD .....	11
1.4 GOALS OF THE PRESENT STUDY.....	12
1.5 THESIS OUTLINE.....	12
<b>CHAPTER 2. SATURATED FATTY ACID-INDUCED HYPERPHOSPHORYLATION OF TAU IN PRIMARY RAT CORTICAL NEURONS .....</b>	<b>14</b>
2.1 INTRODUCTION .....	14
2.2 MATERIALS AND METHODS .....	18
2.2.1 Isolation and Culture of Primary Rat Cortical Neurons and Astroglia.....	18
2.2.2 Lactate Dehydrogenase (LDH) Assay .....	18
2.2.3 Western Blot Analysis.....	19
2.2.4 Immunofluorescence Analysis of Neurons and Astroglia.....	20
2.2.5 Immunostaining of Reactive oxygen Species.....	20
2.2.6 Data Analyses .....	21
2.3 RESULTS AND DISCUSSION.....	21
2.3.1 Direct Treatment of Neurons with Saturated Fatty Acids.....	21
2.3.2 Involvement of Saturated FFAs in Tau Hyperphosphorylation Through Astroglial Mediation .....	22
2.3.3 Involvement of Oxidative Stress in FFA-Astroglia-Induced Tau Hyperphopshorylation in Neurons.....	26
2.4 CONCLUSIONS .....	27



<b>CHAPTER 3. SATURATED FATTY ACID-INDUCED AMYLOIDOGENIC PROCESSING OF APP IN PRIMARY RAT CORTICAL NEURONS.....</b>	<b>28</b>
3.1 INTRODUCTION .....	28
3.2 MATERIALS AND METHODS .....	33
3.2.1 Isolation and Culture of Primary Rat Cortical Neurons and Astroglia .....	33
3.2.2 Western Blot Analysis.....	34
3.2.3 Immunofluorescence Analysis of BACE1 in Neurons .....	34
3.2.4 Data Analyses .....	35
3.3 RESULTS .....	35
3.3.1 Direct Treatment of Neurons with Saturated Fatty acid (Palmitic Acid).....	35
3.3.2 Involvement of Saturated FFAs in BACE1 Up-regulation and Amyloidogenic Processing of APP Through Astroglial Mediation.....	36
3.3.3 Involvement of Oxidative Stress in FFA-Astroglia-Induced BACE1 Up-regulation and Amyloidogenic Processing of APP in Primary Neurons .....	39
3.4 CONCLUSIONS .....	41
<b>CHAPTER 4. SATURATED FATTY ACID-INDUCED ABNORMAL METABOLIC CHANGES ASSOCIATED WITH ALZHEIMER'S DISEASE.....</b>	<b>42</b>
4.1 INTRODUCTION .....	42
4.2 MATERIALS AND METHODS .....	45
4.2.1 Isolation and Culture of Primary Rat Cortical Neurons and Astroglia .....	45
4.2.2 Western Blot Analysis.....	46
4.2.3 Biochemical Measurements of Cellular Metabolites .....	47
4.2.4 Metabolic Flux Analysis (MFA).....	48
4.2.5 Measurement of Intracellular ATP in Astroglia .....	54
4.2.6 Measurement of Intracellular Ceramide in Astroglia .....	55
4.2.7 Data Analyses .....	56
4.3 RESULTS AND DISCUSSION.....	56
4.3.1 FFA-Induced Abnormal Glucose Metabolism .....	56
4.3.2 Cellular Mechanism of FFA-Induced Abnormal Glucose Metabolism in Astroglia.....	59
4.3.3 FFA-Induced Global Metabolic Changes in Astroglia .....	61
4.3.3.1 Verification of the pseudo-steady state assumption and linearity of fluxes over 24 hours.....	62
4.3.3.2 MFA Analysis .....	64
4.4 CONCLUSIONS .....	69
<b>CHAPTER 5. INVOLVEMENT OF CERAMIDE IN FFA-ASTROGLIA-INDUCED PATHOPHYSIOLOGICAL ABNORMALITIES ASSOCIATED WITH AD .....</b>	<b>70</b>

5.1 INTRODUCTION .....	70
5.1 MATERIALS AND METHODS .....	72
5.2.1 Isolation and Culture of Primary Neurons and Astroglia from Rat Cortex and Cerebellum .....	72
5.2.2 Immunostaining of Reactive Oxygen Species (ROS).....	74
5.2.3 Western Blot Analysis.....	74
5.2.4 ELISA measurements of A $\beta$ 40 and A $\beta$ 42 .....	76
5.2.5 Data Analyses .....	76
5.3 RESULTS AND DISCUSSION.....	76
5.3.1. Involvement of Astroglial Ceramide in FFA-Astroglia-Induced ROS production in Neurons .....	76
5.3.2 Involvement of astroglial ceramide in FFA-astroglia-induced amyloidogenesis and tau hyperphosphorylation in neurons.....	78
5.3.3 A possible explanation for the region-specific and cell type-specific damage observed in AD.....	84
5.4 CONCLUSIONS .....	87
<b>CHAPTER 6 CONCLUSIONS .....</b>	<b>88</b>
<b>APPENDIX .....</b>	<b>96</b>
1. Brain cells from older animals .....	96
2. Trans-well experiments.....	96
3. Exogenous addition of ceramide as a positive control .....	97
<b>LIST OF PUBLICATIONS .....</b>	<b>99</b>
<b>BIBLIOGRAPHY .....</b>	<b>100</b>

## **LIST OF TABLES**

Table 4.1 List of the cellular metabolic reactions.....	43
Table 4.2 List of intracellular metabolites.....	46
Table 4.3 List of measured fluxes.....	47
Table 4.4 Ratio of intracellular to extracellular lactate levels.....	57
Table 4.5 Metabolic flux values calculated by MFA.....	58

**Images in this dissertation are presented colored.**

## **LIST OF FIGURES**

**Figure 1.1. The shrinkage of brain in Alzheimer's disease.** The brain regions involved in cognitive functions (frontal and temporal lobes, left and lower part of brain, respectively) show significant shrinkage in AD brain as compared to normal brain.....1

**Figure 1.2. The pathophysiological lesions in AD brain.** (A) Amyloid beta ( $A\beta$ ) plaque and (B) Neurofibrillary tangle (NFT).....2

**Figure 1.3. The decreased glucose metabolism in Alzheimer's disease.** The positron emission tomography (PET) images show significant decline in cerebral glucose metabolism in AD brain as compared to normal brain; red and yellow-high metabolism, blue-low metabolism.....2

**Figure 2.1. The physiology and pathology of tau.** (A) In healthy neurons, tau stabilizes microtubules. (B) In AD, tau hyperphosphorylates and detaches from microtubules leading to tangle formation.....8

**Figure 2.2. Direct treatment of neurons with saturated FFAs.** Primary rat cortical neurons were treated for 24 hours with 0.2mM of either palmitic acid (PA) or stearic acid (SA) or with 5% bovine serum albumin (BSA), vehicle for FFAs (control). Detergent cell lysates from fatty acid-treated and control cells were immunoblotted with PHF-1 and AT8 antibodies, which recognize phosphorylated tau.  $\beta$ -actin is shown as a marker for protein loading. ....15

**Figure 2.3. MAP-2, GFAP and AT8 immunostaining.** (A) Neurons treated directly with FFAs for 24 hours. (B) Astrocytes treated for 12 hours with 0.2mM of either palmitic acid (PA) or stearic acid (SA) or 5% BSA (control). (C) Neurons treated for 24 hours with conditioned media from fatty acid-treated or control astrocytes. (D) Immunofluorescence labeling of phosphorylated tau with AT8 antibody in neurons treated with conditioned media from fatty acid-treated or untreated astrocytes (control). Images were obtained with confocal fluorescence microscopy. (Objective lens magnification- 40X for MAP-2 and GFAP, 63X for AT8).....16

**Figure 2.4. Measurement of LDH release from astroglia treated with PA.** 24h treatment with 0.2mM PA failed to liberate LDH from astroglia as compared to controls. In contrast, 1hr treatment of astroglia with 300mM  $H_2O_2$  (positive control) induced significant LDH liberation after 24h as compared to both control and PA-treated cells. Data are taken from 3 different experiments and are expressed as mean  $\pm$  S.D. One-way

ANOVA with Tukey's post hoc method was used for analyzing the differences between treatment groups. \*,  $p < 0.05$  compared with control.....17

**Figure 2.5. Astroglia-mediated, fatty acid-induced hyperphosphorylation of tau in neurons.** (A) Western blot analysis of hyperphosphorylated tau was performed using phospho-specific antibodies PHF-1 and AT8. (B) Histograms corresponding to PHF-1 and AT8 blots represent quantitative determinations of intensities of the relevant bands. Data represent mean  $\pm$  S.D. of 3 independent experiments. One-way ANOVA with Tukey's post hoc method was used for analyzing the differences between treatment groups. \*,  $p < 0.05$  compared with control; #,  $p < 0.05$  compared with fatty acid treatment.....18

**Figure 2.6. Intracellular accumulation of ROS in neurons.** (A) Astroglia and (B) neurons were stained with CM-H2DCFDA for intracellular ROS detection and examined with confocal fluorescence microscopy (Zeiss LSM 5 Pascal). (Objective lens magnification, 63X).....19

**Figure 3.1. Processing of amyloid precursor protein (APP).** (A) The non-amyloidogenic pathway catalyzed by  $\alpha$ - and  $\gamma$ -secretase. (B) The amyloidogenic pathway catalyzed by  $\beta$ - and  $\gamma$ -secretase.....23

**Figure 3.2. Direct treatment of neurons with palmitic acid.** Primary rat cortical neurons were treated for 24 hours with 0.2mM of palmitic acid (PA) or with 4% bovine serum albumin (BSA), vehicle for PA (control). Detergent cell lysates from PA-treated and control cells were immunoblotted with BACE1 antibody.  $\beta$ -actin is shown as a marker for protein loading. The blots are representative of 3 independent experiments..29

**Figure 3.3. BACE1 immunostaining.** Immunofluorescence labelling of BACE1 in neurons treated for 24 hours with conditioned media from PA-treated (for 24 hours) or untreated astrocytes (control). Images were obtained with confocal fluorescence microscopy (objective lens magnification- 40X).....30

**Figure 3.4. Astroglia-mediated, PA-induced BACE1 upregulation in neurons.** Astrocytes were treated for 12 and 24 hours with 0.2mM of PA or 4% BSA (control), followed by transfer of the astrocytes-conditioned media to neurons (24 hours treatment). (A) Western blot analysis of BACE1 protein levels in neurons.  $\beta$ -actin is shown as a marker for protein loading. (B) Histograms represent quantitative determinations of intensities of the relative bands. Data represent mean  $\pm$  S.D. of three independent experiments. Student's t-test was used for analyzing differences between different treatment groups. \*,  $p < 0.05$  compared with respective control.....31

**Figure 3.5. Immunoblot analysis of presenilin-1 (PS1) levels in neurons treated with astrocytes-conditioned media.** Astrocytes were treated for 24 hours with 0.2mM PA or 5% BSA (control), followed by transfer of the astrocytes-conditioned media to neurons (24 hours treatment), with or without 10mM DMU. Detergent cell lysates from PA-

treated and control cells were immunoblotted for PS1 and PS1-CTF levels. The immunoblot is representative of 3 independent experiments.....32

**Figure 3.6. Oxidative stress involved in astroglia-mediated, PA-induced elevations in BACE1 and C99 levels in neurons.** Astrocytes were treated for 24 hours with 0.2mM PA or 5% BSA (control), followed by transfer of the astrocytes-conditioned media to neurons (24 hours treatment), with or without 10mM DMU. (A) Western blot analysis of BACE1, APP and C99 protein levels in neurons. (B) Histograms represent quantitative determinations of intensities of the relative bands. Data represent mean  $\pm$  S.E. of three independent experiments. One-way ANOVA with Tukey's post hoc method was used for analyzing the differences between treatment groups. \*,  $p < 0.05$  compared with control; \*\*  $p < 0.05$  compared with PA treatment.....33

**Figure 4.1. Conventional view of cerebral glucose metabolism.....37**

**Figure 4.2. Cerebral glucose metabolism based on the novel astrocyte-neuron lactate shuttle hypothesis. ....38**

**Figure 4.3. Astroglial metabolic network.** Boxes represent extracellular metabolites, while ovals represent intracellular metabolites. The direction of reaction assumed in the model is indicated by arrows. ....45

**Figure 4.4. PA downregulates glucose uptake and lactate release by astroglia.** The cortical neurons and astroglia were treated for 24 hours with 0.2mM of PA or 4% BSA. (A) In neurons, PA treatment did not change glucose uptake and lactate production. (B) PA treatment significantly decreased glucose uptake and lactate production by astroglia. AMPK-activator AICAR did not inhibit PA-induced downregulation in glucose metabolism. Data represent mean  $\pm$  S.D. of six experiments. Student's t-test was used for analyzing the differences between the two treatment groups. \*,  $p < 0.05$  compared with respective control. ....50

**Figure 4.5. Measurement of intracellular ATP in astroglia.** The cortical astroglia were treated for 24 hours with 0.2mM of PA or 4% BSA. PA treatment increased cellular ATP production in astroglia. Data represent mean  $\pm$  S.D. of 3 experiments. Student's t-test was used for analyzing the differences between the two treatment groups. \*,  $p < 0.05$  compared with respective control. ....51

**Figure 4.6. PA downregulates GLUT1 level in astroglia.** Astroglia were treated for 24 hours with 0.2mM of PA or 4% BSA. The immunoblot analysis shows that PA-treatment significantly decreased the levels of GLUT1 as compared to the untreated ones.  $\beta$ -actin is shown as a marker for protein loading. Histogram represents quantitative determinations of intensities of the relative bands normalized with actin. Data represent mean  $\pm$  S.D. of three independent experiments. Student's t-test was used for analyzing the differences between the two treatment groups. \*,  $p < 0.05$  compared with respective control.....53

**Figure 4.7. FFA-metabolizing pathways involved in cellular ROS production.....54**

**Figure 4.8A. Time-dependent measurements of intracellular lactate levels.** Astroglia were treated for 6, 12 and 24 hours with 0.2mM of PA or 4% BSA. The cells were trypsinized, washed with TBS and lyzed by using 0.7% perchloric acid. The lactate levels in cell lysate were measured by enzymatic assay. Data represent mean  $\pm$  S.D. of three independent experiments.....56

**Figure 4.8B. Time-dependent measurements of extracellular lactate levels.** Astroglia were treated for 6, 12 and 24 hours with 0.2mM of PA or 4% BSA. The conditioned media were collected and the lactate levels in the media were measured by enzymatic assay. Data represent mean  $\pm$  S.D. of three independent experiments.....57

**Figure 4.9. PA-induced, de novo synthesis of ceramide in astroglia.** Astroglia were treated for 24h with 0.2mM PA or 4% BSA (control), after which cellular lipids were extracted for ceramide determination by HPLC. PA significantly increased ceramide synthesis in astroglia, which was completely inhibited by treatment of astroglia with 2mM L-CS, an inhibitor of de novo synthesis of ceramide. Data are taken from 3 different experiments and are expressed as mean  $\pm$  S.D. One-way ANOVA with Tukey's post hoc method was used for analyzing the differences between treatment groups. \*,  $p < 0.05$  compared with control; #,  $p < 0.05$  compared with PA treatment.....61

**Figure 5.1. Cellular ceramide production.** Ceramide is produced in cells by *de novo* synthesis from serine and palmitoyl-CoA or by breakdown of membrane sphingomyelins.....64

**Figure 5.2. Involvement of astroglial ceramide in PA-astroglia-induced ROS production in neurons.** Co-treatment of astroglia with 2mM L-CS inhibited PA-astroglia-induced ROS production in neurons. The neurons were stained with CM-H2DCFDA for intracellular ROS detection and examined with confocal fluorescence microscopy (Zeiss LSM 5 Pascal). (Objective lens magnification, 40X).....70

**Figure 5.3. The expression of iNOS and IL-6 in astroglia.** The expression of iNOS, but not IL-6 was increased by PA treatment in astroglia. Co-treatment of astroglia with 2mM L-CS inhibited PA-induced iNOS expression in astroglia.  $\beta$ -actin is shown as a marker for protein loading.....71

**Figure 5.4. Involvement of astroglial ceramide in PA-astroglia-induced elevations in BACE1 and amyloidogenic processing of APP in neurons.** In neurons treated with conditioned media from PA-treated astroglia, the levels of (A) BACE1, (B) C99 and (C) A $\beta$ 40 and A $\beta$ 42 were found elevated. These PA-astroglia-induced tau abnormalities were blocked by inhibiting astroglial ceramide synthesis with 2mM L-CS. Data represent mean  $\pm$  S.D. of three independent experiments. One-way ANOVA with Tukey's post hoc method was used for analyzing the differences between treatment groups. \*,  $p < 0.05$  compared with control; #,  $p < 0.05$  compared with PA treatment.....72

**Figure 5.5. Involvement of astroglial ceramide in PA-astroglia-induced tau hyperphosphorylation in neurons.** In neurons treated with conditioned media from PA-

treated astroglia, tau was found pathologically hyperphosphorylated as shown by immunoblotting with PHF-1 and AT8 antibodies. Tau-1 detects dephosphorylated tau, thus showing decreased levels in PA-astroglia-treated neurons. These PA-astroglia-induced tau abnormalities were blocked by inhibiting astroglial ceramide synthesis with 2mM L-CS. Histograms corresponding to PHF-1 and AT8 blots represent quantitative determinations of intensities of the relevant bands normalized with actin. Data represent mean  $\pm$  S.D. of three independent experiments. One-way ANOVA with Tukey's post hoc method was used for analyzing the differences between treatment groups. \*,  $p < 0.05$  compared with control; #,  $p < 0.05$  compared with PA treatment.....73

**Figure 5.6. PA-astroglia-induced activation of AD-specific kinases in neurons is mediated by astroglial ceramide.** Conditioned media from PA-treated astroglia activated (A) GSK-3 (increased levels of phosphorylated GSK-3) and (B) cdk5 (increased cleavage of p35 to p25) but not (C) MAP- Erk1/2 (no change in the levels of phosphorylated MAP- Erk1/2). The treatment of astroglia with 2mM L-CS inhibited PA-astroglia-induced activation of both GSK-3 and cdk5. Data are representative of 3 different experiments.....75

**Figure 5.7. GSK-3 is involved in PA-astroglia-induced tau hyperphosphorylation in neurons.** Astroglia-conditioned media were transferred to neurons, with or without various kinase inhibitors, viz., 10mM LiCl<sub>2</sub> (GSK-3 inhibitor), 10mM Roscovitine (cdk-5 inhibitor) and 30mM PD98059 (MAPK inhibitor). Immunoblot analysis with PHF-1 and AT8 antibodies show that only LiCl<sub>2</sub> inhibited the observed, PA-induced tau hyperphosphorylation in neurons. Histogram data represent mean  $\pm$  S.D. of three independent experiments. One-way ANOVA and Tukey's post hoc method was used for analyzing the differences between treatment groups. \*,  $p < 0.05$  compared with control; #,  $p < 0.05$  compared with PA treatment.....77

**Figure 5.8. Differential effects of cortical and cerebellar astroglia on cortical neurons.** Cortical neurons (CTN) were treated with conditioned media from (A) cortical astroglia (CTA) and (B) cerebellar astroglia (CBA). Western blot analysis of hyperphosphorylated tau was performed using AT8 antibody. Cortical astroglia but not cerebellar astroglia were involved in PA-induced tau hyperphosphorylation in neurons. Data represent mean  $\pm$  S.D. of three independent experiments. Student's t-test was used for analyzing differences between different treatment groups. \*,  $p < 0.05$  compared with control.....79

**Figure 6.1. The "FFA-AD" hypothesis.** Proposed cellular mechanism by which astroglial FFA metabolism may play a central role in causing pathophysiological and metabolic changes associated with AD.....83



## LIST OF ABBREVIATIONS

<b>A<math>\beta</math>:</b>	Amyloid beta
<b>AChE:</b>	Acetylcholine esterase
<b>AD:</b>	Alzheimer's disease
<b>ADDLs:</b>	A $\beta$ -derived diffusible ligands
<b>AMPK:</b>	AMP-activated protein kinase
<b>ApoE4:</b>	Apolipoprotein E4
<b>APP:</b>	Amyloid precursor protein
<b>BACE:</b>	$\beta$ -site APP cleaving enzyme
<b>BBB:</b>	Blood-brain barrier
<b>BSA:</b>	Bovine serum albumin
<b>cdk:</b>	cyclin-dependent kinase
<b>CBA:</b>	Cerebellar astroglia
<b>CTA:</b>	Cortical astroglia
<b>CTN:</b>	Cortical neurons
<b>DAG:</b>	Diacyl glycerol
<b>DMU:</b>	1,3-dimethyl urea
<b>ELISA:</b>	Enzyme-linked immunosorbent assay
<b>FACS:</b>	Fatty acyl-CoA synthetase
<b>FAD:</b>	Familial Alzheimer's disease
<b>FFA:</b>	Free fatty acid
<b>GSK:</b>	Glycogen synthase kinase
<b>4-HNE:</b>	4-hydroxynonenal

**HPLC:** High performance liquid chromatography

**IL-6:** Interleukin-6

**iNOS:** inducible nitric oxide synthase

**L-CS:** L-cycloserine

**LDH:** Lactate dehydrogenase

**MAPK:** Mitogen-activated protein kinase

**MCI:** Mild cognitive impairment

**MFA:** Metabolic flux analysis

**NAC:** N-acetyl cysteine

**NFTs:** Neurofibrillary tangles

**NMDA:** N-methyl D-aspartate

**NO:** Nitric oxide

**PA:** Palmitic acid

**PET:** Positron emission tomography

**PHF:** Paired helical filaments

**PKA:** Protein kinase A

**PKC:** Protein kinase C

**PS:** Presenilin

**ROS:** Reactive oxygen species

**SA:** Stearic acid

**SAD:** Sporadic Alzheimer's disease

**SPT-1:** Serine palmitoyltransferase-1

**TBARS:** Thiobarbituric acid reactive substances

## CHAPTER 1. INTRODUCTION

### 1.1 ALZHEIMER'S DISEASE

Dementia is one of the most complex and heterogeneous age-related disorders and the most common cause of dementia is Alzheimer's disease (AD) <sup>1</sup>. AD is a progressive neurodegenerative disease clinically characterized by severe memory loss and cognitive impairment <sup>2</sup>. As shown in **Figure 1.1**, AD brain exhibits significant shrinkage as compared to healthy controls <sup>3</sup>. Pathologically, AD is characterized by extracellular deposits of amyloid beta (A $\beta$ ) protein and intracellular accumulation of neurofibrillary tangles (NFTs) composed of hyperphosphorylated tau protein (**Figure 1.2**) <sup>3</sup>. In addition to these two classical neuropathological hallmarks, AD brain is also characterized by abnormal metabolic changes; abnormal cerebral glucose metabolism is one of the distinct characteristics of AD brain (**Figure 1.3**) <sup>3-5</sup>.

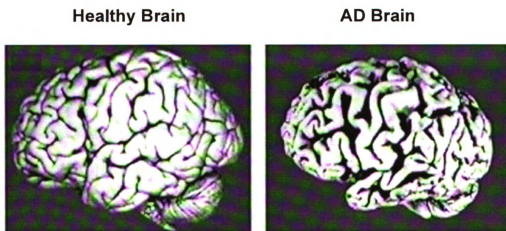


**Figure 1.1. The shrinkage of brain in Alzheimer's disease.** The brain regions involved in cognitive functions (frontal and temporal lobes, left and lower part of brain, respectively) show significant shrinkage in AD brain as compared to normal brain (Figure taken from Ref. 3, with permission from Nature Publishing Group).

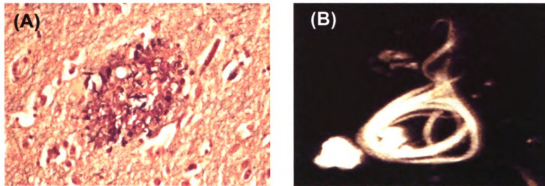


**Figure 1.2. The pathophysiological lesions in AD brain.** (A) Amyloid beta ( $A\beta$ ) plaque and (B) Neurofibrillary tangle (NFT) (Figures taken from [www.alzheimers.org](http://www.alzheimers.org), 08-09-2007).

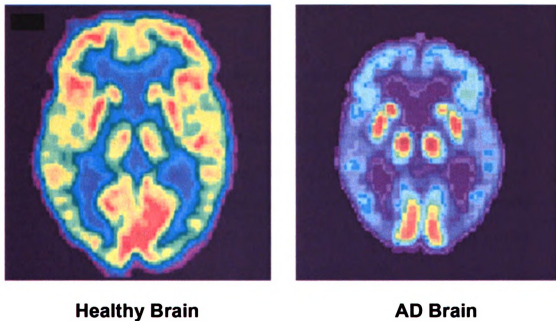


**Figure 1.3. The decreased glucose metabolism in Alzheimer's disease.** The positron emission tomography (PET) images show significant decline in cerebral glucose metabolism in AD brain as compared to normal brain; red and yellow-high metabolism, blue-low metabolism (Figure taken from Ref. 3, with permission from Nature Publishing Group).

AD is classified into two categories- familial Alzheimer's disease (FAD) and sporadic Alzheimer's disease (SAD). FAD has been shown to be associated with the mutations in

APP, presenilin 1 and 2 (PS1 and PS2) genes on chromosome 21, 14 and 1, respectively<sup>6-9</sup>. Of all the AD cases only 5-10% are due to FAD mutations and the mutations in PS1 are the most frequent of the FAD causes<sup>10, 11</sup>. Furthermore, apolipoprotein E4 (ApoE4) gene has been shown to cause slight predisposition to AD<sup>12</sup>. On the other hand, SAD is the major form of AD and comprises 90-95% of all the cases<sup>10</sup>. Unlike FAD, the etiology of SAD is not well understood and several possible risk factors in the development of SAD have been identified. Age is the most significant risk factor for the development of AD. Additional risk factors based upon the epidemiological studies are high fat diet, gender, head trauma and vascular risk factors such as diabetes, ischemia, hypertension, etc.<sup>13</sup>.

AD was first described in 1906 by the German psychiatrist Alois Alzheimer<sup>14</sup>. Today, AD affects approximately 5-10% of the population over 65 years of age and more than 20% over the age of 80 years<sup>15</sup>. It represents 40-70% of all dementia cases<sup>15, 16</sup>. There are approximately 5 million AD patients in the U.S. alone and the total direct/indirect cost associated with the disease is estimated to be more than \$140 billion annually [www.alz.org]. With the increasing aging population in the western world, AD has become one of the leading socio-economical challenges today. At the rate of 1 new patient every 72 seconds, the number of AD patients is expected to grow to 13 million by year 2050 and the associated cost will be more than the total U.S. budget [www.alz.org]. Currently, there is no cure for AD<sup>17</sup>. The available treatments include the use of acetylcholinesterase (AChE) inhibitors (donepezil, rivastigmine and galanthamine) and the N-methyl D-aspartate (NMDA) antagonist, memantine, which have beneficial, but

short-lived effects on the symptoms of AD. This emphasizes a significant need for identifying novel targets for therapeutic intervention in AD.

## **1.2 THE CURRENT HYPOTHESES OF AD**

AD etiology is very complex and a large number of factors are hypothesized to play key roles in the pathogenesis of AD. Based on the extensive literature search, we present variety of such major scientific hypotheses about the pathogenesis of AD below. In case of each of these hypotheses, we present supporting data in terms of epidemiological studies as well as various cell culture and animal models. In addition, the limitations associated with these hypotheses are also explained.

### **1.2.1 The Amyloid Cascade Hypothesis**

The amyloid hypothesis is the most widely studied hypothesis in AD research field. According to this hypothesis, the different gene defects can lead to altered expression or proteolytic processing of amyloid precursor protein (APP) leading to chronic imbalance between A $\beta$  production and clearance. This results in the gradual accumulation of A $\beta$  plaques, which in turn initiates a pathological cascade leading to the gliosis, inflammatory changes, synaptic change, neurofibrillary tangles and neurotransmitter loss<sup>18</sup>. Many studies support the amyloid cascade hypothesis. The brains of AD patients are characterized by the presence of A $\beta$  plaques and their number far exceeds that found in the brains of age-matched healthy controls<sup>19</sup>. Furthermore, the amount of A $\beta$  plaques is highly correlated with the degree of cognitive impairment<sup>20</sup>. In addition, all four genes associated with FAD have been shown to be involved in increased production of A $\beta$

(APP, PS1 and PS2)<sup>21-28</sup> and its aggregation (ApoE4)<sup>29, 30 31</sup>. ApoE4 leads to excessive deposition of A $\beta$  in the brain long before AD symptoms occur<sup>32</sup>. Down's syndrome patients who produce significantly higher amount of A $\beta$  from birth and deposit A $\beta$  plaques in their brains as early as age 12, inevitably develop AD by age the of 50<sup>33</sup>. This further emphasizes the central role of A $\beta$  in the pathogenesis of AD. In addition, in various cell culture models A $\beta$  fibrils have been shown to induce neuronal damage and activate inflammatory cells (microglia and astroglia)<sup>34, 35 36</sup>. Also transgenic animal models expressing human APP gene have been shown to develop A $\beta$  plaques leading to the neuronal and microglial damage. These animal models reproduce most of the major features associated with the AD pathology<sup>37-39</sup>.

Despite these data, the amyloid cascade hypothesis falls short in comprehensively interpreting AD pathology. In addition to the increased A $\beta$  deposition, AD brain is also characterized by the formation of NFTs. In this context, although A $\beta$  has been shown to induce hyperphosphorylation of tau and its tangle formation in cell cultures, the APP transgenic mice do not show formation of NFTs in their brain<sup>40</sup>. Also, NFTs have been shown to occur independent of A $\beta$  plaques<sup>41</sup>. In addition, it is not clear whether the behavioral deficits observed in APP transgenic animals are related exclusively to the increased A $\beta$  production and deposition in these animals. Furthermore, the amyloid cascade hypothesis does not provide an explanation for the region-specific damage observed in AD. Finally, suspension of the A $\beta$  vaccination clinical trial due to the development of encephalitis in a small percentage of individuals further undermined the amyloid cascade hypothesis<sup>42</sup>.

### 1.2.2 The Cholesterol Metabolism and AD

Recently, it has been hypothesized that the abnormalities in cholesterol homeostasis may play a central role in causing synaptic impairment, neuronal degeneration and other hallmarks associated with AD <sup>43</sup>. The hypothesis is based on the observations that statins which inhibit cholesterol synthesis protect against age-associated dementia and AD <sup>44, 45</sup>. Also, the dietary hypercholesterolemia in APP transgenic mice and rabbits has been shown to accelerate A $\beta$  deposition in their brains <sup>46, 47</sup>. Various cell culture studies further support the involvement of abnormal cholesterol metabolism in A $\beta$  production <sup>48-50</sup>. In addition to increased A $\beta$  production, abnormal cholesterol metabolism may lead to neurite degeneration, neuronal cell death, cholinergic dysfunction, oxidative stress and behavioral impairment, thus suggesting its central role in AD pathogenesis <sup>43</sup>.

The main limitation of the cholesterol hypothesis is that the causal factor behind the abnormal brain cholesterol metabolism is not well established. Furthermore, It is not clear how dietary hypercholesterolemia affects brain cholesterol metabolism as it has been shown that the cholesterol pools in the plasma and the brain are independent of each other; in rats where hypercholesterolemia was induced by diet, all the brain cholesterol was synthesized *in situ* and did not come from circulation <sup>51</sup>. Furthermore, although cholesterol levels enhance A $\beta$  production, tau hyperphosphorylation is caused by cellular cholesterol deficiency <sup>52, 53</sup>. Thus, how abnormal cholesterol metabolism may lead to the formation of both the pathophysiological changes associated with AD (A $\beta$  production and tau hyperphosphorylation) is not clear.



### 1.2.3 Oxidative Stress and AD

Age is the most important risk factor for AD and one of the most accepted theories of aging is increased oxidative stress <sup>54</sup>. In this context, it has been hypothesized that the age-associated increase in oxidative stress may play a key role in the pathogenesis of AD. The increased oxidative stress in AD brain can also be attributed to various other factors such as increased levels of metal ions in the brain, inflammatory response from activated microglia and astroglia and increased levels of advanced glycation endproducts (AGEs) associated with AD. Iron has been shown to be increased in NFTs as well as in A $\beta$  plaques and involved in reactive oxygen species (ROS) production <sup>55, 56</sup>. Iron catalyzes the formation of hydroxyl radicals from H<sub>2</sub>O<sub>2</sub> and thus may lead to lipid peroxidation and oxidation of cellular DNA and proteins. The iron-induced lipid peroxidation is further potentiated by aluminum <sup>57</sup>, which also accumulates in neurofibrillary tangle-containing neurons <sup>58</sup>. The activated microglia surround the A $\beta$  plaques <sup>59</sup> and are a source of NO and oxygen radicals <sup>60</sup>, which can react to form peroxynitrite <sup>61</sup>. Furthermore, AGEs in the presence of transition metals can undergo redox cycling with consequent ROS production <sup>62-64</sup>. The role of oxidative stress in AD pathogenesis is supported by various studies where free radicals were shown to be involved in increased A $\beta$  production <sup>65-70</sup> as well as hyperphosphorylation of tau <sup>71-75</sup>, two hallmarks of AD.

Here it is interesting to note that Amyloid- $\beta$  itself has been directly implicated in ROS formation through peptidyl radicals <sup>76-78</sup>. Furthermore, increased oxidative stress has been associated with many other neurodegenerative diseases such as Parkinson's disease and Huntington's disease, which have clinical and pathological features different than AD.

Therefore, it is not clear whether oxidative stress plays a causal role in AD pathogenesis or merely a part of the complex AD etiology.

#### **1.2.4 The Cholinergic Hypothesis of AD**

The cholinergic system in the brain is involved in controlling cerebral blood flow, cortical activity and sleep-wake cycle as well as in modulating cognitive function <sup>79</sup>. The severe deficiency in the brain cholinergic system which is associated with the cognitive impairment has been proposed to be a central aspect of AD pathology <sup>80</sup>. The strong correlation of clinical dementia ratings with the reductions in the cerebral cholinergic markers such as choline acetyltransferase and levels of acetylcholine support the association of cholinergic dysfunction with AD pathology <sup>81, 82</sup>. The direct correlation of dysfunctional cholinergic system and AD pathology is supported by various cell culture and animal model studies that showed a central role of cholinergic system in regulating amyloidogenic processing of APP and hyperphosphorylation of tau, two main characteristics of AD. The activation of muscarinic acetylcholine receptor (M2-mAChR) in SH-SY5Y neuroblastoma cells significantly downregulated level of BACE1, which is involved in amyloidogenic processing of APP <sup>83</sup>. Furthermore, selective lesion of basal forebrain cholinergic neurons in rat brain significantly increased A $\beta$  production and deposition in cortical areas <sup>84, 85</sup>. Also, activation of nicotinic receptors (nAChR) has been shown to decrease amyloidogenic of APP both in cell culture <sup>86, 87</sup> and in vivo <sup>88</sup>. In addition, the activation of mAChR has been shown to prevent tau phosphorylation <sup>89, 90</sup>.

Despite these supporting data, the cholinergic hypothesis has some limitations. It is unclear if the cholinergic dysfunction leads to the A $\beta$  production or A $\beta$  leads to the death of cholinergic neurons associated with AD. Furthermore, basal forebrain cholinergic neuronal loss is not specific to AD and is also associated with many diseases e.g. Parkinson's disease, Parkinsonism with dementing complex of Guam, Pick's disease, Jakob-Creutzfeld disease etc.<sup>79</sup>.

### **1.2.5 Homocysteine and AD**

The elevated plasma level of homocysteine (homocysteinuria) has been proposed to be an independent risk factor for the development of AD<sup>91</sup>. The level of total homocysteine is significantly higher in serum of AD patients compared to healthy subjects<sup>92-98</sup>. The role of homocysteine in AD pathology is further emphasized by the cell culture studies where homocysteine caused oxidative stress, tau hyperphosphorylation and apoptosis in neurons<sup>99, 100</sup>. There is a significant positive correlation between homocysteine and 4-hydroxynonenal (4-HNE), a lipid peroxidation product, in AD<sup>101</sup>. Furthermore, BACE1 and PS1, two important enzymes involved in A $\beta$  production have been shown to be regulated by methylation. In context to this, increased homocysteine levels (caused by the reduction of folate and vitamin B12 in culture medium) cause a reduction of S-adenosylmethionine, the universal methyl-group donor, thus consequently increasing PS1 and BACE1 levels<sup>102</sup>. In this context, a positive correlation between elevated levels of homocysteine and A $\beta$ 40 has been established in AD<sup>103</sup>.

In addition to these supportive data, there are many studies that oppose any key role of homocysteine in AD. It has been observed that although plasma homocysteine levels were higher in AD cases than controls, this difference was not significant and homocysteine levels were not related to cognitive status <sup>104</sup>. This was further supported by another study, which showed that high homocysteine levels were not associated with AD and were not related to a decrease in memory scores over time <sup>105</sup>. Furthermore, homocysteine has been shown to potentiate copper-induced oxidative stress in primary mouse neurons, but homocysteine alone had no effect <sup>106</sup>. Thus, it is clear that the area of homocysteine and AD needs to be further studied. We need additional, long-term studies using a variety of populations to determine if elevated homocysteine level is a significant and consistent risk factor for AD.

#### **1.2.6 The Pathogen Hypothesis of AD**

The pathogen hypothesis proposes a potential role of microbes such as herpes simplex virus 1 (HSV1) and *Chlamydomphila pneumoniae* (Cp) in the pathogenesis of AD. The pathogens have been accepted to play central role in causing many diseases which earlier had been thought to be non-infectious; *Helicobacter pylori* has been shown to cause duodenal ulcers and gastric cancers <sup>107</sup>, which previously were thought of as the result of stress, chemical irritants and genetic mutations. Also, human papillomavirus (HPV) virus has been accepted to cause virtually all cases of cervical cancer <sup>108</sup>. Furthermore, *C. pneumoniae* has been recently suggested to play a role in atherosclerosis <sup>109, 110</sup>. In light of these data, proponents of the pathogen hypothesis suggest its serious consideration in the case of AD, given the fact that the dominant hypothesis in the AD field (the amyloid

cascade hypothesis) remains open to many questions. Interestingly, although various studies showed the presence of HSV1 and Cp in brains of AD patients <sup>111-115</sup>, others failed to confirm these data <sup>116-119</sup>. These contradictory results may be attributed to the fact that both HSV1 and Cp are highly challenging to detect. Recently, an infection-based animal model showed that intranasal inoculation of mice with Cp results in the formation of amyloid plaques in their brain <sup>120</sup>, thus further supporting the pathogen hypothesis of AD. However, these data await further independent replication.

### **1.3 POTENTIAL INVOLVEMENT OF SATURATED FATTY ACIDS IN THE PATHOGENESIS OF AD**

Epidemiological studies suggest that high fat diets significantly increase the risk of AD and the degree of saturation of fatty acids is critical in determining the risk for AD <sup>121</sup>. This notion is further supported by various *in vivo* studies where mice fed a western, high fat (21-40%)-high cholesterol (0.15-1%) diet developed AD-like pathophysiological changes in their brain <sup>122-124</sup>. Diets rich in saturated fats may increase brain uptake of intact free fatty acids (FFAs) from the plasma through the blood brain barrier (BBB) <sup>125</sup>; the BBB is not a barrier for fatty acids <sup>126</sup>. Here, it is interesting to note that diabetes mellitus, which is a significant risk factor for AD <sup>127</sup> is characterized by elevated plasma levels of saturated FFAs <sup>128</sup>. Due to the interaction between the FFA pools in the plasma and the brain <sup>125, 126, 129</sup>, diabetes-associated increases in plasma FFAs may affect the level of FFAs in the brain and in turn increase the risk for AD. Likewise, traumatic brain injury, which has been established as an independent risk factor for AD <sup>130</sup> is associated with elevated levels of palmitic, stearic and arachidonic acids in the brain <sup>131</sup>. Following

traumatic brain injury, palmitic acid increases from ~ 60 to 180  $\mu\text{M}$  and stearic acid from ~ 50 to 350  $\mu\text{M}$  <sup>132</sup>. In addition, the fatty acid profile of NFTs in AD brain has been shown to be rich in palmitic and stearic fatty acids <sup>133</sup>. Similarly, the white matter in AD brain is characterized by high fatty acid content <sup>134</sup>. Finally, apolipoprotein E4 (ApoE4) is an important genetic risk factor for AD and its risk may be further increased by a hyperlipidemic life-style <sup>135</sup>. Despite these accumulating data, the basic mechanism of how elevated levels of fatty acids are involved in the pathogenesis of AD is unclear.

#### **1.4 GOALS OF THE PRESENT STUDY**

The present study was undertaken with the following aims: 1) investigate the possible involvement of saturated fatty acids in causing the pathophysiological and metabolic changes associated with AD; 2) establish the basic mechanism behind these potential, fatty acid-induced abnormalities; and 3) understand the causal interrelation between the neuropathological and metabolic changes. These data may be useful in identifying the possible causal role of elevated levels of saturated fatty acids in the pathogenesis of AD and may further help in identifying novel therapeutic targets.

#### **1.5 THESIS OUTLINE**

In line with the main focus of the present work to investigate a possible causal link between saturated FFAs and AD-associated abnormalities, this dissertation is subdivided as follows: Chapter 2 presents results describing the involvement of saturated FFAs in causing oxidative stress and hyperphosphorylation of tau in neurons through astroglial mediation. Chapter 3 describes the role of saturated FFAs in causing amyloidogenic

processing of amyloid precursor protein (APP) through astroglia-mediated oxidative stress. In Chapter 4, FFA-induced abnormal glucose metabolism is studied. Metabolic flux analysis (MFA) is applied to obtain a comprehensive picture of the global metabolic changes caused by FFA treatment. This led to the identification of abnormal astroglial sphingolipid metabolism as a pathway of interest in relation to the FFA-induced pathophysiological changes observed in neurons. Chapter 5 further establishes the causal role of astroglial ceramide in the FFA-induced, AD-associated pathophysiological abnormalities in neurons. Chapter 6 presents the conclusions based on the present study and future research directions.

## **CHAPTER 2. SATURATED FATTY ACID-INDUCED HYPERPHOSPHORYLATION OF TAU IN PRIMARY RAT CORTICAL NEURONS**

### **2.1 INTRODUCTION**

Neurofibrillary tangles (NFTs) are one of the classical neuropathological hallmarks of AD brain <sup>3</sup>. NFTs have been suggested to play a central role in AD pathogenesis since they have been shown to correlate with the severity of dementia. According to a proposed model of pathological evolution of AD, NFTs appear first in the entorhinal cortex during the preclinical phase, spreading to the hippocampus in the middle phase and, eventually, to the neocortex during the late stage of AD <sup>136</sup>. This strong correlation between the number of NFTs and the disease severity was further supported by many other studies <sup>137, 138</sup>. NFTs are composed of paired helical filaments of tau protein, which is hyperphosphorylated in AD <sup>139</sup>. Physiologically, tau is one of the major microtubule-associated proteins that stabilize the microtubules, which play important structural and functional roles in the neurons (**Figure 2.1A**). Tau is involved in signal transduction <sup>140, 141</sup>, anchoring various protein kinases and phosphatases <sup>142, 143</sup> and interacting with the actin cytoskeleton <sup>144</sup>. Six isoforms of tau exist in the central nervous system, which are derived from a single gene and vary between having 3 or 4 microtubule-binding repeat domains and in the number and size of N-terminal inserts <sup>145</sup>. Interactions between tau and microtubules are regulated by the length and more importantly, phosphorylation of the microtubule-binding repeat domains <sup>146</sup>. Tau has about 30 possible phosphorylation sites <sup>147</sup> and in its phosphorylated form cannot stabilize microtubules <sup>148</sup>. In this context, tau is phosphorylated to a degree of ~8 Pi/mol in AD as compared to ~2 Pi/mol for



normal tau and this hyperphosphorylation of tau in AD leads to the disruption of the cytoskeleton of neurons, which in turn leads to their degeneration, thereby playing an important role in AD pathology (**Figure 2.1B**)<sup>3</sup>.

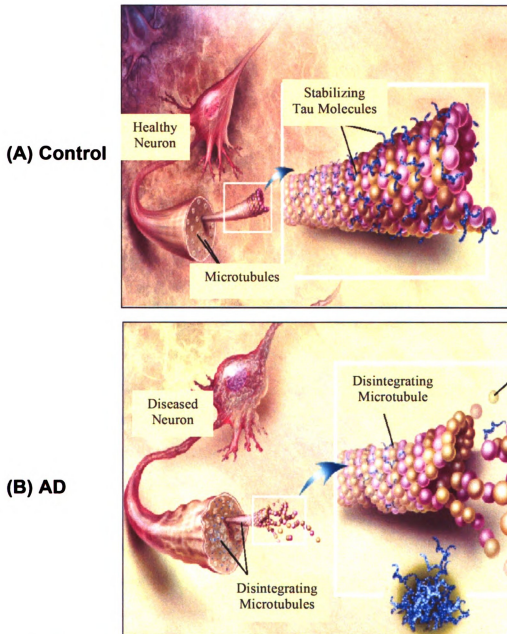


**Figure 2.1. The physiology and pathology of tau.** (A) In healthy neurons, tau stabilizes microtubules. (B) In AD, tau hyperphosphorylates and detaches from microtubules leading to tangle formation (figure taken from [www.alz.org](http://www.alz.org)).

The hyperphosphorylation of tau has been proposed to be critical in promoting aggregation of tau in NFTs <sup>149</sup>. The hyperphosphorylation of tau has been shown to precede the formation of NFTs in degenerating neurons <sup>150, 151</sup>. The importance of hyperphosphorylation of tau in its aggregation is further emphasized by additional studies that showed that the aggregation of tau depends on the degree of its phosphorylation and *in vitro* dephosphorylation of phosphorylated-tau from AD brain prevents its aggregation <sup>152</sup>. Furthermore, in human neuroblastoma cells phosphorylated but not the unphosphorylated tau has been shown to form tau filaments <sup>153</sup>.

The hyperphosphorylation of tau has been suggested to be due to the imbalance between the activities of protein kinases and phosphatases although the actual mechanism is still not well understood. The kinases involved in tau phosphorylation are divided into two groups, proline-directed protein kinases (PDPKs) and non-PDPKs <sup>154</sup>. The PDPKs include glycogen synthase kinase 3 (GSK-3), cycline-dependent kinase 5 (cdk5) and mitogen activated protein kinases (MAPKs). The non-PDPKs include protein kinase C (PKC), protein kinase A (PKA) and Ca<sup>2+</sup>/calmodulin-dependent kinase II (CaMKII). Different kinases may phosphorylate tau at different amino acid residues with some overlapping of sites. The phosphatases involved in dephosphorylation of tau are divided into two major groups, S or T site protein phosphatases and protein tyrosine phosphatases, of which PP-1, PP-2A and PP-2B dephosphorylate tau with a certain degree of overlap in sites <sup>155-157</sup>. AD brain has been characterized by decreased activity of phosphatases <sup>158</sup> and increased activity of various kinases resulting in hyperphosphorylation of tau <sup>148, 159-161</sup>. Increased activity of these tau phosphorylating

kinases in AD has been suggested to be a direct result of increased oxidative stress <sup>162</sup>. Increased oxidative stress, manifested by increased lipid peroxidation and protein oxidation <sup>163, 164</sup> is one of the major and earliest characteristics of AD brain <sup>73, 165</sup>. Lipid peroxidation is an important aspect of AD brain and has been shown to be elevated in the regions of brain affected in AD <sup>166, 167</sup>. There is a strong correlation between thiobarbituric acid reactive substances (TBARS), an indicator of lipid peroxidation, and the presence of NFTs in AD brain <sup>166</sup>. Similarly, the levels of 4-hydroxynonenal (4-HNE) and acrolein have been shown to be elevated in AD brain <sup>168, 169</sup>. Furthermore, protein oxidation is an inevitable aspect of aging and age-related neurodegenerative diseases <sup>76, 170</sup>. Protein oxidation is significantly increased in the cortex and hippocampus of AD brain as compared to age-matched healthy controls <sup>171, 172</sup>.

In addition to increasing the activity of various stress-dependent kinases, which are involved in hyperphosphorylating tau thus leading to its aggregation, oxidative stress in itself has been shown to be involved in forming tau dimers, which are the building blocks of paired helical filaments (PHFs) in NFTs. The aggregation of tau is increased when tau molecules crosslink into dimers by an oxidized disulfide bond at Cys322 <sup>173, 174</sup>. Furthermore, 4-HNE, which has been shown to co-localize with NFTs in AD brain <sup>165, 169, 175</sup>, can act as an adduct to phosphorylated tau and enhance tau filament formation <sup>153</sup>. In summary, oxidative stress and hyperphosphorylation are important pathological events in the formation of tau aggregates, which are one of the characteristics signatures of AD brain. Therefore, the aim of the current study was to investigate possible involvement of saturated fatty acids in causing oxidative stress and hyperphosphorylation of tau.

## **2.2 MATERIALS AND METHODS**

### **2.2.1 Isolation and Culture of Primary Rat Cortical Neurons and Astroglia**

Primary cortical neurons were isolated from one-day-old Sprague-Dawley rat pups and cultured according to the published methods as described in Chandler et al.<sup>176</sup>. The cells were plated on poly-D-Lysine coated, 6-well plates at the concentration of  $2 \times 10^6$  cells per well in fresh cortical medium [Dulbecco's Modified Eagle's Medium (DMEM and all other media are from Invitrogen, CA) supplemented with 10% horse serum (Sigma, MO), 25 mM glucose, 10 mM HEPES (Sigma), 2 mM glutamine (BioSource International, CA), 100 IU/ml penicillin, and 0.1 mg/ml streptomycin]. Three days after incubation (37°C, 5% CO<sub>2</sub>), the medium was subsequently replaced with 2 ml of cortical medium supplemented with 5  $\mu$ M cytosine- $\beta$ -arabinofuranoside (Arac, from Calbiochem, CA). After 2 days, the neuronal culture was switched back to cortical medium without Arac. The experiments were performed on 6-7 day old culture. To obtain primary cultures of astroglial cells, the cortical cells from one-day-old Sprague-Dawley rat pups were cultured in DMEM/Ham's F12 medium (1:1), 10% fetal bovine serum (Biomed, CA), 100 IU/ml penicillin, and 0.1 mg/ml streptomycin<sup>177</sup>. The cells were plated on poly-D-Lysine coated, 6-well plates at the concentration of  $2 \times 10^6$  cells per well. Cells were grown for 8-10 days (37°C, 5% CO<sub>2</sub>) and culture medium was changed every 2 days. 24 hours prior to treatment with fatty acids, the medium was changed to neuronal cell culture medium.

### **2.2.2 Lactate Dehydrogenase (LDH) Assay**

The secreted and intracellular levels of LDH were measured to determine the level of cell toxicity in astroglial cells by using cytotoxicity detection kit (Roche, IN, USA). The

cytotoxicity was determined as the fraction of LDH released into the medium, normalized to the total LDH (released + intracellular), as shown in the equation below-.

$$\%LDH \text{ release} = \frac{LDH \text{ (medium)}}{LDH \text{ (medium+intracellular)}} \times 100$$

### 2.3 Western Blot Analysis

For western blot analysis, cells were washed three times with ice-cold TBS (25 mM Tris, pH 8.0, 140 mM NaCl, and 5 mM KCl) and lysed for 20 minutes by scraping into ice-cold radioimmunoprecipitation assay (RIPA) buffer [1% (v/v) Triton, 0.1% (w/v) SDS, 0.5% (w/v) deoxycholate, 20 mM Tris, pH 7.4, 150 mM NaCl, 100 mM NaF, 1 mM Na<sub>3</sub>VO<sub>4</sub>, 1 mM EDTA, 1 mM EGTA, and 1 mM PMSF, all chemicals from Sigma] <sup>178</sup>. The total cell lysate was obtained by centrifugation at 12,000 rpm for 15 minutes at 4 °C. The total protein concentration was measured by BCA protein assay kit from Pierce (Rockford, IL). Equal amounts of total protein from each condition were run at 200 V on 10% SDS-PAGE gels (BioRad, CA) for phosphorylated tau and actin. The separated proteins were transferred to nitrocellulose membranes for 1 hour at 100 V and incubated at 4 °C overnight with the appropriate primary antibodies [1:200 PHF-1 (from Dr. P. Davies, Albert Einstein, NY), 1:200 AT8 (Pierce Biotechnology, IL), 1:2000 actin (Sigma, MO)]. Blots were washed three times in PBS-Tween (PBS-T) and incubated with appropriate HRP-linked secondary antibodies (Pierce Biotechnology, IL) diluted in PBS-T for 1 hr. After an additional three washes in PBS-T, blots were developed with the Pierce SuperSignal West Femto Maximum Sensitivity Substrate (Pierce Biotechnology) and imaged with the BioRad ChemiDoc. Quantity One software from Bio-Rad was used to quantify the signal intensity of the protein bands.

#### **2.2.4 Immunofluorescence Analysis of Neurons and Astroglia**

To perform confocal immunofluorescence microscopy study, neurons and astroglia cultures were fixed for 20 minutes in 4% paraformaldehyde and permeabilized with 0.1% Triton X-100 and 5% goat serum (Invitrogen) in PBS. Cells were then labeled overnight at 4 °C with appropriate primary antibodies [1:50 MAP-2 (Santa Cruz Biotechnology, CA) for neurons, 1:1000 GFAP (Dako, CA) for astroglia and 1:200 AT8 for hyperphosphorylated tau] in 5% goat serum in PBS. After three PBS washes, primary antibodies were detected with rhodamine conjugated (Chemicon, CA) or Alexa Fluor 594 conjugated (Molecular Probes, OR) secondary antibodies. The cells were visualized with the confocal microscope Zeiss LSM 5 Pascal (Carl Zeiss, Jena, Germany) using a 40× (for MAP-2 and GFAP) or 63× (for AT8) oil-immersion objective lens.

#### **2.2.5 Immunostaining of Reactive Oxygen Species (ROS)**

Intracellular reactive oxygen species (ROS) were detected by staining with the oxidant-sensitive dye 5-(6)-chloromethyl-2',7'-dichlorodihydrofluorescein diacetate (CM-H<sub>2</sub>DCFDA, from Molecular Probes, OR). H<sub>2</sub>DCFDA is cleaved of its ester groups by intracellular esterases and converted into membrane impermeable, nonfluorescent derivative H<sub>2</sub>DCF. Oxidation of H<sub>2</sub>DCF by ROS results in highly fluorescent 2,7-dichlorofluorescein (DCF) <sup>179</sup>. The cells were incubated for 30 minutes at 37 °C with 2 μM CM-H<sub>2</sub>DCFDA in Hanks' Balanced Salt Solution without phenol red (Invitrogen). The cells were then washed three times with PBS and analyzed with confocal microscopy. A 63X oil-immersion objective lens was used for data acquisition.

### 2.2.6 Data Analyses

Data are shown as means  $\pm$  S.D. for indicated number of experiments. Student's t-test and one-way ANOVA with Tukey's *post hoc* method were used to evaluate statistical significances between different treatment groups. Statistical significance was set at  $p < 0.05$ .

## 2.3 RESULTS AND DISCUSSION

### 2.3.1 Direct Treatment of Neurons with Saturated Fatty Acids

Although tau is present in astroglia and oligodendrocytes in the brain and in some peripheral tissues, it is mainly synthesized by neurons<sup>180, 181</sup>. Tau is mainly located in neuronal axons and hyperphosphorylated tau is deposited in dystrophic neurites and neuronal bodies in the form of NFTs. Therefore, to examine the possible involvement of saturated FFAs in the hyperphosphorylation of tau, primary rat cortical neurons were left untreated or treated with 0.2 mM of palmitic acid (PA) or stearic acid (SA) for 24 hours. After 24 hours, the cells were lysed and western blot analysis was performed to determine the cellular levels of hyperphosphorylated tau. There was no change in the levels of phosphorylated tau in rat cortical neurons treated directly with palmitic or stearic acid, as compared to controls (**Figure 2.2**). Furthermore, the morphology of the neurons was not affected by the FFA treatment, as shown by MAP-2 immunostaining (**Figure 2.3A**). The observed lack of FFA effect on neurons may be attributed to the low capacity of primary neurons to take up and metabolize saturated fatty acids<sup>182</sup>.

Previously, primary rat cortical neurons have been shown to possess a very low capacity to take up PA and incorporate it into glycerolipids and sphingolipids <sup>182</sup>.

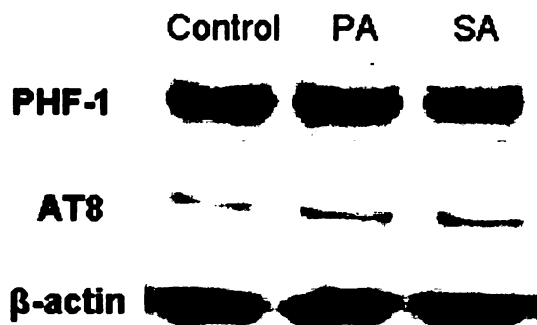


**Figure 2.2. Direct treatment of neurons with saturated FFAs.** Primary rat cortical neurons were treated for 24 hours with 0.2 mM of palmitic acid (PA) or stearic acid (SA) or with 5% bovine serum albumin (BSA), vehicle for FFAs (control). Detergent cell lysates from fatty acid-treated and control cells were immunoblotted with PHF-1 and AT8 antibodies, which recognize phosphorylated tau.  $\beta$ -actin is shown as a marker for protein loading.

### 2.3.2 Involvement of Saturated FFAs in Tau Hyperphosphorylation Through Astroglial Mediation

Compared to primary neurons, primary astroglia possess a significantly higher capacity to utilize saturated fatty acids <sup>182</sup>. The uptake and incorporation of PA into glycerolipids and sphingolipids have been shown to be more than 3 times higher in primary rat cortical astroglia as compared to primary rat cortical neurons <sup>182</sup>. Therefore, we treated cortical astroglia with 0.2 mM of PA or SA for 12 hours and transferred the conditioned media to treat the cortical neurons for 24 hours. The morphologies of the fatty acid-treated astroglia and neurons are shown using GFAP and MAP-2 immunostaining, respectively (**Figures 2.3B and C**). No significant change in the cell morphologies was observed, except, the characteristic dotted MAP-2 labeling of the neurites was less significant in the



neurons treated with conditioned media from FFA-treated astroglia as compared to controls.

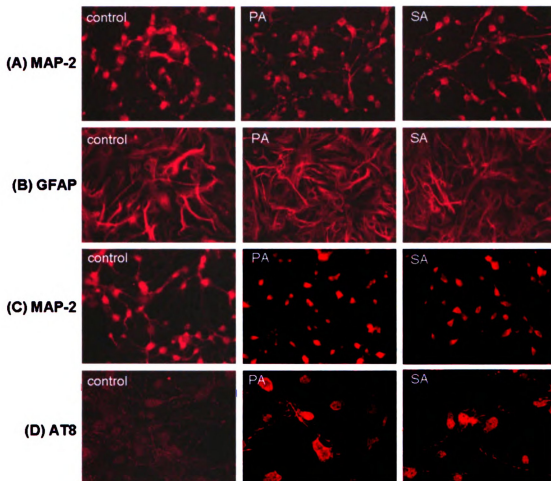


**Figure 2.3. MAP-2, GFAP and AT8 immunostaining.** (A) Neurons treated directly with FFAs for 24 hours. (B) Astrocytes treated for 12 hours with 0.2 mM of either palmitic acid (PA) or stearic acid (SA) or 5% BSA (control). (C) Neurons treated for 24 hours with conditioned media from fatty acid-treated or control astrocytes. (D) Immunofluorescence labeling of phosphorylated tau with AT8 antibody in neurons treated with conditioned media from fatty acid-treated or untreated astrocytes (control). Images were obtained with confocal fluorescence microscopy. (Objective lens magnification- 40X for MAP-2 and GFAP, 63X for AT8).

Furthermore, treatment of astroglia with 0.2mM of PA did not affect the astroglial cell viability compared to controls as measured by % LDH release (**Figure 2.4**). 300  $\mu$ M  $H_2O_2$  treatment was used as a positive control and significantly increased LDH release

from astroglia (Figure 2.4), which is in accordance with a previous study in the literature

183

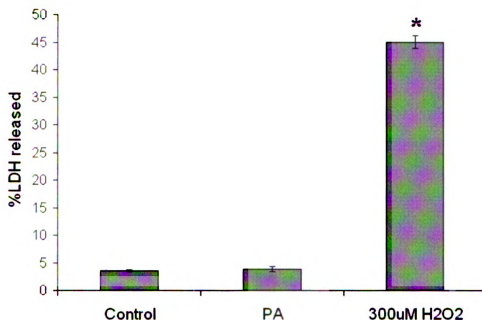


**Figure 2.4. Measurement of LDH release from astroglia treated with PA.** 24hr treatment with 0.2mM PA failed to liberate LDH from astroglia as compared to controls. In contrast, 1hr treatment of astroglia with 300  $\mu$ M H<sub>2</sub>O<sub>2</sub> (positive control) induced significant LDH liberation after 24h as compared to both control and PA-treated cells. Data are taken from 3 different experiments and are expressed as mean  $\pm$  S.D. One-way ANOVA with Tukey's *post hoc* method was used for analyzing the differences between treatment groups. \*,  $p < 0.05$  compared with control.

The conditioned media from FFA-treated astroglia caused significant hyperphosphorylation of tau in cortical neurons, as observed by immunostaining with AT8 (Figure 2.3D) and immunoblotting with AT8 and PHF-1 antibodies (Figure 2.5). AT8 and PHF-1 antibodies recognize tau protein hyperphosphorylated at AD-specific phospho-epitopes; AT8 recognizes tau phosphorylated at Ser202 and Thr205<sup>184</sup>, while PHF-1 is specific for tau phosphorylated at Ser396 and Ser404<sup>185</sup>. Ser202, Ser396 and

Ser404 are three of the nine abnormal phosphorylation sites of the hyperphosphorylated tau associated with NFTs in AD<sup>186</sup>.

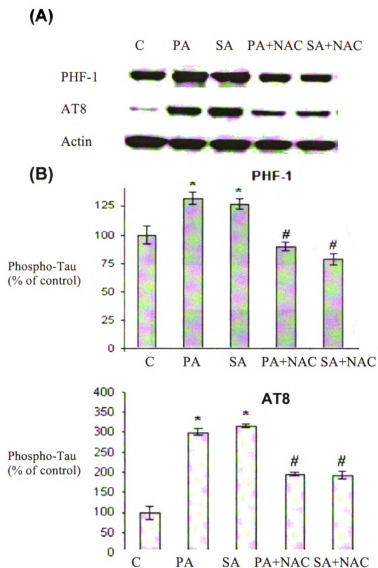
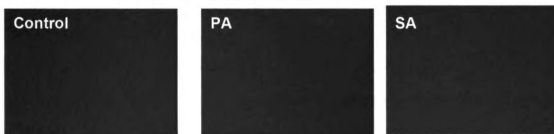


**Figure 2.5. Astroglia-mediated, fatty acid-induced hyperphosphorylation of tau in neurons.** (A) Western blot analysis of hyperphosphorylated tau was performed using phospho-specific antibodies PHF-1 and AT8. (B) Histograms corresponding to PHF-1 and AT8 blots represent quantitative determinations of intensities of the relevant bands. Data represent mean  $\pm$  S.D. of 3 independent experiments. One-way ANOVA with Tukey's *post hoc* method was used for analyzing the differences between treatment groups. \*,  $p < 0.05$  compared with control; #,  $p < 0.05$  compared with fatty acid treatment.

### 2.3.3 Involvement of Oxidative Stress in FFA-Astroglia-Induced Tau Hyperphosphorylation in Neurons

As shown in **Figure 2.6A**, treatment of astroglia with 0.2mM of PA or SA did not cause any ROS production in cortical astroglia. On the other hand, we found that intracellular levels of ROS were elevated in the neurons treated with conditioned media from FFA-treated astroglia as compared to controls (**Figure 2.6B**).

**(A)**



**(B)**

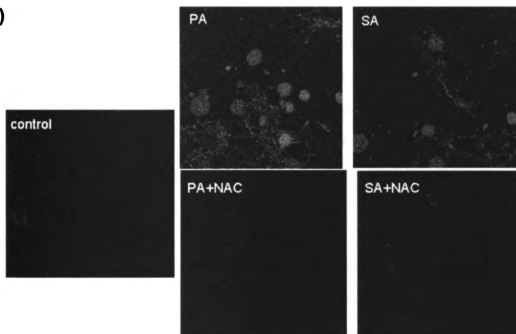


**Figure 2.6. Intracellular accumulation of ROS in neurons.** (A) Astroglia and (B) neurons were stained with CM-H2DCFDA for intracellular ROS detection and examined with confocal fluorescence microscopy. (Objective lens magnification, 63X).

Previously, various *in vitro* and *in vivo* studies have implicated increased oxidative stress in the hyperphosphorylation of tau<sup>71, 72</sup>. 4-HNE and acrolein, the lipid peroxidation products found elevated in AD brain<sup>73</sup>, have been shown to induce hyperphosphorylation of tau in neurons<sup>74, 75</sup>. Furthermore, although acute administration of a high concentration of H<sub>2</sub>O<sub>2</sub> (1mM for 1 hr) decreases tau phosphorylation<sup>187</sup>; chronic exposure of a low concentration of H<sub>2</sub>O<sub>2</sub> (10  $\mu$ M for 24, 48 or 72 hrs), more relevant to AD, increases tau phosphorylation in primary rat cortical neurons (Mark Smith and Xiongwei Zhu, personal communication). Therefore, we treated neurons with 10mM N-acetyl cysteine (NAC), an anti-oxidant. The co-treatment of neurons with NAC inhibited the observed FFA-astroglia-induced increase in ROS levels (**Figure 2.6B**) as well as tau hyperphosphorylation in neurons (**Figure 2.5**).

## 2.4 CONCLUSIONS

In conclusion, saturated FFAs had no direct effect on the neuronal morphology and the level of phosphorylated tau in neurons. In addition, saturated FFAs had no effect on astroglial morphology and viability. However, the conditioned media from FFA-treated astroglia affected the classical dotted MAP-2 labeling of the neuronal axons and also increased the levels of phosphorylated tau in neurons. Furthermore, there was a significant increase in the ROS production in neurons treated with conditioned media from FFA-treated astroglia, without any increase in astroglial ROS levels. The elevated levels of ROS in the neurons were found to be involved in the observed, FFA-astroglia-induced hyperphosphorylation of tau in the neurons. Thus, the present results establish a central role of saturated FFAs in causing hyperphosphorylation of tau in neurons through astroglia-mediated oxidative stress.

## **CHAPTER 3. SATURATED FATTY ACID-INDUCED AMYLOIDOGENIC PROCESSING OF APP IN PRIMARY RAT CORTICAL NEURONS**

### **3.1 INTRODUCTION**

The “amyloid cascade hypothesis”, which suggests the accumulation of aggregated amyloid beta ( $A\beta$ ) in the brain as a main trigger for AD, has been extensively studied since the first characterization of  $A\beta$  deposits in 1984<sup>188</sup>. According to this hypothesis, a chronic imbalance between the production and clearance of  $A\beta$  results in the formation of  $A\beta$  plaques, which leads to a multi-step cascade including reactive gliosis, inflammatory changes, synaptic change and transmitter loss<sup>26, 189-192</sup>. In AD brain, two major types of  $A\beta$  plaques are observed, diffuse plaques and neuritic plaques. Diffuse plaques mainly consist of nonfibrillar  $A\beta$ , while neuritic plaques are more developed consisting of dense  $A\beta$  fibrils together with degenerating dendrites and axons, serum amyloid P,  $\alpha$ 1-antichymotrypsin,  $\alpha$ 1-antitrypsin, sulphated glycosaminoglycans, apolipoproteins E and D, and the neurotrophic factor midkine<sup>193-195</sup>. Recently, the soluble  $A\beta$  intermediates have been shown to play a more important role in AD pathogenesis as compared to the mature neuritic plaques<sup>190, 196, 197</sup>. These soluble  $A\beta$  oligomers,  $A\beta$  protofibrils and  $A\beta$ -derived diffusible ligands (ADDLs) cause synaptic dysfunction, which have been suggested to be an early event in AD-associated memory loss<sup>198</sup>.

$A\beta$  is generated from the proteolytic processing of amyloid precursor protein (APP). APP is an integral type I membrane glycoprotein of 110-120kDa in size and contains a large amino terminal extracellular domain and a small COOH-terminal intracellular domain<sup>199</sup>.

<sup>200</sup>. APP has three major isoforms containing 695, 751 or 770 amino acids. The APP<sub>695</sub> isoform is mostly present in neurons, while the others are present in peripheral and glial cells <sup>201</sup>. APP<sub>751</sub> and APP<sub>770</sub> have serine protease inhibitor domain called Kunitz protease inhibitor domain, while APP<sub>695</sub> lacks this domain. The physiological functions of APP include neuronal survival, cell adhesion, axonal adhesion, neuritic outgrowth, synaptic plasticity and signaling <sup>3, 202</sup>.

The proteolytic processing of APP takes place by sequential cleavage by proteases named  $\alpha$ -,  $\beta$ - and  $\gamma$ -secretase (**Figure 3.1A**). The  $\alpha$ -secretase is a member of the ADAM (a disintegrin and metalloprotease) family such as ADAM17 or TACE (tumor necrosis factor- $\alpha$  converting enzyme), ADAM 9, ADAM10, MDC9 and an aspartyl protease BACE2 <sup>203</sup>. The  $\alpha$ -secretase cleavage of APP may occur at the cell surface, within calveolae or in the trans-Golgi compartment <sup>180, 204</sup>. The  $\alpha$ -secretase has been shown mainly to be active in non-raft regions of the membrane <sup>205, 206</sup>. The  $\alpha$ -secretase cleaves APP within A $\beta$  domain (shown as red) between residues Lys16 and Leu17, thus avoiding the generation of intact A $\beta$  peptides. It leads to the formation of a soluble domain (sAPP $\alpha$ ), which is released into extracellular space and a 10-kDa C-terminal fragment (C83), which remains within the cellular membrane <sup>207</sup>.

The  $\beta$ -secretase, also called BACE ( $\beta$ -site of APP cleaving enzyme), Asp-2 or memapsin-2 is a trans-membrane protein and an aspartic-acid protease <sup>208-210</sup>. BACE contains aspartate residues in its extracellular protein domain which are involved in BACE activity <sup>208</sup>.

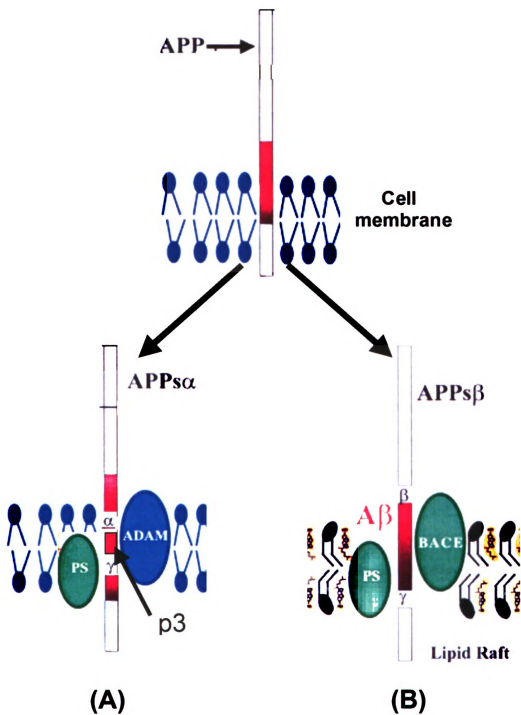


**Figure 3.1. Processing of amyloid precursor protein (APP).** (A) The non-amyloidogenic pathway catalyzed by  $\alpha$ - and  $\gamma$ -secretase. (B) The amyloidogenic pathway catalyzed by  $\beta$ - and  $\gamma$ -secretase.



BACE1 is a major  $\beta$ -secretase involved in the amyloidogenic processing of APP in neurons <sup>211</sup>. Cleavage of APP by  $\beta$ -secretase may occur in endosomes and trans-Golgi compartments <sup>212-214</sup>, which provide an acidic environment that has been shown to be critical for maximal activity of BACE <sup>215</sup>. The  $\beta$ -secretase has been shown mainly to be active in lipid raft regions of the membrane <sup>206, 216, 217</sup>. The  $\beta$ -secretase cleaves APP at the Asp+1 residue of the A $\beta$  region and leads to the generation of a secreted soluble fragment (sAPP $\beta$ ) and a membrane-bound C-terminal fragment (C99).

Both the  $\alpha$ -secretase product of APP (C83) and the  $\beta$ -secretase product of APP (C99) act as immediate substrates for  $\gamma$ -secretase. The  $\gamma$ -secretase is a membrane-bound complex of at least four enzymes including components such as Presenilin 1 and 2 (PS1 and PS2), Nicastrin (Nct), anterior pharynx-defective phenotype (APH-1) and Presenilin enhancer (PEN-2) <sup>218</sup>. The PS1 C-terminal tail (PS1-CTF) is critical for  $\gamma$ -secretase activity <sup>219, 220</sup>. The  $\gamma$ -secretase activity resides in various cellular compartments such as the ER, late-Golgi/trans-Golgi, endosomes and the plasma membrane <sup>221-224</sup>. Similar to the  $\beta$ -secretase, the  $\gamma$ -secretase has been associated with lipid raft microdomains of the membrane <sup>225</sup>. The  $\gamma$ -secretase cleavage of C83 is a non-amyloidogenic pathway, which leads to the generation of a short peptide (p3) containing the C-terminal domain of the A $\beta$  peptide. The physiological or pathological significance of p3 remains unclear. On the other hand, the  $\gamma$ -secretase cleavage of C99 is an amyloidogenic pathway, which leads to the generation of a spectrum of A $\beta$  peptides. The A $\beta$  peptides containing 40 or 42 amino acids (A $\beta$ 40/42) are the two most common amyloidogenic A $\beta$  peptides. Both A $\beta$ 40 and A $\beta$ 42 are produced during normal cellular metabolism but the production of A $\beta$ 42 is

considered to be elevated in AD <sup>226, 227</sup>. A $\beta$ 42 is more prone to aggregation as compared to A $\beta$ 40 <sup>228, 229</sup>. A $\beta$ 42 initially forms non-filamentous, diffuse plaques onto which A $\beta$ 40 starts to aggregate, which leads to the mature, neuritic plaques.

The importance of amyloidogenic processing of APP in AD is emphasized by the involvement of mutations in the APP, presenilin-1 (PS1) and presenilin-2 (PS2) genes, localized on chromosome 21, 14 and 1, respectively, in FAD <sup>230-236</sup>. These APP and PS mutations alter APP processing leading to the pathological increase in the production of total A $\beta$  or A $\beta$ 42 which is highly fibrillogenic <sup>21-24, 189</sup>. In APP mutations linked to FAD, clinical and pathological symptoms are identical to those of the late-onset sporadic AD, which consists of more than 95% of total AD cases. This strongly suggests that amyloidogenic processing of APP plays a central role not only in FAD but also in sporadic AD. Furthermore, ApoE4, a genetic risk factor for AD, has been shown to play an important role in the production and clearance of A $\beta$  <sup>237</sup>. This further suggests that amyloidogenic processing of APP is a central pathological event in AD pathology. In this context, the aim of the current study was to investigate possible involvement of saturated fatty acids in causing amyloidogenic processing of APP, potentially by affecting the levels and/or activities of  $\beta$ - and  $\gamma$ -secretases.

## **3.2 MATERIALS AND METHODS**

### **3.2.1 Isolation and Culture of Primary Rat Cortical Neurons and Astroglia**

Primary neurons and astroglia were isolated from the cortex of one-day-old Sprague-Dawley rat pups and cultured according to the methods as described in chapter 2. The cells were plated on poly-L-Lysine coated, 6-well plates at the concentration of  $2 \times 10^6$  cells per well in fresh cortical medium [Dulbecco's Modified Eagle's Medium (DMEM and all other media are from Invitrogen, CA) supplemented with 10% horse serum (Sigma, MO), 25 mM glucose, 10 mM HEPES (Sigma), 2 mM glutamine (BioSource International, CA), 100 IU/ml penicillin, and 0.1 mg/ml streptomycin]<sup>176</sup>. To obtain pure neuronal cell cultures, after 3 days of incubation (37°C, 5% CO<sub>2</sub>) the medium was replaced with the cortical medium supplemented with 5 µM cytosine-β-arabinofuranoside (Arac, from Calbiochem, CA). After 2 days of Arac treatment, the neuronal culture was switched back to cortical medium without Arac. The neuronal cell culture of more than 95% was obtained by this procedure. The experiments were performed on 6-7 day old neuronal culture. To obtain primary cultures of astroglial cells, the cortical cells from one-day-old Sprague-Dawley rat pups were cultured in DMEM/Ham's F12 medium (1:1), 10% fetal bovine serum (Biomed, CA), 100 IU/ml penicillin, and 0.1 mg/ml streptomycin<sup>177</sup>. Cells were grown for 8-10 days (37°C, 5% CO<sub>2</sub>) and culture medium was changed every 2 days. The astroglial cell culture of more than 95% was obtained by this procedure. 24 hours prior to treatment with fatty acids, the medium was changed to neuronal cell culture medium.

### **3.2.2 Western Blot Analysis**

For western blot analysis, cells were washed three times with ice-cold TBS (25 mM Tris, pH 8.0, 140 mM NaCl, and 5 mM KCl) and lysed for 20 minutes by scraping into scraping into ice-cold radioimmunoprecipitation assay (RIPA) buffer [1% (v/v) Nonidet P-40, 0.1% (w/v) SDS, 0.5% (w/v) deoxycholate, 50 mM Tris, pH 7.2, 150 mM NaCl, 1 mM Na<sub>3</sub>VO<sub>4</sub> and 1 mM PMSF, all chemicals from Sigma]<sup>238</sup>. The total cell lysate was obtained by centrifugation at 12,000 rpm for 15 minutes at 4 °C. The total protein concentration was measured by BCA protein assay kit from Pierce (Rockford, IL). Equal amounts of total protein from each condition were run at 200 V on 10% Tris-HCl gels (for BACE1, actin), 12% Tris-HCl gels (for PS1) and 10-20% Tris-Tricine gels (for APP, C99). The separated proteins were transferred to nitrocellulose membranes for 1 hour at 100 V and incubated at 4 °C overnight with the appropriate primary antibodies [1:1000 BACE1 (chemicon, CA), 1:1000 PS1 (Calbiochem, CA), 1:2000 actin (Sigma, MO), 1:1000 APP/C99 (QED Bioscience Inc, CA)]. Blots were washed three times in PBS-Tween (PBS-T) and incubated with appropriate HRP-linked secondary antibodies (Pierce Biotechnology, IL) diluted in PBS-T for 1 hr. After an additional three washes in PBS-T, blots were developed with the Pierce SuperSignal West Femto Maximum Sensitivity Substrate (Pierce Biotechnology) and imaged with the BioRad ChemiDoc. Quantity One software from Bio-Rad was used to quantify the signal intensity of the protein bands.

### **3.2.3 Immunofluorescence Analysis of BACE1 in Neurons**

To perform confocal immunofluorescence microscopy study, neuronal cultures were fixed for 20 min in 4% paraformaldehyde and permeabilized with 0.1% Triton X-100 and

5% goat serum (Invitrogen) in PBS. Cells were then labeled overnight at 4 °C with the primary antibody [1:100, BACE1] in 5% goat serum in PBS. After three PBS washes, primary antibody was detected with Alexa Fluor 594 conjugated (Molecular Probes, OR) secondary antibody. The cells were visualized with confocal microscope Zeiss LSM 5 Pascal (Carl Zeiss, Jena, Germany) using a 40× oil-immersion objective lens.

### **3.2.4 Data Analyses**

Data are shown as means  $\pm$  S.D. for indicated number of experiments. Student's t-test and one-way ANOVA with Tukey's *post hoc* method were used to evaluate statistical significances between different treatment groups. Statistical significance was set at  $p < 0.05$ .

## **3.3 RESULTS**

### **3.3.1 Direct Treatment of Neurons with Saturated Fatty acid (Palmitic Acid)**

The BACE1 enzyme involved in the first step of amyloidogenic processing of APP has been localized in the brain, mainly in the neurons, thus suggesting that neurons are the prominent source of A $\beta$  peptides in the brain<sup>239</sup>. The BACE1 levels have been shown to be significantly elevated in AD brain as compared to healthy controls<sup>240</sup>. Therefore, to examine the possible effect of saturated FFAs on the BACE1 levels, primary rat cortical neurons were left untreated or treated with 0.2mM of palmitic acid (PA) for 24 hours. In this and all subsequent studies, we treated cells with only PA, since both PA and SA had similar effects as demonstrated in chapter 2. Also, in typical high-fat American diets,

more than 60% of the saturated fat is PA, while SA contributes only 25% of the dietary energy derived from saturated fats <sup>241</sup>. After 24 hrs of direct treatment with PA, the cells were lysed and western blot analysis was performed to determine the cellular levels of BACE1. There was no change in the BACE1 levels in primary rat cortical neurons treated directly with PA as compared to controls (**Figure 3.2**). This lack of FFA effect on neurons may be attributed to the low capacity of primary neurons to take up and metabolize saturated fatty acids <sup>182</sup>. This effect is similar to that shown in Chapter 2, where saturated FFAs had no direct effect on neurons; there was no change in the levels of phosphorylated tau in rat cortical neurons treated directly with both PA and SA.

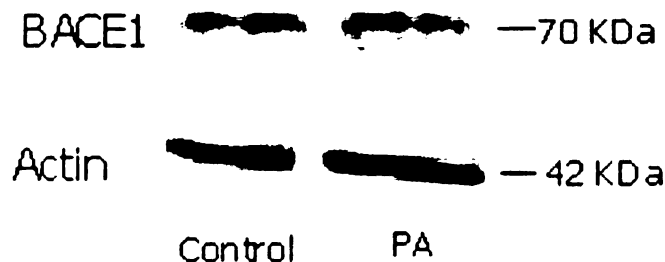


**Figure 3.2. Direct treatment of neurons with palmitic acid.** Primary rat cortical neurons were treated for 24 hours with 0.2mM of palmitic acid (PA) or with 4% bovine serum albumin (BSA), vehicle for PA (control). Detergent cell lysates from PA-treated and control cells were immunoblotted with BACE1 antibody.  $\beta$ -actin is shown as a marker for protein loading. The blots are representative of 3 independent experiments.

### 3.3.2 Involvement of Saturated FFAs in BACE1 Up-regulation and Amyloidogenic Processing of APP Through Astroglial Mediation

As mentioned earlier in Chapter 2, primary astroglia possess a significantly higher capacity (>3 times) to take up and utilize saturated fatty acids <sup>182</sup> and the conditioned media from FFA-treated astroglia significantly increased phosphorylation of tau in

neurons. Therefore, in this study, we first cultured the rat cortical astroglia with 0.2mM PA for 12 or 24 hrs and transferred the conditioned media to treat the cortical neurons for 24 hours. The conditioned media from PA-treated astroglia induced BACE1 upregulation in cortical neurons, as observed by immunofluorescence imaging (**Figure 3.3**) and immunoblotting (**Figure 3.4**).

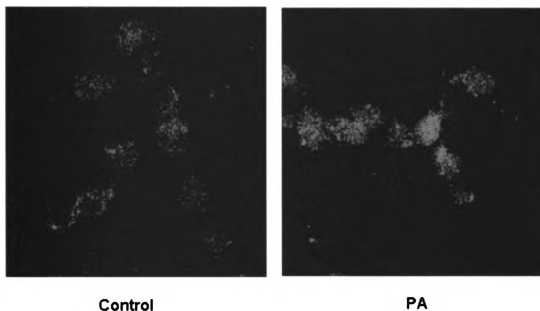


**Figure 3.3. BACE1 immunostaining.** Immunofluorescence labelling of BACE1 in neurons treated for 24 hours with conditioned media from PA-treated (for 24 hours) or untreated astrocytes (control). Images were obtained with confocal fluorescence microscopy (objective lens magnification- 40X).

The PA-induced BACE1 upregulation was observed to be dependent on the length of time that the astroglia were treated with PA, which might be attributed to the time-dependent increase in PA metabolism by the astroglia<sup>182</sup>. BACE1 cleaves APP at the major Asp+1 site and minor Glu+11 site to generate C99 and C89 fragments, respectively<sup>209</sup>. Accordingly, we found increased C99 levels in the PA-astroglia-treated cortical neurons as compared to controls (**Figure 3.6**). C-terminal fragments of APP are found to

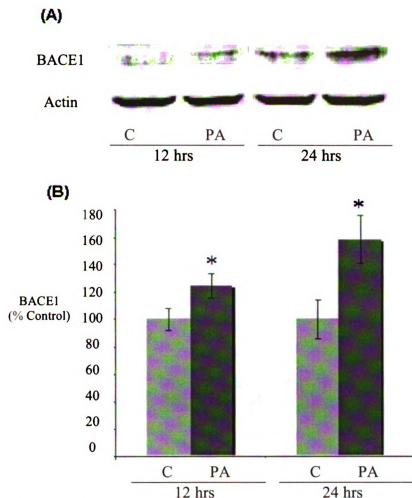


**Figure 3.4. Astroglia-mediated, PA-induced BACE1 upregulation in neurons.** Astrocytes were treated for 12 and 24 hours with 0.2mM of PA or 4% BSA (control), followed by transfer of the astrocytes-conditioned media to neurons (24 hours treatment). (A) Western blot analysis of BACE1 protein levels in neurons.  $\beta$ -actin is shown as a marker for protein loading. (B) Histograms represent quantitative determinations of intensities of the relative bands. Data represent mean  $\pm$  S.D. of three independent experiments. Student's t-test was used for analyzing differences between different treatment groups. \*,  $p < 0.05$  compared with respective control.

be elevated in AD brain and are more toxic to neurons than  $A\beta$ , which is obtained by cleavage of C99 by  $\gamma$ -secretase<sup>242</sup>. The presenilin (PS) complex, including PS, nicastrin, APH-1 and PEN-2, forms a central core of the  $\gamma$ -secretase enzyme and the PS1 C-terminal tail (PS1-CTF) is critical for  $\gamma$ -secretase activity<sup>218</sup>. We found no change in the



levels of PS1-CTF suggesting the  $\gamma$ -secretase activity is unchanged in the PA-astrocytes-treated neurons as compared to controls (**Figure 3.5**). It is noteworthy that a slight increase in BACE1 levels, without any change in  $\gamma$ -secretase activity, has been shown to increase A $\beta$  production significantly <sup>243</sup>. Thus, the increased BACE1 levels in the PA-astrocyte-treated cortical neurons resulting in elevated C99 levels, may be followed by increased A $\beta$  production, despite the lack of change in  $\gamma$ -secretase activity.

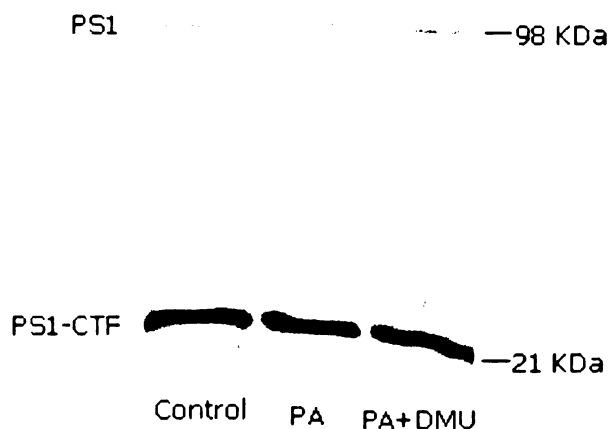
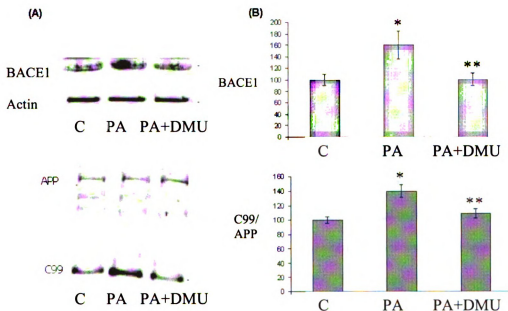


**Figure 3.5. Immunoblot analysis of presenilin-1 (PS1) levels in neurons treated with astrocytes-conditioned media.** Astrocytes were treated for 24 hours with 0.2mM PA or 5% BSA (control), followed by transfer of the astrocytes-conditioned media to neurons (24 hours treatment), with or without 10 mM DMU. Detergent cell lysates from PA-treated and control cells were immunoblotted for PS1 and PS1-CTF levels. The immunoblot is representative of 3 independent experiments.

### 3.3.3 Involvement of Oxidative Stress in FFA-Astroglia-Induced BACE1 Up-regulation and Amyloidogenic processing of APP in Primary Neurons

As shown in Chapter 2, intracellular levels of reactive oxygen species (ROS) were significantly elevated in the neurons cultured with the conditioned media from FFA-treated astroglia as compared to controls. To investigate the possible involvement of

oxidative stress in FFA-induced BACE1 up-regulation and amyloidogenic processing of APP, we treated neurons with 1,3-dimethyl urea (DMU), an antioxidant. The co-treatment of neurons with 10mM DMU inhibited PA-astroglia-induced BACE1 upregulation and increased C99 production in neurons (Figure 3.6).



This suggests a central role of astroglia-mediated oxidative stress in PA-induced upregulation of BACE1 and increased production of C99 in neurons. The role of oxidative stress in causing increased amyloidogenic processing of APP is further supported by various *in vitro* and *in vivo* studies<sup>244</sup>. Oxidative stress has been shown to

increase the expression and activity of BACE1 in NT2 neurons, which was accompanied by a proportional elevation of the c-terminal fragments of APP<sup>65, 66</sup>. H<sub>2</sub>O<sub>2</sub> and UV irradiation have been shown to increase production of A $\beta$  peptides<sup>67-70</sup>, and antioxidants Trolox and dimethyl sulfoxide blocked stress-induced A $\beta$  production<sup>70</sup>. It is noteworthy that A $\beta$  itself can cause oxidative stress and increase its own production<sup>69</sup>, thus sustaining a vicious cycle<sup>68</sup>.

### 3.4 CONCLUSIONS

In conclusion, PA had no direct effect on BACE1 levels and the amyloidogenic processing of APP in neurons. On the other hand, the conditioned media from PA-treated astroglia significantly increased BACE1 levels in neurons, which was dependent on the length of time that the astroglia were treated with PA. This emphasizes a central role of PA metabolism by astroglia in the observed pathological effects in neurons. Furthermore, elevated BACE1 increased amyloidogenic processing of APP, as evident by increased levels of C99 in PA-astroglia-treated neurons as compared to controls. Treatment of neurons with anti-oxidant blocked PA-induced abnormalities in neurons. Thus, the present study illustrates that elevated levels of saturated fatty acids play an important role in the up-regulation of BACE1 and consequent amyloidogenic processing of APP through astroglia-mediated oxidative stress.

## **CHAPTER 4. SATURATED FATTY ACID-INDUCED ABNORMAL METABOLIC CHANGES ASSOCIATED WITH ALZHEIMER'S DISEASE**

### **4.1 INTRODUCTION**

In addition to the two major pathophysiological lesions mentioned earlier (A $\beta$  plaques and NFTs), AD pathology is also characterized by abnormal metabolic changes. Decreased cerebral glucose metabolism is a distinct characteristic of AD <sup>4, 5</sup>. In AD, brain glucose utilization and ATP formation are decreased significantly (approximately 46% and 19% respectively) as compared to healthy controls <sup>245</sup>. *In vivo* imaging of AD brains using positron emission tomography (PET) with 2-[F-18]-fluoro-2-deoxy-D- glucose as a label shows progressive reduction in brain glucose metabolism, which is further correlated with disease severity <sup>246</sup>. In accordance with this, glucose hypometabolism has been suggested to be an important marker for early diagnosis of AD <sup>4</sup>. The metabolic abnormalities observed in AD are widespread in that even the peripheral cells (fibroblasts) from AD patients show decreased metabolic activities <sup>247, 248</sup>. The activities of various metabolic enzymes, mainly pyruvate dehydrogenase,  $\alpha$ -ketoglutarate dehydrogenase, glutamine synthetase, creatine kinase, aconitase and cytochrome oxidase have been shown to be decreased in AD <sup>249-253</sup>. Interestingly, decreased cytochrome oxidase activity in post-mortem brain tissue from AD has been shown to be particularly located in NFT-bearing neurons <sup>254, 255</sup>. The decreased activities of these enzymes may be attributed to the increased oxidative stress in AD, as these enzymes are highly vulnerable to oxidative modification <sup>256</sup>. Also, patients with mild cognitive impairment (MCI), which is characterized by reduced glucose metabolism, often develop AD <sup>257</sup>. Finally, in

patients that are genetically predisposed to AD, cerebral metabolic changes occur well before any pathophysiological signs of the disease manifest <sup>258</sup>.

Glucose is a very important substrate in the efficient physiological functioning of the brain. Glucose, through cellular glycolysis, produces pyruvate that is further oxidized to acetyl-CoA. Acetyl-CoA is utilized by cells to produce cholesterol, acetylcholine and ATP <sup>259</sup>. Thus, decreased glucose metabolism in AD may result in decreased production of these important cellular metabolites. Cholesterol is a primary sterol in cellular membranes and is important in the production of various neurosteroids <sup>260</sup>. Acetyl choline is a very important neurotransmitter involved in various cognitive functions, which have been shown to be decreased in AD <sup>261</sup>. In AD, the activity of choline cetyl transferase has been shown to be decreased in the presynaptic cholinergic neurons which might be attributed to decreased availability of acetylcholine <sup>262</sup>. Muscarinic M1/M3 acetylcholine receptors have been shown to be involved in regulating APP processing and decreased acetylcholine levels may induce increased amyloidogenic processing of APP <sup>263</sup>. In this context, degeneration of cholinergic system in AD has been correlated with disease severity <sup>264</sup>. Finally, ATP is a cellular energy currency required for various cellular functions such as synthesis, folding, transport and degradation of proteins, maintenance of ion homeostasis and synaptic transmission among others <sup>265</sup>. Experimental evidence suggests that decreased glucose metabolism and energy production may lead to increased amyloidogenesis and hyperphosphorylation of tau <sup>266-270</sup>. Taken together, these data suggest that abnormal cerebral metabolism is central to AD pathology and may precede the neuropathological changes associated with the disease <sup>10</sup>.

Traditionally, it is considered that glucose in the brain is mainly metabolized by neurons and it is the substrate of choice for most activity-associated neuronal metabolism (Figure 4.1)<sup>271</sup>. However, recent data suggest that astroglia take-up and metabolize glucose and produce lactate, the latter may be used by neurons as a fuel for metabolic activities and energy production (Figure 4.2)<sup>271-273</sup>. In this context, the aim of the current study was to investigate the possible involvement of saturated fatty acids in causing abnormal glucose metabolism in both neurons and astroglia. Furthermore, we also focus on FFA-induced global metabolic changes in astroglia and their possible involvement in observed FFA-astroglia-induced ROS production in neurons, which in turn is involved in tau hyperphosphorylation and amyloidogenic processing of APP as discussed in chapters 2 and 3.

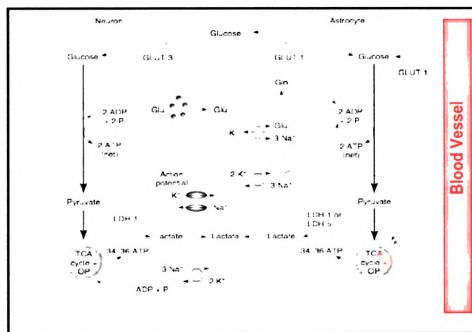
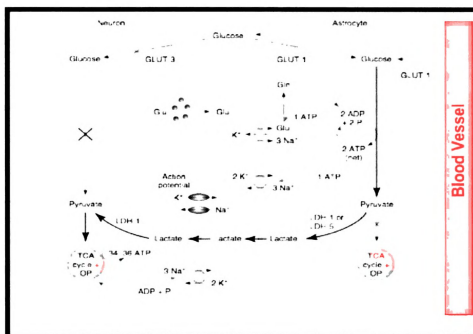


Figure 4.1. Conventional view of cerebral glucose metabolism.



**Figure 4.2. Cerebral glucose metabolism based on the novel astrocyte-neuron lactate shuttle hypothesis.**

## 4.2 MATERIALS AND METHODS

### 4.2.1 Isolation and Culture of Primary Rat Cortical Neurons and Astroglia

Primary neurons and astroglia were isolated from the cortex of one-day-old Sprague-Dawley rat pups and cultured according to the methods as described in chapter 2. The cells were plated on poly-L-Lysine coated, 6-well plates at the concentration of  $2 \times 10^6$  cells per well in fresh cortical medium [Dulbecco's Modified Eagle's Medium (DMEM and all other media are from Invitrogen, CA) supplemented with 10% horse serum (Sigma, MO), 25 mM glucose, 10 mM HEPES (Sigma), 2 mM glutamine (BioSource International, CA), 100 IU/ml penicillin, and 0.1 mg/ml streptomycin]<sup>176</sup>. To obtain

pure neuronal cell cultures, after 3 days of incubation (37°C, 5% CO<sub>2</sub>) the medium was replaced with the cortical medium supplemented with 5µM cytosine-β-arabino-furanoside (Arac, from Calbiochem, CA). After 2 more days, the neuronal culture was switched back to cortical medium without Arac. The neuronal cell culture of more than 95% was obtained by this procedure. The experiments were performed on 6-7 day old neuronal culture. To obtain primary cultures of astroglial cells, the cortical cells from one-day-old Sprague-Dawley rat pups were cultured in DMEM/Ham's F12 medium (1:1), 10% fetal bovine serum (Biomed, CA), 100 IU/ml penicillin, and 0.1 mg/ml streptomycin<sup>177</sup>. Cells were grown for 8-10 days (37°C, 5% CO<sub>2</sub>) and culture medium was changed every 2 days. The astroglial cell culture of more than 95% was obtained by this procedure. 24 hours prior to treatment with fatty acids, the medium was changed to neuronal cell culture medium.

#### **4.2.2 Western Blot Analysis**

For western blot analysis, cells were washed three times with ice-cold TBS (25 mM Tris, pH 8.0, 140 mM NaCl, and 5 mM KCl) and lysed for 20 minutes by scraping into ice-cold radioimmunoprecipitation assay (RIPA) buffer [1% (v/v) Nonidet P-40, 0.1% (w/v) SDS, 0.5% (w/v) deoxycholate, 50 mM Tris, pH 7.2, 150 mM NaCl, 1 mM Na<sub>3</sub>VO<sub>4</sub> and 1 mM PMSF, all chemicals from Sigma]<sup>238</sup>. The total cell lysate was obtained by centrifugation at 12,000 rpm for 15 minutes at 4 °C. The total protein concentration was measured by BCA protein assay kit from Pierce (Rockford, IL). Equal amounts of total protein from each condition were run at 200 V on 10% Tris-HCl gels for detection of GLUT1 and actin. The separated proteins were transferred to nitrocellulose membranes for 1 hour at 100 V and incubated at 4 °C overnight with the appropriate



primary antibodies [1:500 GLUT1, 1:2000 actin]. Blots were washed three times in PBS-Tween (PBS-T) and incubated with appropriate HRP-linked secondary antibodies (Pierce Biotechnology, IL) diluted in PBS-T for 1 hr. After an additional three washes in PBS-T, blots were developed with the Pierce SuperSignal West Femto Maximum Sensitivity Substrate (Pierce Biotechnology) and imaged with the BioRad ChemiDoc. Quantity One software from Bio-Rad was used to quantify the signal intensity of the protein bands.

#### **4.2.3 Biochemical Measurements of Cellular Metabolites**

For measurement of various cellular metabolites the conditioned media were collected immediately after experimental treatment and centrifuged for 10 minutes at 3000 rpm to remove any cell debris. To calculate the glucose uptake and lactate production in particular, their concentrations in the media were measured by using enzymatic glucose (Stanbio Laboratories, TX, USA) and lactate (Trinity Biotech, MO, USA) assays. The glucose uptake and lactate production were calculated by using the differences between the metabolite concentrations in the media before and after the treatment. The data were normalized by using total intracellular protein levels. Similarly, the concentrations of FFA (Assay kit from Roche Biochemicals), beta-hydroxybutyrate and acetoacetate (both assays from Stanbio Laboratories) in the extracellular media were measured according to manufacturer's instructions. High-performance liquid chromatography (HPLC) method (Waters AccQTag amino acid analysis with fluorescence detector) was used to measure concentrations of various amino acids such as Asp, Glu, Gly, Arg, Thr, Ala, Pro, Tyr, Val, Met, Orn, Lys, Ile, Leu and Phe. The concentrations of Ser, Asn, Gln and His were measured by a slight modification of the AccQTag method. The extracellular fluxes of these metabolites were measured for metabolic flux analysis by calculating the changes in

the levels of the metabolites in the cell culture media after 24 hours of treatment. The linearity of some of these fluxes over this interval was verified.

#### 4.2.4 Metabolic Flux Analysis (MFA)

MFA is a powerful mathematical technique that can provide a comprehensive snapshot of the metabolic profile of cells as a function of their environment. The basis of this method is that metabolic pathways have a well-defined stoichiometry relating reactants to products <sup>274</sup>. In MFA, a mass-balance on various intracellular metabolites is performed and under the assumption of pseudo-steady state the differential equations representing the changes in the concentrations of the individual metabolites may be written as algebraic summation of the fluxes associated with that metabolite <sup>275</sup>. These pseudo-steady state balances for all the intracellular metabolites under consideration can be written in matrix form as:

$$S \cdot v = 0$$

where,  $S$  is the stoichiometric matrix and  $v$  is the vector of metabolic fluxes. If  $m$  numbers of fluxes are measured, then it is possible to divide the matrix  $S$  into two submatrices,  $S_m$  and  $S_u$ , corresponding to the measured and unknown fluxes, respectively. This leads to-

$$S_m \cdot v_m + S_u \cdot v_u = 0$$

$$\therefore v_u = (S_u)^{-1} \cdot (-S_m \cdot v_m)$$

Thus, with the knowledge of the stoichiometry and measured fluxes  $v_m$ , the vector of the unknown fluxes  $v_u$  can be calculated.

#### Assumptions

The assumptions pertaining to the MFA model employed in the current study are as follows:

- i. Pseudo-steady state assumption. The intracellular metabolites are assumed to be under the condition of pseudo-steady state in that there is no significant intracellular accumulation of any metabolite. Experiments were conducted to verify the pseudo-steady state assumption.
- ii. Linearity of metabolic fluxes over 24 hour period. Fluxes of the uptake or release of metabolites were assumed to be linear over the 24 hour period, that is the net change in the extracellular concentration of a given metabolite after 24 hours duration represents the flux of that metabolite.
- iii. The metabolites are distributed uniformly inside the cell. Based on this assumption, a single MFA model could be applied to perform metabolite balances for the entire cell and separate models were not needed for the individual cellular compartments or organelles. This assumption has been successfully employed previously in various MFA studies <sup>276 275</sup>.
- iv. Urea cycle is not active in brain tissue. Urea cycle, present in liver, is critical in efficiently clearing up ammonia. However, the urea cycle is not present in the brain. The brain depends on the amidation reaction (glutamate to glutamine) catalyzed by glutamine synthetase, to clear ammonia <sup>277</sup>. Therefore, the present model consisted of the glutamine synthetase reaction and the urea cycle reactions were not included.
- v. Glycerol is converted by the cells to glycerol-3-phosphate, which leads to dicylglycerol (DAG) formation or to glyceraldehyde-3-phosphate, the latter enters glycolysis leading to the production of pyruvate. However, the enzyme involved in the conversion of glycerol-3-phosphate to glyceraldehyde-3-phosphate, glycerol-3-

phosphate dehydrogenase, is not expressed in astroglia <sup>278</sup>. Therefore, only the DAG formation reaction is included in the present model.

Based on these assumptions, a MFA model consisting of 71 cellular metabolic reactions involved in the metabolism of glucose, amino acids and lipids was constructed (**Table 4.1** and **Figure 4.3**). The model consisted of 54 intracellular metabolites as shown in **Table 4.2**. A total of 23 metabolic fluxes were measured (**Table 4.3**), yielding an over-determined system of equations, which was solved by least-squares fit using the Moore-Penrose pseudo-inverse calculation. This method has been successfully used in our laboratory to study FFA-induced abnormalities in HepG2 cells <sup>275</sup>.

**Table 4.1. List of the cellular metabolic reactions**

Flux #	Equation
<b>Glycolysis</b>	
1	G+ATP → G-6-P
2	G-6-P → F-6-P
3	F-6-P +ATP → Glyceraldehyde-3-P + DHAP
4	DHAP → Glyceraldehyde-3-P
5	Glyceraldehyde-3-P → 3-PGA
6	3PGA → PEP + NADH (+ 2ATP)
7	PEP → Pyr
8	Pyruvate + NADH → (Lactate)
9	Pyruvate → Acetyl-CoA + NADH +CO2
<b>TCA cycle</b>	
10	Acetyl-CoA + OAA → Citrate
11	Citrate → α-KetoGlutarate + NADPH +CO2
12	α-Ketoglutarate → Succinyl-CoA + NADH + CO2
13	Succinyl-CoA → Fumavate + FADH2 + ATP
14	Fumarate → OAA + NADH
<b>Pentose-phosphate pathway</b>	
15	G-6-P → 12 NADPH + 6 CO2
16	CO2 out
<b>Ketone Body production</b>	
17	2 Acetyl-COA → Acetoacetyl-CoA
18	Acetoacetyl-CoA → Acetoacetate

**Table 4.1 Continued**

- 19 Acac out
- 20 Acetoacetate + NADH  $\rightarrow$  (B-OH butyrate)

**Oxygen uptake and Oxidative Phosphorylation**

- 21 O<sub>2</sub> (In)
- 22 NADH + 0.5 O<sub>2</sub>  $\rightarrow$  2.5 ATP
- 23 FADH<sub>2</sub> + 0.5 O<sub>2</sub>  $\rightarrow$  2 ATP

**FFA synthesis and oxidation**

- 25 8 Acetyl-CoA + 14 NADH  $\rightarrow$  FA-CoA
- 69 Glycerol + ATP  $\rightarrow$  Glycerol-3-P
- 68 2FA-CoA + Glycerol-3-P  $\rightarrow$  DAG
- 26 FA-CoA + DAG  $\rightarrow$  TG
- 24 FA-CoA (In)

**Amino acid metabolism**

- 27 Ser (In)
- 28 3-PGA + Glu  $\rightarrow$  Ser + a-KG + NADH
- 29 Gln In
- 30 Asp (In)
- 31 Glu (In)
- 32 Gly (In)
- 33 Gly  $\rightarrow$  2 CO<sub>2</sub> + NH<sub>3</sub> + NADH + THF + ATP
- 34 NH<sub>4</sub> (In)
- 35 Arg (In)
- 36 Thr In
- 37 Ala (In)
- 38 Glu + Pyr  $\rightarrow$  Ala + aKG
- 49 Pro In
- 40 Tyr (In)
- 41 Tyr + aKG + 2 O<sub>2</sub>  $\rightarrow$  Glu + CO<sub>2</sub> + Acetoacetate + Fumarate
- 42 Val (In)
- 43 Orn IN
- 44 Lys IN
- 45 Ile IN
- 46 Lue In
- 47 Phe In
- 48 Gln  $\rightarrow$  Glu + NH<sub>4</sub>
- 59 Orn + a-KG + 0.5 NADPH + 0.5 NADH  $\rightarrow$  Pro
- 50 Asp + NH<sub>4</sub>  $\rightarrow$  Asn
- 51 Thr  $\rightarrow$  Pyr + CO<sub>2</sub> + NH<sub>4</sub> + 2 NADH + FADH<sub>2</sub>
- 52 Val + aKG  $\rightarrow$  Glu + CO<sub>2</sub> + 2NADH + FADH<sub>2</sub> + Succ-CoA
- Lys + 2 aKG + NADPH  $\rightarrow$  2Glu + Acetoacetyl-CoA + 2CO<sub>2</sub> + 4 NADH +
- 53 FADH<sub>2</sub>
- 54 Ile + aKG  $\rightarrow$  Glu + Succ-CoA + Acetyl-CoA + NADH + FADH<sub>2</sub>
- 54 Leu + aKG  $\rightarrow$  Glu + HMG-CoA + NADH + FADH<sub>2</sub>

**Table 4.1 Continued**

- 56 Phe + O<sub>2</sub> → Tyr  
 59 α-KG + NH<sub>4</sub> + NADPH → Glu  
 70 Cys + O<sub>2</sub> + α-KG → Glu + Pyr + SO<sub>4</sub>  
 71 Cystine → 2 Cys

**Synthesis of Cholesterol and Cholesteryl ester**

- 60 Acetoacetyl-CoA + Acetyl-CoA → HMG-CoA  
 61 HMG-CoA + 2 NADPH (+ 3ATP) → IPP  
 62 2 IPP → Geranyl-PP  
 63 Geranyl-PP + IPP → Farnesyl-PP  
 64 2 Farnesyl-PP + 0.5 NADPH + 0.5 NADH → Squalene  
 65 Squalene + O<sub>2</sub> + NADPH → Lanosterol  
 66 Lanosterol + 10.5 NADPH + 4.5 NADH + 10 O<sub>2</sub> → Chol + 3 CO<sub>2</sub>  
 67 Chol + FA-CoA → Cholesterol Ester

**Sphingolipid Metabolism**

- 57 Ser + 1 Palm-CoA + 1 FA-CoA + NADPH → Ceramide + CO<sub>2</sub> + FADH<sub>2</sub>  
 58 Ceramide + PhosphatidylCholine → Sphingomyelin

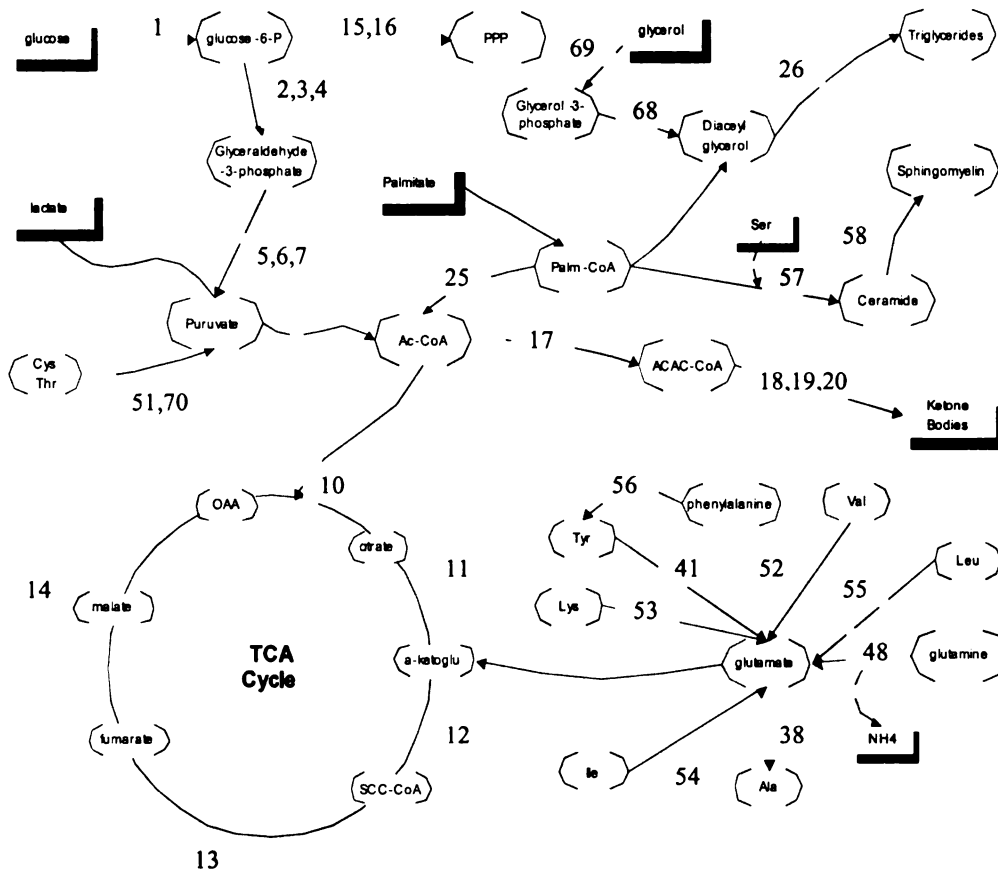


**Figure 4.3. Astroglial metabolic network.** Boxes represent extracellular metabolites, while ovals represent intracellular metabolites. The direction of reaction assumed in the model is indicated by arrows.

**Table 4.2. List of intracellular metabolites**

	Metabolite
1	glucose-6-P
2	fructose-6-P
3	glyceraldehyde-3-P
4	3-PGA
5	DHAP
6	Phosphoenolpyruvate
7	Pyruvate
8	CO <sub>2</sub>
9	acetyl-CoA
10	Oxaloacetate
11	Citrate
12	$\alpha$ -ketoglutarate
13	succinyl-CoA
14	Fumate
15	Acetoacetate
16	acetoacetyl-CoA
17	B-OH
18	O <sub>2</sub>
19	Glycerol-3-P
20	Palm-CoA
21	NADH
22	NADPH
23	FADH <sub>2</sub>
24	Ser
25	NH <sub>4</sub>
26	Glu
27	Gln
28	Val
29	Ile
30	Leu
31	Arg
32	Orn
33	Ala
34	Gly
35	Tyr
36	Thr
37	Lys
38	Phe
39	Pro
40	Asp
41	Asn
42	Cys
43	Ceramide
44	Sphingomyelin

	<b>Table 4.2 Continued</b>
45	HMG-CoA
46	Isopentenyl-PP
47	Geranyl-PP
48	Farnesyl-PP
49	Squalene
50	Lanosterol
51	Cholesterol
52	Cholesterol Ester
53	DAG
54	Sulfate

**Table 4.3. List of measured fluxes**

Flux #	Metabolite
1	Glucose
8	Lactate
19	Acetoacetate
20	Beta-hydroxybutyrate
21	O <sub>2</sub> In
24	Palm
27	Ser
29	Gln
30	Asp
31	Glu
32	Gly
34	NH <sub>4</sub>
35	Arg
36	Thr
37	Ala
39	Pro
40	Tyr
42	Val
43	Orn
44	Lys
45	Ile
46	Leu
47	Phe

#### **4.2.5 Measurement of Intracellular ATP in Astroglia**

To measure the intracellular ATP levels, astroglia were washed with ice-cold PBS and then lysed with 0.7% perchloric acid (PCA). The PCA was neutralized by using 0.7N



NaOH. The neutralized samples were used to measure intracellular ATP levels with a luciferase-based chemiluminescent assay (Molecular Probes, CA).

#### **4.2.5 Measurement of Intracellular Ceramide in Astroglia**

Astroglia were washed with ice-cold PBS and then lipids were extracted by using a chloroform/methanol method as described by Bligh and Dyer<sup>279</sup>. The organic phase was dried under N<sub>2</sub> and the ceramide was measured after its deacylation to sphingolipid base and derivitization with o-phthaldehyde (OPA) as described earlier<sup>280</sup>. Briefly, the dried lipids from the organic phase were re-suspended in 500 µl of 1N KOH in methanol and incubated at 100°C for 1 hour to deacylate ceramide to free sphingolipid bases. The lipids were then dissolved in 50 µl of methanol and 50 µl of OPA reagent is added to this. The OPA reagent was prepared by mixing 99 ml of boric acid (3% w/v in water, pH 10.5), 1ml of ethanol containing 50 mg OPA (Sigma) and 50 µl of β-mercaptoethanol (Sigma). The derivatized sample aliquots (20 µl) were quantified by high performance liquid chromatography (HPLC) using Nova Pak C18 column (60 Å, 4 µm, 3.9 mm X 150 mm; from Waters, MA, USA). Fluorescent-labeled lipids were eluted isocratically by using methanol:5mM potassium phosphate (pH 7.0) (90:10, v/v) at a flow rate of 0.6 ml/min and detected with a fluorescence detector (excitation wavelength 340 nm, emission wavelength 455 nm). A standard curve obtained by running known amounts of ceramide (type III, from bovine brain sphingomyelin; from Sigma) was used as a comparison to determine the ceramide levels in the experimental samples.

#### **4.2.6 Data Analyses**

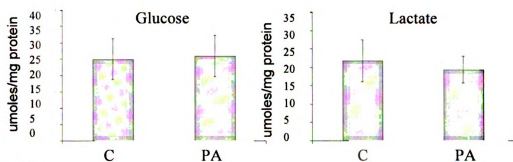
Data are shown as means  $\pm$  S.D. for indicated number of experiments. Student's t-test and one-way ANOVA with Tukey's *post hoc* method were used to evaluate statistical significances between different treatment groups. Statistical significance was set at  $p < 0.05$ .

### **4.3 RESULTS AND DISCUSSION**

#### **4.3.1 FFA-Induced Abnormal Glucose Metabolism**

To study the effects of PA on cellular glucose metabolism, neurons and astroglia were treated with 0.2mM of PA for 24 hours. As shown in **Figure 4.4A**, there was no change in the glucose uptake and lactate production in neurons treated with PA as compared to the untreated ones. This is in line with the observed, lack of direct effect of PA on neurons in terms of AD-associated pathophysiological changes as discussed earlier (Chapters 2 and 3) and may similarly be attributed to the low affinity of primary neurons towards PA<sup>182</sup>. However, as mentioned earlier, astroglia have a higher capacity to take up and metabolize PA<sup>182</sup>. Thus, in the case of astroglia, PA may compete with glucose for cellular uptake. Previously, PA has been shown to inhibit glycolysis in primary hepatocytes<sup>281, 282</sup>. Furthermore, high fat diet has been shown to increase palmitate oxidation and decrease fructose oxidation in isolated primary hepatocytes<sup>283</sup>. We found that PA treatment significantly decreased basal glucose uptake and lactate release from astroglia (**Figure 4.4B**).

(A)



(B)

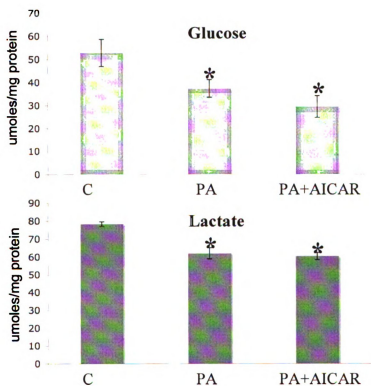


**Figure 4.4. PA downregulates glucose uptake and lactate release by astroglia.** The cortical neurons and astroglia were treated for 24 hours with 0.2mM of PA or 4% BSA. (A) In neurons, PA treatment did not change glucose uptake and lactate production. (B) PA treatment significantly decreased glucose uptake and lactate production by astroglia. AMPK-activator AICAR did not inhibit PA-induced downregulation in glucose metabolism. Data represent mean  $\pm$  S.D. of six experiments. Student's t-test was used for analyzing the differences between the two treatment groups. \*,  $p < 0.05$  compared with respective control.

Here it is imperative to note that although PA did not directly affect glucose metabolism in neurons, PA-astroglia-induced ROS production in neurons (as discussed in chapter 2) may affect glucose uptake and metabolism in neurons; oxidative stress has been shown to affect the activities of glucose transporter and glycolytic enzymes and in turn affect glucose uptake and metabolism in neurons<sup>284-286</sup>. To investigate perturbed astroglial metabolism due to PA treatment, we measured cellular ATP production in astroglia. We expected PA-treatment to decrease astroglial ATP production in light of our observation that PA decreases glucose uptake. We, however, found that there was an increase in ATP production in the PA-treated astroglia as compared to the untreated ones (Figure 4.5).

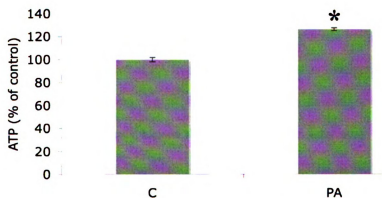


**Figure 4.5. Measurement of intracellular ATP in astroglia.** The cortical astroglia were treated for 24 hours with 0.2mM of PA or 4% BSA. PA treatment increased cellular ATP production in astroglia. Data represent mean  $\pm$  S.D. of 3 experiments. Student's t-test was used for analyzing the differences between the two treatment groups. \*,  $p < 0.05$  compared with respective control.

Increased ATP production in PA-treated astroglia may be due to the uptake and increased oxidation of PA by astroglia. In support of this, previously it has been shown that although PA inhibits glucose oxidation, PA-oxidation itself makes up for this and thereby prevents ATP loss, which otherwise would be expected due to the reduced glucose

oxidation<sup>287, 288</sup>. Furthermore, it has been shown that although glucose utilization is reduced in AD brain, oxygen consumption and CO<sub>2</sub> production are unchanged or even increased as compared to healthy controls<sup>289, 290</sup>. Thus, it has been hypothesized that substrates other than glucose (e.g. FFAs and endogenous amino acids) may be oxidized in AD brain<sup>245</sup>, which may partially compensate for the energy deficit observed in AD brain due to decreased glucose metabolism<sup>291</sup>.

#### **4.3.2 Cellular Mechanism of FFA-Induced Abnormal Glucose Metabolism in Astroglia**

We hypothesized that the observed, PA-induced abnormal glucose metabolism may be due to the potential effect of PA on the level of astroglial glucose transporter (GLUT1) or due to possible involvement of PA in perturbing the signaling mechanism involved in the cellular glucose metabolism, e.g. AMP-activated protein kinase (AMPK). Along those lines, it has been previously shown that polyunsaturated fatty acids (arachidonic acid) deficiency results in down-regulation of the glucose transporter in astroglia<sup>292</sup>. However, the effects of elevated levels of saturated fatty acids on astroglial glucose transporters have not been studied. AMPK is a serine-threonine kinase, which is involved in regulating cellular metabolism<sup>293</sup>. It was first isolated from liver and is also expressed in many other tissues including lung, kidney, heart, skeletal muscle, and brain<sup>294</sup>. At the sub-cellular level in the brain, AMPK is expressed in both neurons and astroglia; however, its activity is 3X higher in astroglia as compared to neurons<sup>295</sup>. The importance of AMPK in AD research is emphasized by the fact that inflammation is central to the AD pathology and AMPK activation has been shown to inhibit the production of

inflammatory cytokines in astrocytes<sup>296</sup>. AMPK activation has also been shown to protect cortical and hippocampal neurons from oxygen-glucose deprivation<sup>297</sup>. Therefore, we treated astroglia for 24 hours with a cell-permeable pharmacological activator of AMPK, 5-aminoimidazole-4-carboxamide ribonucleoside (AICAR). Co-treatment of PA-treated astroglia with 0.25mM AICAR did not increase glucose uptake and lactate production as compared to astroglia treated with PA (**Figure 4.4B**). This suggests that AMPK may not be involved in the observed PA-induced abnormal glucose metabolism in astroglia. On the other hand, we found that the level of astroglial glucose transporter (GLUT1) was significantly downregulated in PA-treated astroglia as compared to untreated cells (**Figure 4.6**). Thus, the observed downregulation in glucose uptake by astroglia in the presence of PA may be attributed to the PA-induced downregulation of GLUT1 levels in astroglia. Interestingly, AD brain is characterized by significant reductions in GLUT1 levels<sup>298</sup>, and disease severity is associated with progressive decline in GLUT1 gene expression<sup>299</sup>.

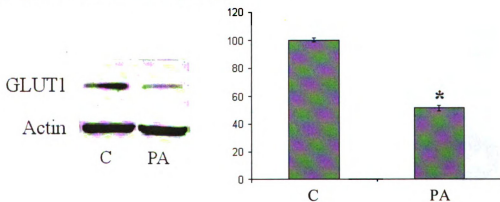


**Figure 4.6. PA downregulates GLUT1 level in astroglia.** Astroglia were treated for 24 hours with 0.2mM of PA or 4% BSA. The immunoblot analysis shows that PA-treatment significantly decreased the levels of GLUT1 as compared to the untreated ones.  $\beta$ -actin is shown as a marker for protein loading. Histogram represents quantitative determinations of intensities of the relative bands normalized with actin. Data represent mean  $\pm$  S.D. of three independent experiments. Student's t-test was used for analyzing the differences between the two treatment groups. \*,  $p < 0.05$  compared with respective control.

### 4.3.3 FFA-Induced Global Metabolic Changes in Astroglia

Abnormal metabolism precedes the cascade of neuropathological changes in AD pathology<sup>10</sup>. Decreased glucose metabolism and energy production have been shown to be involved in increased amyloidogenesis and hyperphosphorylation of tau in neurons<sup>266-270</sup>. However, as we showed here, PA treatment did not affect the glucose metabolism in neurons but only in astroglia. Therefore, we hypothesized that metabolic changes, other than the abnormal glucose metabolism induced by PA in astroglia may be involved in causing the observed, PA-astroglia-induced pathophysiologic changes in neurons (chapters 2 and 3). The main focus was to investigate various FFA-metabolizing pathways in astroglia that may potentially be involved in causing cellular ROS production, specifically in neurons, as is observed in our studies. Based on extensive literature review, we propose 3 major pathways by which PA may induce cellular ROS production (Figure 4.7).

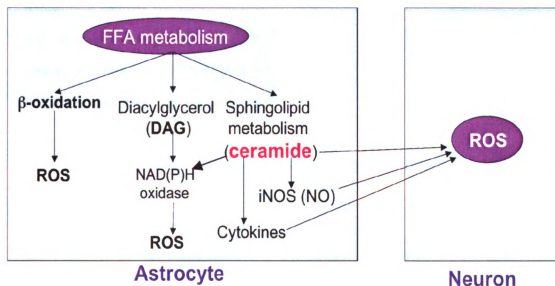


Figure 4.7. FFA-metabolizing pathways involved in cellular ROS production.

Elevated levels of PA may lead to its increased cycling through  $\beta$ -oxidation pathways in mitochondria and other organelles such as peroxisomes and glyoxysomes. The increased oxidation of PA may lead to enhanced cellular ROS production<sup>300</sup>. PA may also increase diacylglycerol (DAG) production, which in turn may activate NAD(P)H oxidase and increase cellular ROS<sup>300, 301</sup>. However, as shown earlier in Chapter 2, PA did not induce ROS production in astroglia (**Figure 2.6**), which may suggest the lack of or minimal activation of these two pathways ( $\beta$ -oxidation and DAG production) in PA-treated astroglia. Finally, PA may also be metabolized by the cells to synthesize ceramide<sup>302</sup>. Ceramides are also potent intracellular activators of NAD(P)H oxidase<sup>303</sup> and thus may increase cellular ROS production. More importantly, ceramide secreted from astrocytes may directly act on neurons and mediate oxidative stress-induced effects in neurons<sup>304</sup>. Furthermore, PA-induced increase in ceramide levels may induce secretion of cytokines<sup>305</sup> or other signaling molecules, e.g., NO<sup>306</sup> by astrocytes, which in turn may elevate production of ROS in the neurons<sup>307, 308</sup>. Thus, taken together, these data may suggest the sphingolipid pathway (ceramide) to be predominantly activated in PA-treated astroglia and ceramide to be a possible mediator of the FFA-induced pathological damage in neurons as shown in our present studies. We sought to support this hypothesis by using mathematical modeling (MFA) and additional experiments.

#### **4.3.3.1 Verification of the pseudo-steady state assumption and linearity of fluxes over 24 hours**

To verify whether the pseudo-steady state assumption for MFA is valid, intracellular and extracellular lactate concentrations were measured after 6, 12 and 24 hour treatments.



Lactate was the metabolite of choice due to its highest flux, which offered two advantages <sup>275</sup>-(1) due to its highest molar synthesis, it is likely the most concentrated metabolite, simplifying accurate detection, and (2) its highest molar change provides the most stringent test of the pseudo-steady state assumption. As shown in **Figures 4.8A and B**, both the intracellular and extracellular concentrations of lactate increased with time in response to PA treatment. The extracellular lactate release was approximately linear over the 24 hour period for both the control and PA treatments. Furthermore, as shown in **Table 4.4**, the changes in the intracellular lactate levels were about a thousand-fold smaller as compared to changes in the extracellular lactate levels. This indicates that the intracellular accumulation of lactate is negligible and the pseudo-steady state hypothesis is valid.

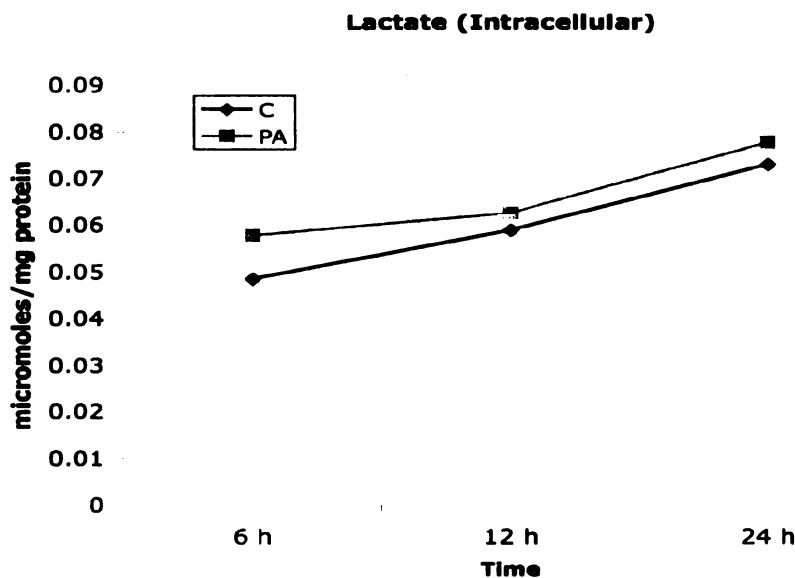


**Figure 4.8A. Time-dependent measurements of intracellular lactate levels.** Astroglia were treated for 6, 12 and 24 hours with 0.2mM of PA or 4% BSA. The cells were trypsinized, washed with TBS and lyzed by using 0.7% perchloric acid. The lactate levels in cell lysate were measured by enzymatic assay. Data represent mean  $\pm$  S.D. of three independent experiments.

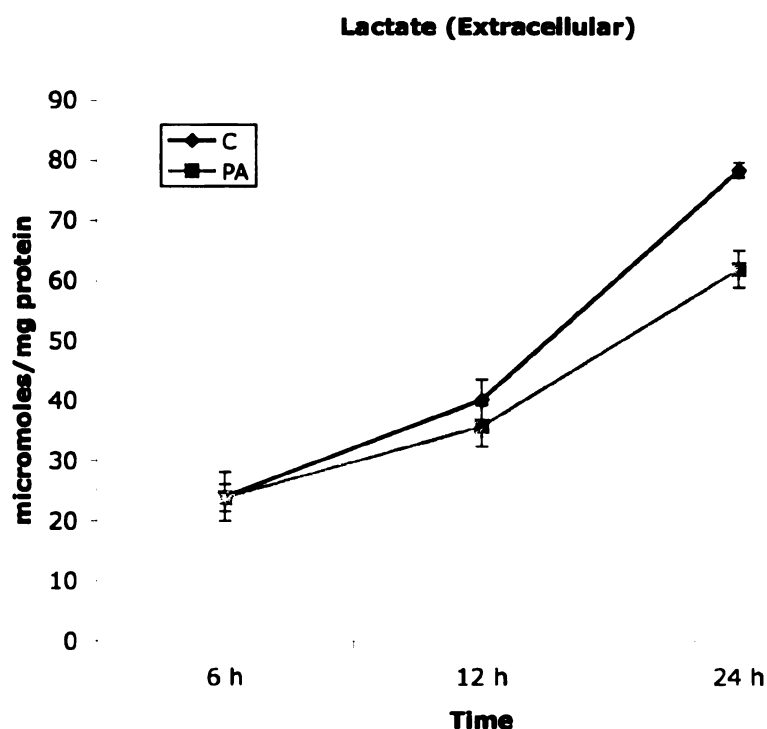


**Figure 4.8B. Time-dependent measurements of extracellular lactate levels.** Astroglia were treated for 6, 12 and 24 hours with 0.2mM of PA or 4% BSA. The conditioned media were collected and the lactate levels in the media were measured by enzymatic assay. Data represent mean  $\pm$  S.D. of three independent experiments

	24h Intra	24h Extra	Ratio (Intra/Extra)
Control	0.07303	78.35371	9.32E-04
PA	0.077786	61.93194	1.26E-03

**Table 4.4. Ratio of intracellular to extracellular lactate levels.**

#### 4.3.3.2 MFA analysis

**Table 4.5** shows a complete list of fluxes calculated from MFA analysis for both the control and PA-treated astroglia. Firstly, in both the control and PA-treated cells fatty acid synthesis but not the fatty acid oxidation, was more prominent (**flux 25, Table 4.5**). In PA-treated astroglia fatty acid synthesis was lower as compared to controls, which

might be attributed to the exogenously added PA. In this context, there is evidence that astrocytes do synthesize fatty acids <sup>309</sup> and exogenous addition of fatty acids decrease the endogenous fatty acid synthesis <sup>310</sup>. Secondly, in PA-treated cells, glycerol uptake was significantly decreased (**flux 69, Table 4.5**). Previously, PA treatment has been shown to decrease glycerol uptake in HepG2 cells <sup>275</sup>. As glycerol is involved in DAG production, PA-induced decrease in glycerol uptake may further contribute to decreased synthesis of DAG in the PA-treated astroglia (**flux 68, Table 4.5**). Finally, flux through *de novo* synthesis of ceramide was significantly elevated in PA-treated astroglia as compared to controls (**flux 57, Table 4.5**). Experimental measurements also showed higher intracellular ceramide levels in PA-treated astroglia as compared to controls and co-treatment of astroglia with 2mM L-cycloserine (L-CS), an inhibitor of *de novo* synthesis of ceramide, inhibited PA-induced ceramide increase (**Figure 4.9**), thus further validating the MFA findings.

**Table 4.5. Metabolic flux values calculated by MFA**

Flux #	Equation	Control		Palmitate	
		Average	Error	Average	Error
1	G+ATP → G-6-P	52.8850	5.8490	37.4540	3.8160
2	G-6-P → F-6-P	52.7431	5.8491	37.2262	3.8160
3	F-6-P +ATP → Glyceraldehyde-3-P + DHAP	52.7431	5.8491	37.2262	3.8160
4	DHAP → Glyceraldehyde-3-P	52.7431	5.8491	37.2262	3.8160
5	Glyceraldehyde-3-P → 3-PGA	105.4862	11.6982	74.4523	7.6320
6	3PGA → PEP + NADH (+ 2ATP)	104.1620	11.7016	72.4859	7.6465
7	PEP → Pyr	104.1620	11.7016	72.4859	7.6465
8	Pyruvate + NADH → (Lactate)	78.3500	1.2500	61.9300	3.1000
9	Pyruvate → Acetyl-CoA + NADH +CO2	24.4819	11.7797	9.1674	8.2970

**Table 4.5 Continued.**

10	Acetyl-CoA + OAA → Citrate	5.8041	1.0401	5.0068	0.9997
	Citrate → α-KetoGlutarate + NADPH	6.1589	1.035	5.4583	1.0044
11	+CO <sub>2</sub>				
	α-Ketoglutarate → Succinyl-CoA +	0.7998	1.1461	0.1808	1.5399
12	NADH + CO <sub>2</sub>				
	Succinyl-CoA → Fumarate + FADH <sub>2</sub> +	4.7440	1.0824	3.8455	1.1778
13	ATP				
		5.4492	1.0467	4.5552	1.0048
14	Fumarate → OAA + NADH				
		0.1419	0.0359	0.2278	0.0047
15	G-6-P → 12 NADPH + 6 CO <sub>2</sub>				
		39.0347	10.9023	25.7209	7.8214
16	CO <sub>2</sub> out				
		1.2702	0.9366	0.9077	1.2612
17	2 Acetyl-CoA → Acetoacetyl-CoA				
		1.9907	0.8355	2.1769	0.9631
18	Acetoacetyl-CoA → Acetoacetate				
		2.3390	0.8040	2.4320	0.8280
19	Acac out				
	Acetoacetate + NADH → (B-OH	0.0020	0	0.0030	0.0010
20	butyrate)				
		24.5230	2.1000	23.2030	2.1000
21	O <sub>2</sub> (In)				
		33.2840	3.7417	32.5936	4.4499
22	NADH + 0.5 O <sub>2</sub> → 2.5 ATP				
		13.5899	1.1080	12.5787	1.1972
23	FADH <sub>2</sub> + 0.5 O <sub>2</sub> → 2 ATP				
		0.1510	0.0210	1.0600	0.1450
24	FA-CoA (In)				
	<b>8 Acetyl-CoA + 14 NADH →</b>	<b>3.3083</b>	<b>1.5521</b>	<b>1.2357</b>	<b>1.1552</b>
25	<b>FA-CoA</b>				
		0.8802	0.5339	0.2139	0.4917
26	FA-CoA + DAG → TG				
		0.7100	0.0380	0.7260	0.0790
27	Ser (In)				
		1.3241	0.2431	1.9665	0.4702
28	3-PGA + Glu --> Ser + α-KG + NADH				
		-4.7620	0.7520	-4.8990	1.8360
29	Gln In				
		0.2140	0.0030	0.2050	0.0010
30	Asp (In)				
		-0.9460	0.1830	-0.5090	0.4850
31	Glu (In)				
		1.7060	0.1180	2.9720	0.9830
32	Gly (In)				
	Gly → 2 CO <sub>2</sub> + NH <sub>3</sub> + NADH + THF +	1.5013	0.1373	2.5585	0.9404
33	ATP				
		3.5020	0.1760	4.0760	0.0220
34	NH <sub>4</sub> (In)				

**Table 4.5 Continued.**

35	Arg (In)	1.5340	0.1240	1.4980	0.2810
		1.7910	0.4230	2.0220	0.5570
36	Thr In	-2.5070	0.2100	-2.1700	0.1290
37	Ala (In)	2.7117	0.2138	2.5835	0.1973
38	Glu + Pyr → Ala + aKG	-0.6020	0.0360	-0.4570	0.0530
39	Pro In	-0.3900	0.0980	-0.2940	0.2420
40	Tyr (In)	0.3503	0.2274	0.2581	0.4920
	Tyr + aKG + 2 O <sub>2</sub> → Glu + CO <sub>2</sub> +				
41	Acetoacetate + Fumarate	0.1580	0.0350	0.4430	0.3480
42	Val (In)	-0.0440	0.0060	-0.0380	0.0110
43	Orn IN	1.7030	0.4310	2.7340	0.0560
44	Lys IN	3.1310	0.2010	2.6940	0.2630
45	Ile IN	2.1720	0.1600	1.5910	0.3230
46	Lue In	0.4400	0.1230	0.4760	0.0500
47	Phe In	-4.8166	0.6129	-5.2744	1.4865
48	Gln → Glu + NH <sub>4</sub>	0.1016	0.0309	-0.0163	0.0557
	Orn + a-KG + 0.5 NADPH + 0.5 NADH				
49	--> Pro	0.2094	0.0402	0.3092	0.0776
50	Asp + NH <sub>4</sub> → Asn	1.5863	0.4071	1.6085	0.5480
	Thr → Pyr + CO <sub>2</sub> + NH <sub>4</sub> + 2 NADH +				
51	FADH <sub>2</sub>	0.3082	0.1005	0.4811	0.3861
	Val + aKG → Glu + CO <sub>2</sub> + 2NADH +				
52	FADH <sub>2</sub> + Succ-CoA	1.2936	0.3607	1.9070	0.3133
	Lys + 2 aKG + NADPH → 2Glu +				
	Acetoacetyl-CoA + 2CO <sub>2</sub> + 4 NADH +				
53	FADH <sub>2</sub>	3.2812	0.2044	2.7321	0.3272
	Ile + aKG → Glu + Succ-CoA + Acetyl-				
54	CoA + NADH + FADH <sub>2</sub>	1.9673	0.1710	1.1775	0.3420
	Leu + aKG → Glu + HMG-CoA + NADH				
55	+ FADH <sub>2</sub>	0.5902	0.1461	0.5141	0.2304
56	Phe + O <sub>2</sub> → Tyr				
	<b>Ser + 1 Palm-CoA + 1 FA-CoA</b>	<b>0.4094</b>	<b>0.1607</b>	<b>0.8270</b>	<b>0.3105</b>
	<b>+ NADPH → Ceramide + CO<sub>2</sub></b>				
57	<b>+ FADH<sub>2</sub></b>				
	Ceramide + PhosphatidylCholine →	0.2047	0.0804	0.4135	0.1552
58	Sphingomyelin				
59	a-KG + NH <sub>4</sub> + NADPH --> Glu	1.3589	0.5890	2.2459	1.3018

**Table 4.5 Continued.**

	Acetoacetyl-CoA + Acetyl-CoA →	-1.9673	0.1710	-1.1775	0.3420
60	HMG-CoA				
61	HMG-CoA + 2 NADPH (+ 3 ATP) → IPP	-0.0000	0.0000	-0.0000	0.0000
		-0.0000	0.0000	-0.0000	0.0000
62	2 IPP → Geranyl-PP				
		-0.0000	0.0000	-0.0000	0.0000
63	Geranyl-PP + IPP → Farnesyl-PP				
	2 Farnesyl-PP + 0.5 NADPH + 0.5	0.0000	0.0000	0.0000	0.0000
64	NADH → Squalene				
	Squalene + O <sub>2</sub> + NADPH →	-0.0000	0.0000	-0.0000	0.0000
65	Lanosterol				
	Lanosterol + 10.5 NADPH + 4.5 NADH	0.0000	0.0000	0.0000	0.0000
66	+ 10 O <sub>2</sub> → Chol + 3 CO <sub>2</sub>				
		-0.0000	0.0000	-0.0000	0.0000
67	Chol + FA-CoA → Cholesterol Ester				
	2FA-CoA + Glycerol-3-P →	<b>0.8802</b>	<b>0.5339</b>	<b>0.2139</b>	<b>0.4917</b>
68	DAG				
		0.8802	0.5339	0.2139	0.4917
69	Glycerol + ATP → Glycerol-3-P				
		-0.2047	0.0804	-0.4135	0.1552
70	Cys + O <sub>2</sub> + α-KG → Glu + Pyr + SO <sub>4</sub>				
		-0.1024	0.0402	-0.2067	0.0776
71	Cystine → 2 Cys				

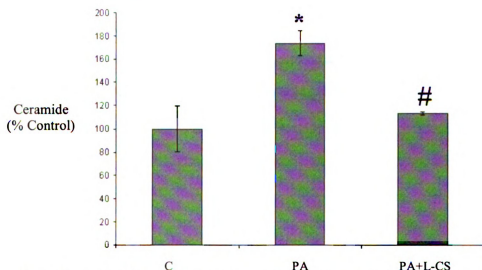


**Figure 4.9. PA-induced, de novo synthesis of ceramide in astroglia.** Astroglia were treated for 24h with 0.2mM PA or 4% BSA (control), after which cellular lipids were extracted for ceramide determination by HPLC. PA significantly increased ceramide synthesis in astroglia, which was completely inhibited by treatment of astroglia with 2mM L-CS, an inhibitor of de novo synthesis of ceramide. Data are taken from 3 different experiments and are expressed as mean  $\pm$  S.D. One-way ANOVA with Tukey's post hoc method was used for analyzing the differences between treatment groups. \*,  $p < 0.05$  compared with control; #,  $p < 0.05$  compared with PA treatment.

#### 4.4 CONCLUSIONS

In conclusion, PA had no direct effect on either glucose uptake and lactate production in neurons. On the other hand, PA significantly decreased both glucose uptake and lactate release in astroglia. The observed downregulation in glucose uptake by astroglia in the presence of PA may be attributed to PA-induced downregulation of astroglial glucose transporter (GLUT1) levels. In addition to these PA-induced abnormalities in astroglial glucose metabolism, we also showed by using MFA that flux through *de novo* synthesis of ceramide is elevated in PA-treated astroglia as compared to control. This MFA finding was further validated experimentally; PA-treated astroglia had elevated intracellular levels of ceramide as compared to controls, which were decreased by the astroglial treatment with L-CS, which inhibits serine palmitoyltransferase-1 (SPT-1), an enzyme that catalyzes the first committed step of *de novo* synthesis of ceramide. Thus, the present data establish a central role of saturated FFAs in causing abnormalities in astroglial glucose metabolism and further warrant investigating a possible causal role of increased astroglial ceramide levels in FFA-astroglia-induced pathological changes in neurons.

## **CHAPTER 5. INVOLVEMENT OF CERAMIDE IN FFA-ASTROGLIA-INDUCED PATHOPHYSIOLOGICAL ABNORMALITIES ASSOCIATED WITH AD**

### **5.1 INTRODUCTION**

Ceramides are one of the most important sphingolipids and are composed of sphingosine and fatty acid, which are joined in an amide bond. Ceramides are involved in the synthesis of sphingomyelin, one of the major components of the cellular lipid bilayer, thus playing a critical role in structural integrity of cell membranes. In addition, ceramides also act as signaling molecules and are involved in many important signaling functions such as cell growth, differentiation, cell death etc. <sup>311</sup>. Ceramides are synthesized in cells through two pathways- (1) the sphingomyelinase (Smase) pathway and (2) the *de novo* synthesis pathway (**Figure 5.1**). Smase is regulated by the cellular redox state; increased oxidative stress activates Smase <sup>312</sup>. Currently, there are five different enzymes characterized as Smases based on their pH dependence, cation dependence and cellular localization <sup>312</sup>. Smases break down membrane sphingomyelins into ceramide and free fatty acids. On the other hand, the *de novo* synthesis of ceramide uses serine and palmitoyl-CoA to synthesize ceramide and is initiated by serine palmitoyltransferase (SPT-1), which is the rate-limiting step of ceramide synthesis. Ketosphinganine formed in this first reaction is then converted to sphinganine by ketosphinganine reductase. A double bond is introduced to sphinganine by dihydroceramide synthase leading to the production of dihydroceramide, which is converted to ceramide by dihydroceramide desaturase.



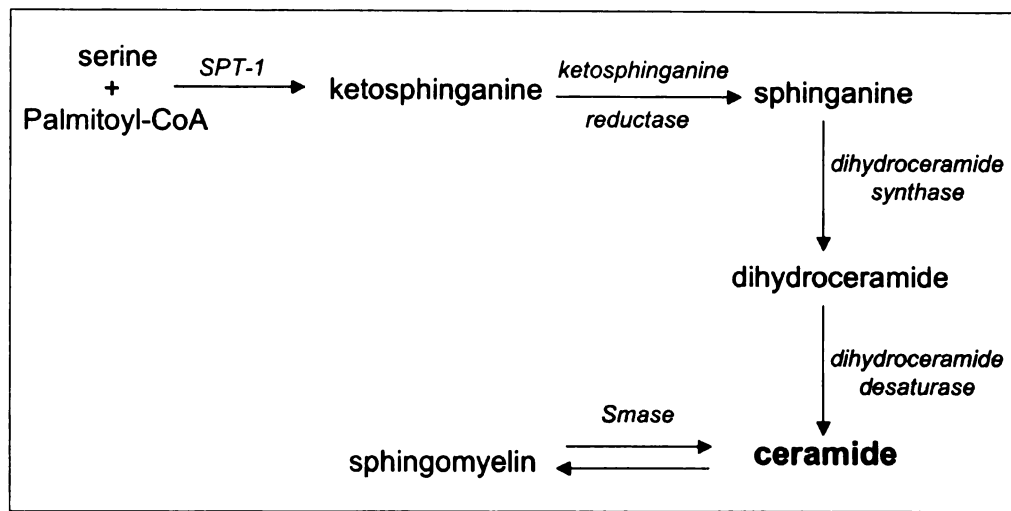


**Figure 5.1. Cellular ceramide production.** Ceramide is produced in cells by *de novo* synthesis from serine and palmitoyl-CoA or by breakdown of membrane sphingomyelins.

Abnormal ceramide metabolism has been implicated in many diseases such as diabetes, AIDS and neurodegenerative disorders <sup>311</sup>. Ceramides may induce insulin resistance associated with diabetes and inhibition of ceramide synthesis has been shown to ameliorate glucocorticoid-, saturated-fat-, and obesity-induced insulin resistance <sup>313</sup>. Ceramide level has been also shown to be elevated in the cerebrospinal fluid of AIDS patients; elevated cerebral ceramides may be involved in neuronal cell death thus leading to the dementia often associated with AIDS <sup>314</sup>. In AD brain, ceramide levels were found elevated as compared to those of healthy controls, and the levels were higher in the affected regions (cortex and hippocampus) as compared to the unaffected regions (cerebellum) of the AD brain <sup>315, 316</sup>, thus suggesting a central role of elevated ceramide levels in AD pathology. On the sub-cellular level, immunohistochemical analysis of AD brain showed abnormal expression of ceramides in the astroglia as compared to neurons <sup>317</sup>. In addition, ceramides have also been shown to be elevated in the white matter of AD

brain <sup>318</sup>. The involvement of increased ceramide levels in AD pathogenesis is further emphasized by a recent study that showed that the gene expression of the enzymes involved in the *de novo* synthesis of ceramides is significantly upregulated in AD brain <sup>319</sup>. In addition, increased ceramide synthesis has been implicated in A $\beta$ -induced death of neurons <sup>320, 321</sup> and oligodendrocytes <sup>322</sup> in AD. In chapters 2 and 3, we showed that saturated fatty acids induced tau hyperphosphorylation and amyloidogenic processing of APP in neurons through astroglia-mediated oxidative stress. Furthermore, in chapter 4 we showed that astroglia treatment with PA significantly increased *de novo* synthesis of ceramide. Therefore, the aim of the current study was to investigate the possible involvement of PA-induced, increased astroglial ceramide levels in causing AD-associated, pathophysiological changes observed in neurons.

## **5.2 MATERIALS AND METHODS**

### **5.2.1 Isolation and Culture of Primary Neurons and Astroglia from Rat**

#### **Cortex and Cerebellum**

Primary cortical neurons and astroglia were isolated from the brains of one-day-old Sprague-Dawley rat pups and cultured according to the methods as described in chapter 2. The cells were plated on poly-L-Lysine coated, 6-well plates at the concentration of  $2 \times 10^6$  cells per well in fresh cortical medium [Dulbecco's Modified Eagle's Medium (DMEM and all other media are from Invitrogen, CA) supplemented with 10% horse serum (Sigma, MO), 25 mM glucose, 10 mM HEPES (Sigma), 2 mM glutamine (BioSource International, CA), 100 IU/ml penicillin, and 0.1 mg/ml streptomycin] <sup>176</sup>.

To obtain pure neuronal cell cultures, the medium was replaced with the cortical medium supplemented with 5  $\mu$ M cytosine- $\beta$ -arabinofuranoside (Arac, from Calbiochem, CA) after 3 days of incubation (37°C, 5% CO<sub>2</sub>). After 2 more days, the neuronal culture was switched back to cortical medium without Arac. The neuronal cell culture of more than 95% was obtained by this procedure. The experiments were performed on 6-7 day old neuronal culture. Primary cerebellar neurons were isolated from 7-day-old rat pups, according to enzyme digestion and trituration techniques described previously<sup>323</sup>. Briefly, dissected cerebellar tissue was placed in a cerebellar buffer solution containing 136.89mM NaCl, 5.36mM KCl, 0.34mM Na<sub>2</sub>HPO<sub>4</sub>, 0.44mM KH<sub>2</sub>PO<sub>4</sub>, 5.55mM dextrose, 20.02mM Hepes, and 4.17mM NaHCO<sub>3</sub>, PH 7.4. Cerebellar tissue was minced, transferred to 0.025% trypsin solution in cerebellar buffer, and incubated in water bath for 15 minutes at 37°C. 0.04% DNase I solution in cerebellar medium (DMEM supplemented with 10% horse serum, 25mM KCl, 5 mg/ml insulin, 50  $\mu$ M GABA, 100IU/ml penicillin, and 0.1 mg/ml streptomycin) was then added to inactivate trypsin. After the supernatant was collected from the trituration steps, cerebellar neurons were separated from the debris into 4% BSA solution in cerebellar buffer supplemented with 0.03% MgSO<sub>4</sub>. Finally, the purified neurons were plated onto poly-D-Lysine coated six-well culture dishes at a density of  $2.0 \times 10^5$  cells/ml in 2ml of fresh cerebellar medium. One day after incubation (37°C, 10% CO<sub>2</sub>/95% air), half the medium was subsequently replaced with fresh cerebellar medium supplemented with 20 $\mu$ M cytosine- $\beta$ -arabinofuranoside. Total medium was replaced with fresh cerebellar medium after three days. Afterwards, half of the fresh cerebellar medium was replaced every third day. The experiments were performed on 10-12 day old neuronal culture. To obtain primary

cultures of astroglial cells, the cortical and cerebellar cells from one-day-old and seven-day-old Sprague-Dawley rat pups, respectively were cultured in DMEM/Ham's F12 medium (1:1), 10% fetal bovine serum (Biomed, CA), 100 IU/ml penicillin, and 0.1 mg/ml streptomycin<sup>177</sup>. Cells were grown for 8-10 days (37°C, 5% CO<sub>2</sub>) and culture medium was changed every 2 days. The astroglial cell culture of more than 95% was obtained by this procedure. 24 hours prior to treatment with fatty acids, the medium was changed to neuronal cell culture medium.

### **5.2.2 Immunostaining of Reactive Oxygen Species (ROS)**

Intracellular reactive oxygen species (ROS) were detected by staining with the oxidant-sensitive dye 5-(6)-chloromethyl-2',7'-dichlorodihydrofluorescein diacetate (CM-H<sub>2</sub>DCFDA, from Molecular Probes, OR). H<sub>2</sub>DCFDA is cleaved of the ester groups by intracellular esterases and converted into membrane impermeable, nonfluorescent derivative H<sub>2</sub>DCF. Oxidation of H<sub>2</sub>DCF by ROS results in highly fluorescent 2,7-dichlorofluorescein (DCF)<sup>179</sup>. The cells were incubated for 30 minutes at 37 °C with 2µM CM-H<sub>2</sub>DCFDA in Hanks' Balanced Salt Solution without phenol red (Invitrogen). The cells were then washed three times with PBS and analyzed with confocal microscopy (Zeiss LSM 5 Pascal). A 63X oil-immersion objective lens was used for data acquisition.

### **5.2.3 Western Blot Analysis**

For Western blotting, the following antibodies were used: BACE1 (Chemicon, CA, USA), APP/C99 (QED Bioscience Inc., CA, USA), AT8 (Pierce Biotechnology, IL, USA), PHF-1 (from Dr. P. Davies, Albert Einstein, NY, USA), Tau-1 (Chemicon), GSK-3α/β (Chemicon), Phospho GSK-3α/β (Sigma), MAP Erk1/2 (Cell Signaling), Phospho

MAP Erk1/2 (Cell Signaling Technology, MA, USA), cdk5 (Santa Cruz Biotechnology, CA, USA), p35/p25 (Santa Cruz) and actin (Sigma). To extract membrane proteins (BACE1 and APP/C99), cells were washed three times with ice-cold TBS (25 mM Tris, pH 8.0, 140 mM NaCl, and 5 mM KCl) and lysed for 20 minutes by scraping into ice-cold radioimmunoprecipitation assay (RIPA) buffer [1% (v/v) Nonidet P-40, 0.1% (w/v) SDS, 0.5% (w/v) deoxycholate, 50 mM Tris, pH 7.2, 150 mM NaCl, 1 mM Na<sub>3</sub>VO<sub>4</sub> and 1 mM PMSF, all chemicals from Sigma]<sup>238</sup>. To extract all other proteins, RIPA buffer containing 1% (v/v) Triton, 0.1% (w/v) SDS, 0.5% (w/v) deoxycholate, 20 mM Tris, pH 7.4, 150 mM NaCl, 100 mM NaF, 1 mM Na<sub>3</sub>VO<sub>4</sub>, 1 mM EDTA, 1 mM EGTA, and 1 mM PMSF [all chemicals from Sigma] was used<sup>178</sup>. The total cell lysate was obtained by centrifugation at 12,000 rpm for 15 minutes at 4 °C. The total protein concentration was measured by BCA protein assay kit from Pierce (Rockford, IL, USA). Equal amounts of total protein from each condition were run at 200 V on SDS-PAGE gels (BioRad, CA, USA). The separated proteins were transferred to nitrocellulose membranes for 1 hour at 100 V and incubated at 4 °C overnight with the appropriate primary antibodies [1:1000 BACE1, 1:1000 APP/C99, 1:200 AT8, 1:200 PHF-1, 1:2000 Tau-1, 1:1000 GSK-3 $\alpha/\beta$ , 1:1000 Phospho GSK-3 $\alpha/\beta$ , 1:1000 MAP Erk1/2, 1:1000 Phospho MAP Erk1/2, 1:1000 cdk5, 1:1000 P35/p25, 1:500 GLUT1, 1:2000 actin]. Blots were washed three times in PBS-Tween (PBS-T) and incubated with appropriate HRP-linked secondary antibodies (Pierce) diluted in PBS-T for 1 hr at room temperature. After washing three times in PBS-T, blots were developed with the Pierce SuperSignal West Femto Maximum Sensitivity Substrate (Pierce) and imaged with the BioRad ChemiDoc. Quantity One software from Bio-Rad was used to quantify the signal intensity of the protein bands.

#### **5.2.4 ELISA measurements of A $\beta$ 40 and A $\beta$ 42**

For A $\beta$  measurements, the media and neuronal cells were collected after 24 hours of treatment. The media were treated with protease inhibitor cocktail (Sigma, MO, USA) and cleared by brief centrifugation (3000 rpm, 5 minutes, 40C). A $\beta$ 40 and A $\beta$ 42 in the media were measured by using colorimetric sandwich ELISA according to the manufacturer's instructions (Wako Chemicals, VA, USA). The cells were lysed and the intracellular protein was measured by using the BCA protein assay kit from Pierce (Rockford, IL, USA), which was used to normalize the A $\beta$ 40 and A $\beta$ 42 values.

#### **5.2.5 Data Analyses**

Data are shown as means  $\pm$  S.D. for indicated number of experiments. Student's t-test and one-way ANOVA with Tukey's *post hoc* method were used to evaluate statistical significances between different treatment groups. Statistical significance was set at  $p < 0.05$ .

### **5.3 RESULTS AND DISCUSSION**

#### **5.3.1. Involvement of Astroglial Ceramide in FFA-Astroglia-Induced ROS Production in Neurons**

In chapter 2, we showed that treatment of neurons with the conditioned media from FFA-treated astroglia increased ROS production in neurons. This suggests a central role of astroglial FFA metabolism in the observed FFA-astroglia-induced ROS production in neurons. Furthermore, our literature-based hypothesis followed by mathematical and

experimental studies suggested astroglial ceramide as a possible mediator of ROS production in neurons (as discussed in chapter 4). In this context, here we found that inhibition of *de novo* synthesis of ceramide in PA-treated astroglia by using 2 mM L-CS, significantly inhibited PA-astroglia-induced ROS production in neurons (**Figure 5.2**). The treatment of neurons directly with L-CS did not inhibit the PA-astroglia-induced ROS production observed in neurons. This further emphasizes the role of astroglial ceramide in causing ROS production in neurons.

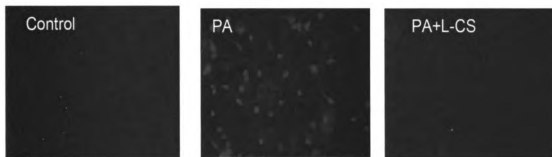


**Figure 5.2. Involvement of astroglial ceramide in PA-astroglia-induced ROS production in neurons.** Co-treatment of astroglia with 2mM L-CS inhibited PA-astroglia-induced ROS production in neurons. The neurons were stained with CM-H2DCFDA for intracellular ROS detection and examined with confocal fluorescence microscopy. (Objective lens magnification, 40X).

As mentioned earlier, ceramide secreted from astroglia can act directly on neurons and mediate the oxidative stress-induced effects in the neurons<sup>304</sup>. In addition, PA-induced increase in ceramide levels can induce the secretion of cytokines (e.g. IL-6)<sup>305</sup> or other signaling molecules, e.g. NO<sup>306</sup> by astrocytes, which in turn may elevate the production of ROS in the neurons<sup>307, 308</sup>. In this context, we found that PA treatment did not induce IL-6 expression in astroglia, however it increased the level of inducible nitric oxide synthase (iNOS) in astroglia, which was blocked by the co-treatment of astroglia with 2mM L-CS, thus suggesting an involvement of ceramide in astroglial iNOS expression (**Figure 5.3**).

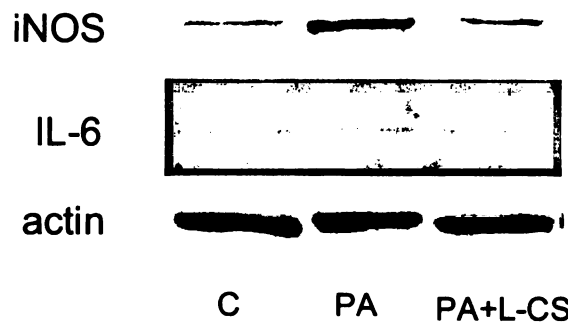


**Figure 5.3. The expression of iNOS and IL-6 in astroglia.** The expression of iNOS, but not IL-6 was increased by PA treatment in astroglia. Co-treatment of astroglia with 2mM L-CS inhibited PA-induced iNOS expression in astroglia.  $\beta$ -actin is shown as a marker for protein loading.

### 5.3.2 Involvement of astroglial ceramide in FFA-astroglia-induced amyloidogenesis and tau hyperphosphorylation in neurons

We treated cortical astroglia with 0.2mM PA for 24 hours and then used the astroglia-conditioned media to treat cortical neurons for 24 hours. After 24 hours of treatment, the media were collected for measurement of secreted A $\beta$  levels and the neurons were washed, lysed and the total cellular protein was used for western blot analysis of a number of proteins. As shown in **Figure 5.4**, treatment of neurons with the conditioned media from PA-treated astroglia significantly increased BACE1 levels and consequent amyloidogenic processing of APP leading to the formation of c-terminal fragments of APP (C99) (**Figure 5.4**). C99 is processed by  $\gamma$ -secretase to form A $\beta$ . BACE1 is a rate-limiting enzyme in the amyloidogenic processing of APP and a slight increase in BACE1 levels leads to a dramatic increase in the production of A $\beta$ <sub>40/42</sub><sup>243</sup>. Indeed, we found that the PA-astroglia-treated neurons significantly increased secretion of A $\beta$ <sub>40</sub> and A $\beta$ <sub>42</sub> as compared to controls (**Figure 5.4**).



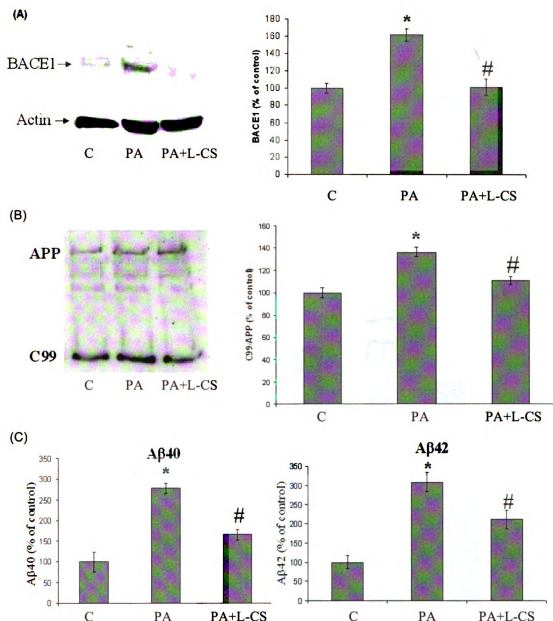


**Figure 5.4. Involvement of astroglial ceramide in PA-astroglia-induced elevations in BACE1 and amyloidogenic processing of APP in neurons.** In neurons treated with conditioned media from PA-treated astroglia, the levels of (A) BACE1, (B) C99 and (C) Aβ40 and Aβ42 were found elevated. These PA-astroglia-induced tau abnormalities were blocked by inhibiting astroglial ceramide synthesis with 2mM L-CS. Data represent mean ± S.D. of three independent experiments. One-way ANOVA with Tukey's post hoc method was used for analyzing the differences between treatment groups. \*,  $p < 0.05$  compared with control; #,  $p < 0.05$  compared with PA treatment.

In addition, phosphorylation of tau was significantly increased in neurons treated with the conditioned media from PA-treated astroglia as observed by immunoblotting with two different antibodies, PHF-1 and AT8 (**Figure 5.5**). As mentioned earlier, PHF-1 and AT8 antibodies recognize tau protein hyperphosphorylated at two different, AD-specific phospho-epitopes. In addition to PHF-1 and AT8 antibodies, we also carried out immunoblotting with Tau-1 antibody, which detects all the isoforms of dephosphorylated tau, thus acting as a negative control. As expected, dephosphorylated Tau-1 was significantly decreased in PA-astroglia-treated neurons as compared to control-astroglia-treated neurons (**Figure 5.5**).

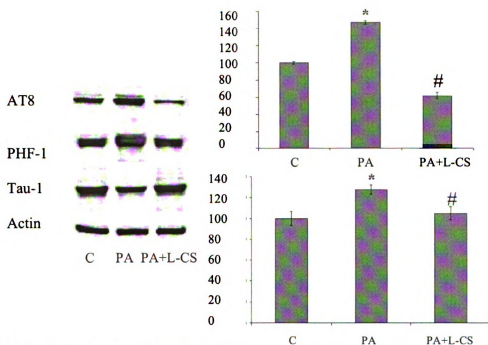


**Figure 5.5. Involvement of astroglial ceramide in PA-astroglia-induced tau hyperphosphorylation in neurons.** In neurons treated with conditioned media from PA-treated astroglia, tau was found pathologically hyperphosphorylated as shown by immunoblotting with PHF-1 and AT8 antibodies. Tau-1 detects dephosphorylated tau, thus showing decreased levels in PA-astroglia-treated neurons. These PA-astroglia-induced tau abnormalities were blocked by inhibiting astroglial ceramide synthesis with 2mM L-CS. Histograms corresponding to PHF-1 and AT8 blots represent quantitative determinations of intensities of the relevant bands normalized with actin. Data represent mean  $\pm$  S.D. of three independent experiments. One-way ANOVA with Tukey's post hoc method was used for analyzing the differences between treatment groups. \*,  $p < 0.05$  compared with control; #,  $p < 0.05$  compared with PA treatment.

As PA treatment was found to elevate *de novo* synthesis of ceramide in astroglia, we wanted to investigate a possible involvement of astroglial ceramide in the observed, PA-astroglia-induced amyloidogenesis and tau hyperphosphorylation in neurons. For this, we treated astroglia with 2mM L-CS together with 0.2mM PA for 24 hours and then transferred the astroglia-conditioned medium to the neurons (24 hours treatment). The inhibition of astroglial ceramide synthesis by L-CS treatment blocked PA-astroglia-induced BACE1 upregulation, A $\beta$  production and hyperphosphorylation of tau (**Figures 5.4 and 5.5**), strongly suggesting a central role of astroglial ceramide in causing AD-associated pathophysiological changes in neurons. Previously, exogenous addition of ceramide to neurons has been shown to induce A $\beta$  production<sup>324</sup>. Furthermore, increased tau phosphorylation has been reported in cholesterol-deficient neurons, which had a significant increase in ceramide levels<sup>325</sup>. Our findings reported here, however, are the first to demonstrate a direct causal role of astroglial PA metabolism and endogenously synthesized ceramide in astroglia, in causing A $\beta$  production and tau hyperphosphorylation in neurons, two characteristic signatures of AD pathology.

We further studied the possible activation of various AD-related kinases (GSK-3 $\alpha/\beta$ , cdk5 and MAPK Erk1/2)<sup>75</sup>, one or more of which may be responsible for the observed PA-astroglia-induced tau hyperphosphorylation, and potentially activated by ceramide. An increase in the phosphorylation of these enzymes was used as an indicator of their activation. As shown in **Figure 5.6A**, levels of phosphorylated GSK-3 $\alpha/\beta$  (Tyr279/Tyr216) were significantly increased in PA-astroglia-treated neurons as compared to controls, without any significant change in the levels of total GSK-3 $\alpha/\beta$ .

GSK-3 $\alpha$  phosphorylated at Tyr279 and GSK3- $\beta$  phosphorylated at Tyr216 suggest increased activity <sup>326</sup>. In addition to activating GSK-3 $\alpha/\beta$ , PA-treatment also increased the cleavage of cdk5 activator p35 to p25 (**Figure 5.6B**). p25 accumulates in the brains of AD patients and the conversion of p35 to p25 suggests augmented activity of cdk5 <sup>327, 328</sup>. Finally, there was no change in the levels of both total and phosphorylated MAPK Erk1/2 in the PA-astroglia-treated neurons as compared to control-astroglia-treated ones (**Figure 5.6C**), suggesting no change in its activity. The treatment of astroglia with 2mM L-CS inhibited both the PA-astroglia-induced increase in the level of phosphorylated GSK-3 $\alpha/\beta$  and the cleavage of p35 to p25 (**Figure 5.6A and B**).

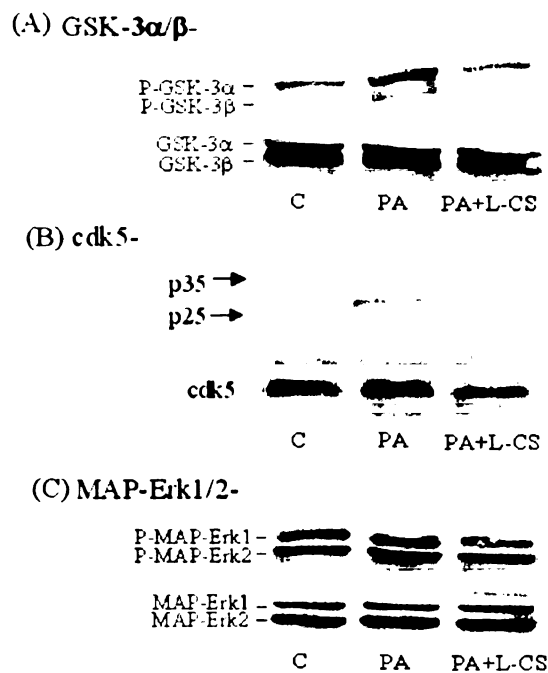


**Figure 5.6. PA-astroglia-induced activation of AD-specific kinases in neurons is mediated by astroglial ceramide.** Conditioned media from PA-treated astroglia activated (A) GSK-3 (increased levels of phosphorylated GSK-3) and (B) cdk5 (increased cleavage of p35 to p25) but not (C) MAP- Erk1/2 (no change in the levels of phosphorylated MAP- Erk1/2). The treatment of astroglia with 2mM L-CS inhibited PA-astroglia-induced activation of both GSK-3 and cdk5. Data are representative of 3 different experiments.

To further evaluate the possible involvement of these enzymes in PA-astroglia-induced tau hyperphosphorylation in neurons, we treated neurons with pharmacological inhibitors of these enzymes; 10mM LiCl (for GSK-3 $\alpha/\beta$ ), 10 $\mu$ M Roscovitine (for cdk5) and 30 $\mu$ M PD98059 (for MAPK Erk1/2). Treatment with PD98059 did not inhibit PA-astroglia-induced tau hyperphosphorylation in neurons (**Figure 5.7**), which is in agreement with the lack of activation of MAPK Erk1/2 (**Figure 5.6C**). Furthermore, although cdk5 was activated in neurons (**Figure 5.6B**), co-treatment of neurons with a potent cdk5 inhibitor, roscovitine, did not inhibit the observed PA-astroglia-induced hyperphosphorylation of tau (**Figure 5.7**). This suggests that PA-astroglia-induced hyperphosphorylation of tau in primary rat cortical neurons is independent of the observed activation of the cdk5 pathway. Our results agree with a previous report that showed that cleavage of p35 to p25 and subsequent activation of cdk5 were not involved in the hyperphosphorylation of tau in primary rat hippocampal neurons <sup>329</sup>. On the other hand, GSK-3 inhibitor (LiCl) inhibited the PA-astroglia-induced hyperphosphorylation of tau in neurons (**Figure 5.7**). Previously, GSK-3 has been shown to be involved in causing both tau hyperphosphorylation and A $\beta$  production and thus, is central and essential in the development of AD. GSK-3 $\beta$  is involved in hyperphosphorylation of tau and its other isoform, GSK-3 $\alpha$ , is involved in A $\beta$  production by regulating the activity of  $\gamma$ -secretase <sup>330, 331</sup>. These studies together with our present data further emphasize the central role of PA-induced, abnormal astroglial ceramide metabolism in causing AD-associated pathophysiological characteristics.

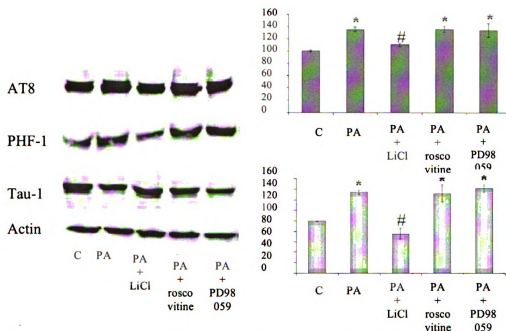


**Figure 5.7. GSK-3 is involved in PA-astroglia-induced tau hyperphosphorylation in neurons.** Astroglia-conditioned media were transferred to neurons, with or without various kinase inhibitors, viz., 10mM LiCl2 (GSK-3 inhibitor), 10mM Roscovitine (cdk-5 inhibitor) and 30mM PD98059 (MAPK inhibitor). Immunoblot analysis with PHF-1 and AT8 antibodies show that only LiCl inhibited the observed, PA-induced tau hyperphosphorylation in neurons. Histogram data represent mean  $\pm$  S.D. of three independent experiments. One-way ANOVA and Tukey's post hoc method was used for analyzing the differences between treatment groups. \*,  $p < 0.05$  compared with control; #,  $p < 0.05$  compared with PA treatment.

### 5.3.3 A possible explanation for the region-specific and cell type-specific damage observed in AD

AD is a peculiar neurodegenerative disease in that the observed pathophysiological and metabolic damages are found to be region-specific and cell type-specific. Basal forebrain, cortex and hippocampus are affected while cerebellum is relatively spared. Also, cholinergic neurons are most affected<sup>332, 333</sup>. Here, it is interesting to note that different brain regions show differential FFA metabolic activities; the activity of fatty acyl-CoA synthetase (FACS) is 10X lower in cerebellum as compared to the other affected brain regions<sup>334</sup>. FACS is the first enzyme involved in cellular FFA metabolism, which

converts fatty acid to fatty acyl-CoA, which is then utilized by the cells in catabolic (e.g.  $\beta$ -oxidation) and anabolic (e.g. ceramide synthesis) pathways<sup>335</sup>. ceramide production in cerebellum is 2X and 4X lower as compared to cortex and hippocampus, respectively<sup>336</sup>. These studies together with our present data may suggest that under pathologically elevated levels of saturated FFAs, cerebellum may be less likely to be affected by abnormal FFA metabolism due to its lower activity level of FACS and consequent, lower levels of ceramide, as compared to cortex and hippocampus. This may explain in part the region-specific damage observed in AD brain. To further investigate this hypothesis, we carried out experiments, whereby we treated cortical neurons (CTN) with the conditioned media from cortical astrocytes (CTA) and from cerebellar astrocytes (CBA). In line with the results discussed earlier, the conditioned media from PA-treated CTA increased tau hyperphosphorylation in CTN (**Figure 5.8A**). The conditioned media from PA-treated CBA, however, did not increase the phosphorylation of tau in CTN (**Figure 5.8B**).

Furthermore, we had previously shown that FFA metabolism by astroglia results in increased reactive oxygen species (ROS) production in neurons<sup>337, 338</sup>. The elevated ROS, in turn, were found to be involved in causing BACE1 upregulation and tau hyperphosphorylation in neurons<sup>337, 338</sup>, suggesting a central role of oxidative stress in the FFA-induced damage. Thus, elevated FFA metabolism associated with higher FACS activity in the affected regions (basal forebrain, cortex and hippocampus) may lead to increased oxidative stress in these regions compared to unaffected ones (cerebellum). In this context, it is interesting to note that in AD brains, oxidative stress markers are higher in the affected regions than in the unaffected ones<sup>339, 340</sup>. The increased oxidative stress

may be particularly damaging to the basal forebrain cholinergic neurons as these neurons have been shown to lack an important anti-oxidative enzyme, seleno-glutathione peroxidase<sup>341</sup>. This may account, in part, for the cell type-specific damage observed in AD pathology; substantial loss of basal forebrain cholinergic neurons is a distinct feature of AD<sup>342</sup>. Furthermore, these basal forebrain cholinergic neurons, through their long ascending projections, innervate cortical and hippocampal regions<sup>343</sup> and the increased oxidative stress in these regions of AD brain may lead to the degeneration of these projections from the cholinergic neurons. In this context, it is also interesting to note that A $\beta$  plaques, hallmarks of AD, have been shown to be specifically located where the projection of the basal forebrain cholinergic neurons degenerate<sup>344, 345</sup>.

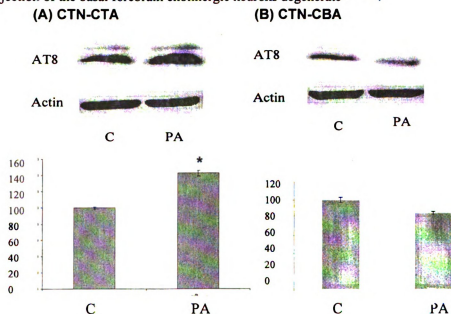


**Figure 5.8. Differential effects of cortical and cerebellar astroglia on cortical neurons.** Cortical neurons (CTN) were treated with conditioned media from (A) cortical astroglia (CTA) and (B) cerebellar astroglia (CBA). Western blot analysis of hyperphosphorylated tau was performed using AT8 antibody. Cortical astroglia but not cerebellar astroglia were involved in PA-induced tau hyperphosphorylation in neurons. Data represent mean  $\pm$  S.D. of three independent experiments. Student's t-test was used for analyzing differences between different treatment groups. \*,  $p < 0.05$  compared with control.



## 5.4 CONCLUSIONS

In conclusion, astroglial ceramide was found to be involved in the observed PA-astroglia-induced ROS production in neurons. Astroglial ceramide was also found involved in the PA-astroglia-induced hyperphosphorylation of tau in neurons. Although astroglial ceramide activated both GSK-3 $\alpha/\beta$  and cdk5 in neurons, only GSK-3 $\alpha/\beta$  was found to be involved in PA-astroglia-induced hyperphosphorylation of tau. Furthermore, Astroglial ceramide increased BACE1 levels and consequent amyloidogenic processing of APP leading to the production of A $\beta$ 40/42. Thus, the present results establish a central role of astroglial fatty acid metabolism and consequent increase in the *de novo* synthesis of astroglial ceramide in causing two of the major pathophysiological changes associated with AD, tau hyperphosphorylation and A $\beta$  production.

## CHAPTER 6 CONCLUSIONS AND FUTURE DIRECTIONS

### 6.1 Conclusions

The objective of this dissertation was to investigate the potential involvement of saturated fatty acids in causing AD-associated pathophysiological and abnormal metabolic changes. Our studies established a complex functional interaction between neuronal and non-neuronal (astroglial) cells, leading to the AD-specific abnormalities under the conditions of pathologically elevated levels of saturated fatty acids. It was shown that saturated fatty acids had no direct deleterious effects on neurons; however, they caused increased oxidative stress in neurons through astroglial mediation. Fatty acid-induced oxidative stress played a central role in the hyperphosphorylation of tau and amyloidogenic processing of APP, two of the important characteristics of AD pathology. Both metabolic modeling (MFA) and experimental data suggested a key role of astroglial ceramide in causing FFA-induced, AD-associated abnormalities in neurons. Note that this was the first-ever attempt to apply MFA to comprehensively study the primary astroglial metabolism. Our data place “astroglial fatty acid metabolism” at the center of the pathogenic cascade in AD and also suggest “astroglial ceramide” as a potentially important target for therapeutic intervention in AD.

Based on our findings, we hypothesize the following sequence of cellular events by which saturated FFAs may play a central role in the pathogenesis of AD (**Figure 6.1**). The brain experiences chronically elevated levels of saturated FFAs. Saturated FFAs are taken up and metabolized by astroglia, downregulating astroglial GLUT1 levels and glucose metabolism. Astroglial FFA metabolism also results in increased levels of

ceramides. Ceramides then induce secretion of cytokines (e.g. IL-1 $\beta$ , TNF- $\alpha$  etc.) or other signaling molecules (e.g. NO, due to increased expressed iNOS expression) by astroglia, which may induce ROS production in neurons. Increased oxidative stress in neurons causes BACE1 upregulation and GSK-3 activation resulting in increased A $\beta$  production and hyperphosphorylation of tau, respectively. The sequence of events suggested here is similar to that observed in AD pathology- decreased glucose metabolism is an early event, which together with increased oxidative stress precedes the pathophysiological changes observed in AD (NFTs and A $\beta$  plaques). Furthermore, the present “FFA-AD” hypothesis also provides a possible explanation for the region-specific and cell type-specific damage observed in AD (Chapter 5).

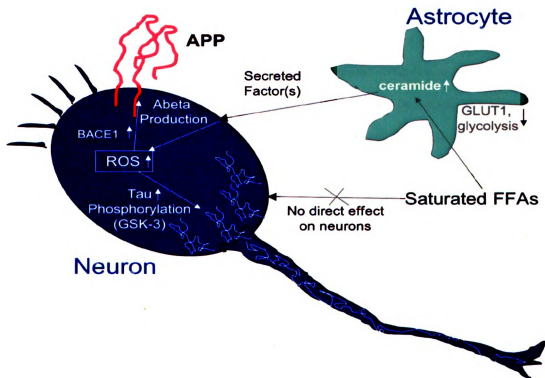


**Figure 6.1. The “FFA-AD” hypothesis.** Proposed cellular mechanism by which astroglial FFA metabolism may play a central role in causing pathophysiological and metabolic changes associated with AD.

The low level of ceramide production in cerebellar astroglia as compared to cortical and hippocampal astroglia <sup>336</sup>, may play a key role in the little damage observed in cerebellum of AD brain as opposed to other regions. Due to the low flux of saturated FFAs through sphingolipid pathway in cerebellar astroglia, FFAs may be diverted to other metabolic pathways, e.g.  $\beta$ -oxidation of fatty acids, which may lead to the increased production of ketone bodies. Here it is interesting to note that ketone bodies have been shown to act as anti-oxidants in that they protect neuronal cells from A $\beta$ -induced oxidative damage <sup>346</sup>. This may further explain why cerebellum is relatively spared in AD.

It is also noteworthy that the single-most factor strongly correlated with AD is aging. Therefore, any hypothesis to explain AD pathology must provide an explanation for the correlation between aging and incidence of AD. Increased oxidative stress has been strongly associated with aging, which might be a result of decreased anti-oxidant enzymatic capacity with aging <sup>54, 347</sup>. Under these conditions, enhanced production of ROS induced by saturated FFAs may make the brain more vulnerable to increased oxidative damage as compared to age-matched controls with low levels of saturated FFAs. Thus, our present hypothesis may explain the link between age and the higher incidence of AD.

Despite these supporting data, our “FFA-AD” hypothesis is unable to explain the AD pathology comprehensively at this juncture. Specifically, although our cell-culture studies showed potential involvement of saturated fatty acids in causing both the

amyloidogenesis and the hyperphosphorylation of tau, in animals high fat diet has been shown to cause only increased A $\beta$  production but not the tau hyperphosphorylation and the NFT formation associated with it <sup>122-124</sup>. The reason behind these disparities between *in vitro* and *in vivo* findings is not well understood. In addition, some studies suggest the tau protein abnormalities initiate the AD cascade, while others emphasize A $\beta$  deposits as the causative factors in AD <sup>348</sup>. Our present data is unable to shed any light on this ongoing debate.

Furthermore, in the present studies we established a central role of FA-induced oxidative stress in causing AD-associated abnormalities. However, oxidative stress has been shown to be central to many other brain diseases, e.g. Parkinson's disease <sup>349</sup>, in addition to AD. Therefore, it is not clear how FFA-induced oxidative stress is specific to AD pathology. In other words, it is not clear how FFA-induced oxidative stress would lead to AD-specific changes but would not induce abnormalities associated with other diseases, in which oxidative stress plays a key role. All the high fat diet animal models show only AD-specific changes in their brain. Our current data does not provide any explanation for this important, fundamental question.

In addition, AD follows a specific spatio-temporal pattern of neurodegeneration, where neurodegeneration starts at the basal forebrain and with time proceeds to entorhinal cortex, hippocampus, parts of limbic system and associative cortex <sup>350</sup>. The basal forebrain cholinergic neurons lack an important anti-oxidative enzyme, seleno-glutathione peroxidase <sup>341</sup>. This may explain their higher vulnerability to the FFA-

induced increased oxidative stress. It is not clear, however, how saturated fatty acids would contribute to the characteristic spatio-temporal neuronal damage observed in AD.

Furthermore, our present data explain the potential involvement of saturated fatty acids in the increased A $\beta$  production. However, it is not just the increased production of A $\beta$ , but also its aggregation that is important in AD pathology. To be specific, neither monomeric nor mature aggregated polymeric forms, but the intermediate oligomeric forms of A $\beta$  are responsible for the AD-associated neurotoxicity<sup>351</sup>. In fact, a very recent study showed that accelerating A $\beta$  fibrillization which reduced A $\beta$  oligomer levels, helped in reducing functional deficits in AD mouse models<sup>352</sup>. Our present data do not answer if (and how) saturated fatty acids play a role in the A $\beta$  oligomerization.

Here, it is also important to note that the risk of AD is higher in women as compared to men<sup>353</sup>. It is not clear if saturated fatty acids play any role in the gender-specificity associated with AD. The decreased level of estrogen hormone in menopausal women has been suggested to increase the risk for AD in women<sup>354</sup>. It is not clear at present, if there is any correlation between saturated fatty acids and estrogen levels, that may lead to increased risk for AD development in women as compared to men, under the condition of elevated levels of saturated FFAs.

Finally, our present studies established a central role of astroglia in causing FFA-induced, AD-associated abnormalities. The critical role of astroglia in AD pathology has been suggested previously by many studies. Increased expression of iNOS in astroglia and

consequent increase in NO levels has been shown to stimulate A $\beta$  production and hyperphosphorylation of tau in neurons<sup>355, 356</sup>. Furthermore, reactive astrogliosis associated with AD has been suggested to induce glutamate release, which may lead to excitotoxicity and cell death in neurons<sup>357, 358</sup>. In addition, astroglial apoptosis has been associated with AD and A $\beta$  has been shown to induce astroglial cell death<sup>359, 360</sup>. This astroglial cell death may result in the “loss of good function”, to support the neurons under normal conditions. Together these data place astroglia at the centre stage of AD pathology. However, the major limitation of all these studies, including ours, is that the astroglia are used in these studies as a whole population. It would be worthwhile to investigate the possible involvement of Type I and Type II astroglia separately, in causing AD-associated damage. These data may prove invaluable in finding novel clues that may further help in establishing the in-depth disease mechanism.

## **6.2 Future Directions**

Our cell-culture based studies presented in this dissertation have provided important information regarding the key role of saturated fatty acids in causing AD-associated abnormalities. As discussed above, many questions remain unanswered and thus, need further scientific investigation. The focus of the future investigation will be specifically on the following studies as discussed below.

### **6.2.1 *In vivo* studies**

Future work should focus on animal studies where cerebral FFA metabolism will be studied in terms of the *de novo* synthesis of ceramide at the regional (e.g. cortex,

hippocampus vs. cerebellum) as well as sub-cellular (astroglia vs. neurons) levels in response to various diets and stimuli in APP transgenic mice, e.g. Tg2576. This line of mice expresses human APP695 with the 670/671 “Swedish” double mutation and show clear age-dependent A $\beta$  deposition and memory deficits <sup>39</sup>. It would be a significant step forward in AD research if saturated FFAs are shown to exert their risk for the development of AD *in vivo*, through a similar mechanism as observed in the current *in vitro* studies. Furthermore, the potential importance of ceramide as a therapeutic target for AD should also be further studied in these animals by using pharmacological inhibitors of *de novo* synthesis of ceramide, e.g. L-CS, D-serine, myriocin (ISP-1), fumonisin B1, viridifungin A, sphingofungin B or lipoxamycin. Decreased A $\beta$  production and its deposition in the brains of these mice would serve as measures of the potential protective effects of these ceramide inhibitors.

### **6.2.2 Delivery of ceramide inhibitors through the blood-brain barrier (BBB)**

With the use of ceramide inhibitors *in vivo*, one of the greatest challenges, which also presents a great research opportunity, is to find ways for efficient transport of these inhibitors across the BBB. In its neuroprotective role, the BBB prevents the delivery of many important therapeutic agents to the brain; more than 98% of currently available therapeutics cannot pass through the BBB <sup>361</sup>. Future studies should investigate the use of novel delivery systems, e.g. nanoparticles, as carriers of ceramide inhibitors to the brain. In addition to their ability to cross the BBB, these vehicles should also be engineered so as to deliver ceramide inhibitors specifically to astroglia, e.g. by attaching astroglia-



specific antibody (GFAP) to nanoparticles. In addition to their use in AD, these successful delivery vehicles will also prove useful in treating other brain diseases.

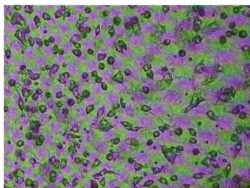
### **6.2.3 Studying pathways downstream to ceramide**

One of the major limitations with ceramide as a therapeutic target is its important role as a signaling molecule in many physiological processes. In addition, the currently available ceramide inhibitors mentioned earlier have very high toxicities, weak inhibition activity and also exhibit low specificity<sup>362, 363</sup>. Thus, it would also be worthwhile to focus future studies on the pathways downstream of ceramide generation that may be involved in FFA-induced, AD-associated abnormalities, e.g. ceramide-induced secretion of inflammatory cytokines or other signaling molecules such as NO from astroglia.

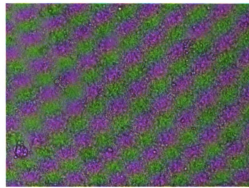
## APPENDIX

### 1. Brain cells from older animals

In our studies we used cortical neurons and astroglia from 1-2-day old rat pups. As AD is strongly associated with aging, use of brain cells from older animals would be more appropriate for these AD studies. However, it is difficult to isolate the cortical cells from the brains of older rats and their viability reduced significantly; the cortical cells isolated from 7-day old rat pups started dying after 2 days in culture.



Day 1

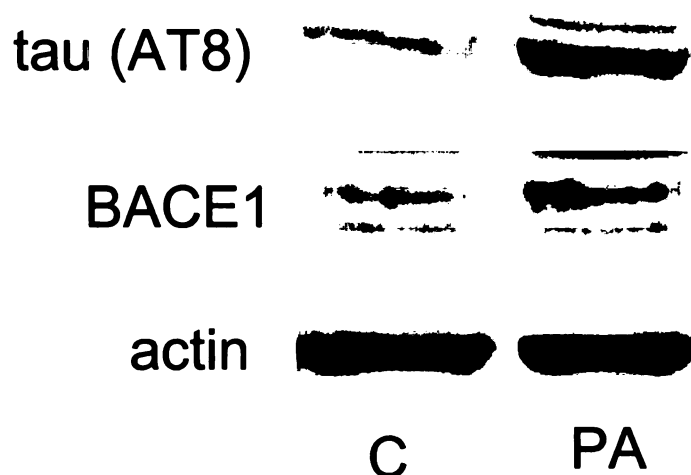


Day 2

### 2. Trans-well experiments

In our studies, the conditioned media from astroglia were transferred to neurons, so the two cell types did not share the same growth environment. Physiologically, however, neurons and astroglia are in close proximity and share common growth environment where secreted factors from both the neurons and astroglia may affect both these cell types. We investigated the possible effect of potential factors secreted from the neurons that may affect astroglia, which in turn may modulate the observed astroglial effects on

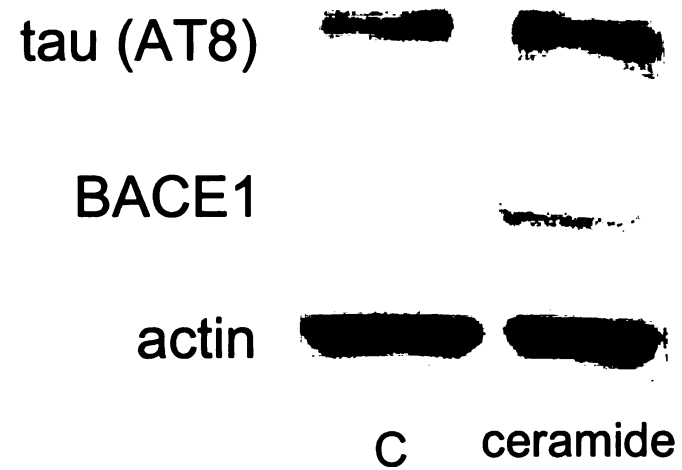
the neurons using trans-well tissue culture. The astroglia were plated in the well inserts and neurons in the wells. The cells were then treated with either 0.2mM PA or 4% BSA (control) and levels of BACE1 and phosphorylated tau in neurons were studied. We found that PA-treatment significantly increased levels of BACE1 and phosphorylated tau in neurons, similar to our non-trans-well experiments.



### 3. Exogenous addition of ceramide as a positive control

Our studies showed a central role of astroglial ceramide in the FFA-astroglia-induced, AD-associated pathophysiological changes observed in neurons. The role of astroglial ceramide was confirmed by HPLC measurement of elevated ceramide and also by using a pharmacological inhibitor of ceramide synthesis in astroglia. As a positive control, we exogenously added 10 $\mu$ M C-6 ceramide (a synthetic analog of ceramide, Sigma) to astroglia for 24hr, followed by the transfer of the astroglia-conditioned media to neurons (24hr treatment). We found that C-6 ceramide significantly increased levels of BACE1

and phosphorylated tau in neurons, thus further emphasizing role of ceramide in causing AD-associated abnormalities.



## LIST OF PUBLICATIONS

This thesis is based on our following original publications-

- 1) **Patil, S.** and Chan, C., "Palmitic and Stearic fatty acids induce Alzheimer-like hyperphosphorylation of tau in primary rat cortical neurons", **Neuroscience Letters**, 384: 288-293 (2005).
- 2) **Patil, S.**, Lufang, S., Masserang, A. and Chan, C., "Palmitic acid-treated astrocytes induce BACE1 upregulation and accumulation of C-terminal fragment of APP in primary cortical neurons", ", **Neuroscience Letters**, 406: 55-59 (2006).
- 3) **Patil, S.**, Li, Z. and Chan, C., "Cellular to Tissue Informatics: Approaches to Optimizing Cellular Function of Engineered Tissue", **Advances in Biochemical Engineering / Biotechnology**, eds. K. Lee and D. Kaplan, 102: 139-159 (2006).
- 4) **Patil, S.**, Melrose, J. and Chan, C., "Involvement of astroglial ceramide in palmitic acid-induced Alzheimer-like changes in primary neurons", (Accepted, **European Journal of Neuroscience**).
- 5) **Patil, S.**, Balu, D., Melrose J. and Chan, C., "Brain region specificity of palmitic acid-induced Alzheimer-like changes in primary neurons", (In Preparation).

## BIBLIOGRAPHY

1. Korczyn, A. D.; Vakhapova, V., The prevention of the dementia epidemic. *J Neurol Sci* **2007**, 257, (1-2), 2-4.
2. Wang, D. C.; Chen, S. S.; Lee, Y. C.; Chen, T. J., Amyloid-beta at sublethal level impairs BDNF-induced arc expression in cortical neurons. *Neurosci Lett* **2006**, 398, (1-2), 78-82.
3. Mattson, M. P., Pathways towards and away from Alzheimer's disease. *Nature* **2004**, 430, (7000), 631-9.
4. Mosconi, L., Brain glucose metabolism in the early and specific diagnosis of Alzheimer's disease. *Eur J Nucl Med Mol Imaging* **2005**, 32, (4), 486-510.
5. Ogawa, M.; Watabe, H.; Teramoto, N.; Miyake, Y.; Hayashi, T.; Iida, H.; Murata, T.; Magata, Y., Understanding of cerebral energy metabolism by dynamic living brain slice imaging system with [18F]FDG. *Neurosci Res* **2005**, 52, (4), 357-361.
6. Goate, A.; Chartier-Harlin, M. C.; Mullan, M.; Brown, J.; Crawford, F.; Fidani, L.; Giuffra, L.; Haynes, A.; Irving, N.; James, L., Segregation of a missense mutation in the amyloid precursor protein gene with familial Alzheimer's disease. *Nature* **1991**, 349, (6311), 704-6.
7. Mullan, M.; Crawford, F.; Axelman, K.; Houlden, H.; Lilius, L.; Winblad, B.; Lannfelt, L. A pathogenic mutation for probable Alzheimer's disease in the APP gene at the N-terminus of beta-amyloid. *Nat Genet* **1992**, (1), 345-7.
8. Sherrington, R.; Rogaev, E. I.; Liang, Y.; Rogaeva, E. A.; Levesque, G.; Ikeda, M.; Chi, H.; Lin, C.; Li, G.; et al., Cloning of a gene bearing missense mutations in early-onset familial Alzheimer's disease. *Nature* **1995**, 375, (6534), 754-60.
9. Levy-Lahad, E.; Wasco, W.; Poorkaj, P.; Romano, D. M.; Oshima, J.; Pettingell, W. H.; Yu, C. E.; Jondro, P. D.; Schmidt, S. D.; Wang, K., Candidate gene for the chromosome 1 familial Alzheimer's disease locus. *Science* **1995**, 269, (5226), 973-7.
10. Hoyer, S., Brain glucose and energy metabolism abnormalities in sporadic Alzheimer disease. Causes and consequences: an update. *Exp Gerontol* **2000**, 35, (9-10), 1363-1372.

11. Rogaeva, E. A.; Fafel, K. C.; Song, Y. Q.; Medeiros, H.; Sato, C.; Liang, Y.; Richard, E.; Rogaev, E. I.; Frommelt, P.; Sadovnick, A. D.; Meschino, W.; Rockwood, K.; Boss, M. A.; Mayeux, R.; St George-Hyslop, P., Screening for PS1 mutations in a referral-based series of AD cases: 21 novel mutations. *Neurology* **2001**, *57*, (4), 621-5.
  
12. Corder, E. H.; Saunders, A. M.; Strittmatter, W. J.; Schmechel, D. E.; Gaskell, P. C.; Small, G. W.; Roses, A. D.; Haines, J. L.; Pericak-Vance, M. A., Gene dose of apolipoprotein E type 4 allele and the risk of Alzheimer's disease in late onset families. *Science* **1993**, *261*, (5123), 921-3.
  
13. Haan Mary, N.; Wallace, R., Can dementia be prevented? Brain aging in a population-based context. *Annu Rev Public Health* **2004**, *25*, 1-24.
  
14. Alzheimer, A.; Stelzmann, R. A.; Schnitzlein, H. N.; Murtagh, F. R., An English translation of Alzheimer's 1907 paper, "Über eine eigenartige Erkankung der Hirnrinde". *Clin Anat* **1995**, *8*, (6), 429-31.
  
15. Wimo, A.; Jonsson, L.; Winblad, B., An estimate of the worldwide prevalence and direct costs of dementia in 2003. *Dement Geriatr Cogn Disord* **2006**, *21*, (3), 175-81.
  
16. Fratiglioni, L.; De Ronchi, D.; Aguero-Torres, H., Worldwide prevalence and incidence of dementia. *Drugs Aging* **1999**, *15*, (5), 365-75.
  
17. Wolf-Klein, G.; Pekmezaris, R.; Chin, L.; Weiner, J., Conceptualizing Alzheimer's disease as a terminal medical illness. *Am J Hosp Palliat Care* **2007**, *24*, (1), 77-82.
  
18. Selkoe, D. J., Toward a comprehensive theory for Alzheimer's disease. Hypothesis: Alzheimer's disease is caused by the cerebral accumulation and cytotoxicity of amyloid beta-protein. *Ann N Y Acad Sci* **2000**, *924*, 17-25.
  
19. Perry, E. K.; Tomlinson, B. E.; Blessed, G.; Bergmann, K.; Gibson, P. H.; Perry, R. H., Correlation of cholinergic abnormalities with senile plaques and mental test scores in senile dementia. *Br Med J* **1978**, *2*, (6150), 1457-9.
  
20. Cummings, B. J.; Cotman, C. W., Image analysis of beta-amyloid load in Alzheimer's disease and relation to dementia severity. *Lancet* **1995**, *346*, (8989), 1524-8.

21. Citron, M.; Oltersdorf, T.; Haass, C.; McConlogue, L.; Hung, A. Y.; Seubert, P.; Vigo-Pelfrey, C.; Lieberburg, I.; Selkoe, D. J., Mutation of the beta-amyloid precursor protein in familial Alzheimer's disease increases beta-protein production. *Nature* **1992**, 360, (6405), 672-4.
22. Cai, X. D.; Golde, T. E.; Younkin, S. G., Release of excess amyloid beta protein from a mutant amyloid beta protein precursor. *Science* **1993**, 259, (5094), 514-6.
23. Haass, C.; Hung, A. Y.; Selkoe, D. J.; Teplow, D. B., Mutations associated with a locus for familial Alzheimer's disease result in alternative processing of amyloid beta-protein precursor. *J Biol Chem* **1994**, 269, (26), 17741-8.
24. Suzuki, N.; Cheung, T. T.; Cai, X. D.; Odaka, A.; Otvos, L., Jr.; Eckman, C.; Golde, T. E.; Younkin, S. G., An increased percentage of long amyloid beta protein secreted by familial amyloid beta protein precursor (beta APP717) mutants. *Science* **1994**, 264, (5163), 1336-40.
25. Citron, M.; Vigo-Pelfrey, C.; Teplow, D. B.; Miller, C.; Schenk, D.; Johnston, J.; Winblad, B.; Venizelos, N.; Lannfelt, L.; Selkoe, D. J., Excessive production of amyloid beta-protein by peripheral cells of symptomatic and presymptomatic patients carrying the Swedish familial Alzheimer disease mutation. *Proc Natl Acad Sci U S A* **1994**, 91, (25), 11993-7.
26. Scheuner, D.; Eckman, C.; Jensen, M.; Song, X.; Citron, M.; Suzuki, N.; Bird, T. D.; Hardy, J.; Hutton, M.; Kukull, W.; Larson, E.; Levy-Lahad, E.; Viitanen, M.; Peskind, E.; Poorkaj, P.; Schellenberg, G.; Tanzi, R.; Wasco, W.; Lannfelt, L.; Selkoe, D.; Younkin, S., Secreted amyloid beta-protein similar to that in the senile plaques of Alzheimer's disease is increased in vivo by the presenilin 1 and 2 and APP mutations linked to familial Alzheimer's disease. *Nat Med* **1996**, 2, (8), 864-70.
27. Citron, M.; Westaway, D.; Xia, W.; Carlson, G.; Diehl, T.; Levesque, G.; Johnson-Wood, K.; Lee, M.; Seubert, P.; Davis, A.; Kholodenko, D.; Motter, R.; Sherrington, R.; Perry, B.; Yao, H.; Strome, R.; Lieberburg, I.; Rommens, J.; Kim, S.; Schenk, D.; Fraser, P.; St George Hyslop, P.; Selkoe, D. J., Mutant presenilins of Alzheimer's disease increase production of 42-residue amyloid beta-protein in both transfected cells and transgenic mice. *Nat Med* **1997**, 3, (1), 67-72.
28. Duff, K.; Eckman, C.; Zehr, C.; Yu, X.; Prada, C. M.; Perez-tur, J.; Hutton, M.; Buee, L.; Harigaya, Y.; Yager, D.; Morgan, D.; Gordon, M. N.; Holcomb, L.; Refolo, L.; Zenk, B.; Hardy, J.; Younkin, S., Increased amyloid-beta42(43) in brains of mice expressing mutant presenilin 1. *Nature* **1996**, 383, (6602), 710-3.



29. Schmechel, D. E.; Saunders, A. M.; Strittmatter, W. J.; Crain, B. J.; Hulette, C. M.; Joo, S. H.; Pericak-Vance, M. A.; Goldgaber, D.; Roses, A. D., Increased amyloid beta-peptide deposition in cerebral cortex as a consequence of apolipoprotein E genotype in late-onset Alzheimer disease. *Proc Natl Acad Sci U S A* **1993**, 90, (20), 9649-53.
30. Rebeck, G. W.; Reiter, J. S.; Strickland, D. K.; Hyman, B. T., Apolipoprotein E in sporadic Alzheimer's disease: allelic variation and receptor interactions. *Neuron* **1993**, 11, (4), 575-80.
31. Greenberg, S. M.; Rebeck, G. W.; Vonsattel, J. P.; Gomez-Isla, T.; Hyman, B. T., Apolipoprotein E epsilon 4 and cerebral hemorrhage associated with amyloid angiopathy. *Ann Neurol* **1995**, 38, (2), 254-9.
32. Polvikoski, T.; Sulkava, R.; Haltia, M.; Kainulainen, K.; Vuorio, A.; Verkkoniemi, A.; Niinisto, L.; Halonen, P.; Kontula, K., Apolipoprotein E, dementia, and cortical deposition of beta-amyloid protein. *N Engl J Med* **1995**, 333, (19), 1242-7.
33. Lemere, C. A.; Blusztajn, J. K.; Yamaguchi, H.; Wisniewski, T.; Saido, T. C.; Selkoe, D. J., Sequence of deposition of heterogeneous amyloid beta-peptides and APO E in Down syndrome: implications for initial events in amyloid plaque formation. *Neurobiol Dis* **1996**, 3, (1), 16-32.
34. Pike, C. J.; Burdick, D.; Walencewicz, A. J.; Glabe, C. G.; Cotman, C. W., Neurodegeneration induced by beta-amyloid peptides in vitro: the role of peptide assembly state. *J Neurosci* **1993**, 13, (4), 1676-87.
35. Lorenzo, A.; Yankner, B. A., Beta-amyloid neurotoxicity requires fibril formation and is inhibited by congo red. *Proc Natl Acad Sci U S A* **1994**, 91, (25), 12243-7.
36. Meda, L.; Cassatella, M. A.; Szendrei, G. I.; Otvos, L., Jr.; Baron, P.; Villalba, M.; Ferrari, D.; Rossi, F., Activation of microglial cells by beta-amyloid protein and interferon-gamma. *Nature* **1995**, 374, (6523), 647-50.
37. Games, D.; Adams, D.; Alessandrini, R.; Barbour, R.; Berthelette, P.; Blackwell, C.; Carr, T.; Clemens, J.; Donaldson, T.; Gillespie, F.; et al., Alzheimer-type neuropathology in transgenic mice overexpressing V717F beta-amyloid precursor protein. *Nature* **1995**, 373, (6514), 523-7.
38. Masliah, E.; Sisk, A.; Mallory, M.; Mucke, L.; Schenk, D.; Games, D., Comparison of neurodegenerative pathology in transgenic mice overexpressing V717F

beta-amyloid precursor protein and Alzheimer's disease. *J Neurosci* **1996**, 16, (18), 5795-811.

39. Hsiao, K.; Chapman, P.; Nilsen, S.; Eckman, C.; Harigaya, Y.; Younkin, S.; Yang, F.; Cole, G., Correlative memory deficits, Abeta elevation, and amyloid plaques in transgenic mice. *Science* **1996**, 274, (5284), 99-102.

40. Blurton-Jones, M.; Laferla, F. M., Pathways by which Abeta facilitates tau pathology. *Curr Alzheimer Res* **2006**, 3, (5), 437-48.

41. Price, J. L., Aging, preclinical Alzheimer disease, and early detection. *Alzheimer Dis Assoc Disord* **2003**, 17 Suppl 2, S60-2.

42. Birmingham, K.; Frantz, S., Set back to Alzheimer vaccine studies. *Nat Med* **2002**, 8, (3), 199-200.

43. Koudinov, A. R.; Koudinova, N. V., Cholesterol homeostasis failure as a unifying cause of synaptic degeneration. *J Neurol Sci* **2005**, 229-230, 233-40.

44. Jick, H.; Zornberg, G. L.; Jick, S. S.; Seshadri, S.; Drachman, D. A., Statins and the risk of dementia. *Lancet* **2000**, 356, (9242), 1627-31.

45. Wolozin, B.; Kellman, W.; Ruosseau, P.; Celesia, G. G.; Siegel, G., Decreased prevalence of Alzheimer disease associated with 3-hydroxy-3-methylglutaryl coenzyme A reductase inhibitors. *Arch Neurol* **2000**, 57, (10), 1439-43.

46. Refolo, L. M.; Malester, B.; LaFrancois, J.; Bryant-Thomas, T.; Wang, R.; Tint, G. S.; Sambamurti, K.; Duff, K.; Pappolla, M. A., Hypercholesterolemia accelerates the Alzheimer's amyloid pathology in a transgenic mouse model. *Neurobiol Dis* **2000**, 7, (4), 321-31.

47. Sparks, D. L.; Scheff, S. W.; Hunsaker, J. C., 3rd; Liu, H.; Landers, T.; Gross, D. R., Induction of Alzheimer-like beta-amyloid immunoreactivity in the brains of rabbits with dietary cholesterol. *Exp Neurol* **1994**, 126, (1), 88-94.

48. Bodovitz, S.; Klein, W. L., Cholesterol modulates alpha-secretase cleavage of amyloid precursor protein. *J Biol Chem* **1996**, 271, (8), 4436-40.

49. Racchi, M.; Baetta, R.; Salvietti, N.; Ianna, P.; Franceschini, G.; Paoletti, R.; Fumagalli, R.; Govoni, S.; Trabucchi, M.; Soma, M., Secretory processing of amyloid precursor protein is inhibited by increase in cellular cholesterol content. *Biochem J* **1997**, 322 (Pt 3), 893-8.
50. Simons, M.; Keller, P.; De Strooper, B.; Beyreuther, K.; Dotti, C. G.; Simons, K., Cholesterol depletion inhibits the generation of beta-amyloid in hippocampal neurons. *Proc Natl Acad Sci U S A* **1998**, 95, (11), 6460-4.
51. Morell, P.; Jurevics, H., Origin of cholesterol in myelin. *Neurochem Res* **1996**, 21, (4), 463-70.
52. Fan, Q. W.; Yu, W.; Senda, T.; Yanagisawa, K.; Michikawa, M., Cholesterol-dependent modulation of tau phosphorylation in cultured neurons. *J Neurochem* **2001**, 76, (2), 391-400.
53. Sawamura, N.; Gong, J. S.; Garver, W. S.; Heidenreich, R. A.; Ninomiya, H.; Ohno, K.; Yanagisawa, K.; Michikawa, M., Site-specific phosphorylation of tau accompanied by activation of mitogen-activated protein kinase (MAPK) in brains of Niemann-Pick type C mice. *J Biol Chem* **2001**, 276, (13), 10314-9.
54. Harman, D., Aging: a theory based on free radical and radiation chemistry. *J Gerontol* **1956**, 11, (3), 298-300.
55. Smith, M. A.; Harris, P. L.; Sayre, L. M.; Perry, G., Iron accumulation in Alzheimer disease is a source of redox-generated free radicals. *Proc Natl Acad Sci U S A* **1997**, 94, (18), 9866-8.
56. Sayre, L. M.; Perry, G.; Harris, P. L.; Liu, Y.; Schubert, K. A.; Smith, M. A., In situ oxidative catalysis by neurofibrillary tangles and senile plaques in Alzheimer's disease: a central role for bound transition metals. *J Neurochem* **2000**, 74, (1), 270-9.
57. Oteiza, P. I., A mechanism for the stimulatory effect of aluminum on iron-induced lipid peroxidation. *Arch Biochem Biophys* **1994**, 308, (2), 374-9.
58. Good, P. F.; Perl, D. P.; Bierer, L. M.; Schmeidler, J., Selective accumulation of aluminum and iron in the neurofibrillary tangles of Alzheimer's disease: a laser microprobe (LAMMA) study. *Ann Neurol* **1992**, 31, (3), 286-92.

59. Cras, P.; Kawai, M.; Siedlak, S.; Mulvihill, P.; Gambetti, P.; Lowery, D.; Gonzalez-DeWhitt, P.; Greenberg, B.; Perry, G., Neuronal and microglial involvement in beta-amyloid protein deposition in Alzheimer's disease. *Am J Pathol* **1990**, 137, (2), 241-6.
60. Colton, C. A.; Gilbert, D. L., Production of superoxide anions by a CNS macrophage, the microglia. *FEBS Lett* **1987**, 223, (2), 284-8.
61. Good, P. F.; Werner, P.; Hsu, A.; Olanow, C. W.; Perl, D. P., Evidence of neuronal oxidative damage in Alzheimer's disease. *Am J Pathol* **1996**, 149, (1), 21-8.
62. Yan, S. D.; Yan, S. F.; Chen, X.; Fu, J.; Chen, M.; Kuppusamy, P.; Smith, M. A.; Perry, G.; Godman, G. C.; Nawroth, P.; et al., Non-enzymatically glycosylated tau in Alzheimer's disease induces neuronal oxidant stress resulting in cytokine gene expression and release of amyloid beta-peptide. *Nat Med* **1995**, 1, (7), 693-9.
63. Yan, S. D.; Chen, X.; Schmidt, A. M.; Brett, J.; Godman, G.; Zou, Y. S.; Scott, C. W.; Caputo, C.; Frappier, T.; Smith, M. A.; et al., Glycosylated tau protein in Alzheimer disease: a mechanism for induction of oxidant stress. *Proc Natl Acad Sci U S A* **1994**, 91, (16), 7787-91.
64. Munch, G.; Kuhla, B.; Luth, H. J.; Arendt, T.; Robinson, S. R., Anti-AGEing defences against Alzheimer's disease. *Biochem Soc Trans* **2003**, 31, (Pt 6), 1397-9.
65. Tamagno, E.; Bardini, P.; Obbili, A.; Vitali, A.; Borghi, R.; Zaccheo, D.; Pronzato, M. A.; Danni, O.; Smith, M. A.; Perry, G.; Tabaton, M., Oxidative Stress Increases Expression and Activity of BACE in NT2 Neurons. *Neurobiol Dis* **2002**, 10, (3), 279-288.
66. Tamagno, E.; Guglielmotto, M.; Bardini, P.; Santoro, G.; Davit, A.; Di Simone, D.; Danni, O.; Tabaton, M., Dehydroepiandrosterone reduces expression and activity of BACE in NT2 neurons exposed to oxidative stress. *Neurobiol Dis* **2003**, 14, (2), 291-301.
67. Frederikse, P. H.; Garland, D.; Zigler, J. S., Jr.; Piatigorsky, J., Oxidative stress increases production of b-amyloid precursor protein and b-amyloid (A.b) in mammalian lenses, and A.b has toxic effects on lens epithelial cells. *J Biol Chem* **1996**, 271, (17), 10169-74.

68. Zhang, L.; Zhao, B.; Yew, D. T.; Kusiak, J. W.; Roth, G. S., Processing of Alzheimer's amyloid precursor protein during H<sub>2</sub>O<sub>2</sub>-induced apoptosis in human neuronal cells. *Biochem Biophys Res Commun* **1997**, 235, (3), 845-848.
69. Olivieri, G.; Baysang, G.; Meier, F.; Muller-Spahn, F.; Stahelin, H. B.; Brockhaus, M.; Brack, C., N-acetyl-L-cysteine protects SHSY5Y neuroblastoma cells from oxidative stress and cell cytotoxicity: effects on b-amyloid secretion and tau phosphorylation. *J Neurochem* **2001**, 76, (1), 224-233.
70. Misonou, H.; Morishima-Kawashima, M.; Ihara, Y., Oxidative Stress Induces Intracellular Accumulation of Amyloid b-Protein (A.b) in Human Neuroblastoma Cells. *Biochemistry* **2000**, 39, (23), 6951-6959.
71. Lovell, M. A.; Xiong, S.; Xie, C.; Davies, P.; Markesbery, W. R., Induction of hyperphosphorylated tau in primary rat cortical neuron cultures mediated by oxidative stress and glycogen synthase kinase-3. *J Alzheimers Dis* **2004**, 6, (6), 659-671.
72. Nakashima, H.; Ishihara, T.; Yokota, O.; Terada, S.; Trojanowski, J. Q.; Lee, V. M. Y.; Kuroda, S., Effects of  $\alpha$ -tocopherol on an animal model of tauopathies. *Free Radic Biol Med* **2004**, 37, (2), 176-186.
73. Montine, T. J.; Neely, M. D.; Quinn, J. F.; Beal, M. F.; Markesbery, W. R.; Roberts, L. J.; Morrow, J. D., Lipid peroxidation in aging brain and Alzheimer's disease. *Free Radic Biol Med* **2002**, 33, (5), 620-626.
74. Mattson, M. P.; Fu, W.; Waeg, G.; Uchida, K., 4-Hydroxynonenal, a product of lipid peroxidation, inhibits dephosphorylation of the microtubule-associated protein tau. *NeuroReport* **1997**, 8, (9-10), 2275-2281.
75. Gomez-Ramos, A.; Diaz-Nido, J.; Smith Mark, A.; Perry, G.; Avila, J., Effect of the lipid peroxidation product acrolein on tau phosphorylation in neural cells. *J Neurosci Res* **2003**, 71, (6), 863-70.
76. Butterfield, D. A.; Boyd-Kimball, D., Amyloid beta-peptide(1-42) contributes to the oxidative stress and neurodegeneration found in Alzheimer disease brain. *Brain Pathol* **2004**, 14, (4), 426-32.
77. Hensley, K.; Carney, J. M.; Mattson, M. P.; Aksenova, M.; Harris, M.; Wu, J. F.; Floyd, R. A.; Butterfield, D. A., A model for beta-amyloid aggregation and neurotoxicity

based on free radical generation by the peptide: relevance to Alzheimer disease. *Proc Natl Acad Sci U S A* **1994**, 91, (8), 3270-4.

78. Sayre, L. M.; Zagorski, M. G.; Surewicz, W. K.; Krafft, G. A.; Perry, G., Mechanisms of neurotoxicity associated with amyloid beta deposition and the role of free radicals in the pathogenesis of Alzheimer's disease: a critical appraisal. *Chem Res Toxicol* **1997**, 10, (5), 518-26.

79. Schliebs, R.; Arendt, T., The significance of the cholinergic system in the brain during aging and in Alzheimer's disease. *J Neural Transm* **2006**, 113, (11), 1625-44.

80. Bartus, R. T., On neurodegenerative diseases, models, and treatment strategies: lessons learned and lessons forgotten a generation following the cholinergic hypothesis. *Exp Neurol* **2000**, 163, (2), 495-529.

81. Bierer, L. M.; Haroutunian, V.; Gabriel, S.; Knott, P. J.; Carlin, L. S.; Purohit, D. P.; Perl, D. P.; Schmeidler, J.; Kanof, P.; Davis, K. L., Neurochemical correlates of dementia severity in Alzheimer's disease: relative importance of the cholinergic deficits. *J Neurochem* **1995**, 64, (2), 749-60.

82. Sofic, E.; Gotz, M.; Frolich, L.; Burger, R.; Heckers, S.; Riederer, P.; Jellinger, K.; Beckmann, H., Reflection of changes in membrane constituents in various regions of Alzheimer brains to differential scanning thermograms. *J Neural Transm Suppl* **1990**, 32, 259-67.

83. Zuchner, T.; Perez-Polo, J. R.; Schliebs, R., Beta-secretase BACE1 is differentially controlled through muscarinic acetylcholine receptor signaling. *J Neurosci Res* **2004**, 77, (2), 250-7.

84. Rossner, S.; Ueberham, U.; Schliebs, R.; Perez-Polo, J. R.; Bigl, V., The regulation of amyloid precursor protein metabolism by cholinergic mechanisms and neurotrophin receptor signaling. *Prog Neurobiol* **1998**, 56, (5), 541-69.

85. Lin, L.; Georgievska, B.; Mattsson, A.; Isacson, O., Cognitive changes and modified processing of amyloid precursor protein in the cortical and hippocampal system after cholinergic synapse loss and muscarinic receptor activation. *Proc Natl Acad Sci U S A* **1999**, 96, (21), 12108-13.

86. Efthimiopoulos, S.; Vassilacopoulou, D.; Ripellino, J. A.; Tezapsidis, N.; Robakis, N. K., Cholinergic agonists stimulate secretion of soluble full-length amyloid

precursor protein in neuroendocrine cells. *Proc Natl Acad Sci U S A* **1996**, 93, (15), 8046-50.

87. Seo, J.; Kim, S.; Kim, H.; Park, C. H.; Jeong, S.; Lee, J.; Choi, S. H.; Chang, K.; Rah, J.; Koo, J.; Kim, E.; Suh, Y., Effects of nicotine on APP secretion and Abeta- or CT(105)-induced toxicity. *Biol Psychiatry* **2001**, 49, (3), 240-7.

88. Utsuki, T.; Shoaib, M.; Holloway, H. W.; Ingram, D. K.; Wallace, W. C.; Haroutunian, V.; Sambamurti, K.; Lahiri, D. K.; Greig, N. H., Nicotine lowers the secretion of the Alzheimer's amyloid beta-protein precursor that contains amyloid beta-peptide in rat. *J Alzheimers Dis* **2002**, 4, (5), 405-15.

89. Hellstrom-Lindahl, E.; Moore, H.; Nordberg, A., Increased levels of tau protein in SH-SY5Y cells after treatment with cholinesterase inhibitors and nicotinic agonists. *J Neurochem* **2000**, 74, (2), 777-84.

90. Wang, H. Y.; Li, W.; Benedetti, N. J.; Lee, D. H., Alpha 7 nicotinic acetylcholine receptors mediate beta-amyloid peptide-induced tau protein phosphorylation. *J Biol Chem* **2003**, 278, (34), 31547-53.

91. Seshadri, S.; Beiser, A.; Selhub, J.; Jacques, P. F.; Rosenberg, I. H.; D'Agostino, R. B.; Wilson, P. W.; Wolf, P. A., Plasma homocysteine as a risk factor for dementia and Alzheimer's disease. *N Engl J Med* **2002**, 346, (7), 476-83.

92. Joosten, E.; Lesaffre, E.; Riezler, R.; Ghekiere, V.; Dereymaeker, L.; Pelemans, W.; Dejaeger, E., Is metabolic evidence for vitamin B-12 and folate deficiency more frequent in elderly patients with Alzheimer's disease? *J Gerontol A Biol Sci Med Sci* **1997**, 52, (2), M76-9.

93. Miller, J. W.; Green, R.; Mungas, D. M.; Reed, B. R.; Jagust, W. J., Homocysteine, vitamin B6, and vascular disease in AD patients. *Neurology* **2002**, 58, (10), 1471-5.

94. Nilsson, K.; Gustafson, L.; Hultberg, B., Plasma homocysteine is a sensitive marker for tissue deficiency of both cobalamines and folates in a psychogeriatric population. *Dement Geriatr Cogn Disord* **1999**, 10, (6), 476-82.

95. Quadri, P.; Fragiaco, C.; Pezzati, R.; Zanda, E.; Tettamanti, M.; Lucca, U., Homocysteine and B vitamins in mild cognitive impairment and dementia. *Clin Chem Lab Med* **2005**, 43, (10), 1096-100.

96. Ravaglia, G.; Forti, P.; Maioli, F.; Martelli, M.; Servadei, L.; Brunetti, N.; Porcellini, E.; Licastro, F., Homocysteine and folate as risk factors for dementia and Alzheimer disease. *Am J Clin Nutr* **2005**, 82, (3), 636-43.
97. Teunissen, C. E.; van Boxtel, M. P.; Jolles, J.; de Vente, J.; Vreeling, F.; Verhey, F.; Polman, C. H.; Dijkstra, C. D.; Blom, H. J., Homocysteine in relation to cognitive performance in pathological and non-pathological conditions. *Clin Chem Lab Med* **2005**, 43, (10), 1089-95.
98. Tucker, K. L.; Qiao, N.; Scott, T.; Rosenberg, I.; Spiro, A., 3rd, High homocysteine and low B vitamins predict cognitive decline in aging men: the Veterans Affairs Normative Aging Study. *Am J Clin Nutr* **2005**, 82, (3), 627-35.
99. Ho, P. I.; Ortiz, D.; Rogers, E.; Shea, T. B., Multiple aspects of homocysteine neurotoxicity: glutamate excitotoxicity, kinase hyperactivation and DNA damage. *J Neurosci Res* **2002**, 70, (5), 694-702.
100. Kruman, II; Culmsee, C.; Chan, S. L.; Kruman, Y.; Guo, Z.; Penix, L.; Mattson, M. P., Homocysteine elicits a DNA damage response in neurons that promotes apoptosis and hypersensitivity to excitotoxicity. *J Neurosci* **2000**, 20, (18), 6920-6.
101. Selley, M. L.; Close, D. R.; Stern, S. E., The effect of increased concentrations of homocysteine on the concentration of (E)-4-hydroxy-2-nonenal in the plasma and cerebrospinal fluid of patients with Alzheimer's disease. *Neurobiol Aging* **2002**, 23, (3), 383-8.
102. Fuso, A.; Seminara, L.; Cavallaro, R. A.; D'Anselmi, F.; Scarpa, S., S-adenosylmethionine/homocysteine cycle alterations modify DNA methylation status with consequent deregulation of PS1 and BACE and beta-amyloid production. *Mol Cell Neurosci* **2005**, 28, (1), 195-204.
103. Flicker, L.; Martins, R. N.; Thomas, J.; Acres, J.; Taddei, K.; Norman, P.; Jamrozik, K.; Almeida, O. P., Homocysteine, Alzheimer genes and proteins, and measures of cognition and depression in older men. *J Alzheimers Dis* **2004**, 6, (3), 329-36.
104. Mizrahi, E. H.; Jacobsen, D. W.; Debanne, S. M.; Traore, F.; Lerner, A. J.; Friedland, R. P.; Petot, G. J., Plasma total homocysteine levels, dietary vitamin B6 and folate intake in AD and healthy aging. *J Nutr Health Aging* **2003**, 7, (3), 160-5.



105. Luchsinger, J. A.; Tang, M. X.; Shea, S.; Miller, J.; Green, R.; Mayeux, R., Plasma homocysteine levels and risk of Alzheimer disease. *Neurology* **2004**, 62, (11), 1972-6.
106. White, A. R.; Huang, X.; Jobling, M. F.; Barrow, C. J.; Beyreuther, K.; Masters, C. L.; Bush, A. I.; Cappai, R., Homocysteine potentiates copper- and amyloid beta peptide-mediated toxicity in primary neuronal cultures: possible risk factors in the Alzheimer's-type neurodegenerative pathways. *J Neurochem* **2001**, 76, (5), 1509-20.
107. Cilley, R. E.; Brighton, V. K., The significance of *Helicobacter pylori* colonization of the stomach. *Semin Pediatr Surg* **1995**, 4, (4), 221-7.
108. Lowy, D. R.; Schiller, J. T., Prophylactic human papillomavirus vaccines. *J Clin Invest* **2006**, 116, (5), 1167-73.
109. Campbell, L. A.; Kuo, C. C., Chlamydia pneumoniae and atherosclerosis. *Semin Respir Infect* **2003**, 18, (1), 48-54.
110. de Boer, O. J.; van der Wal, A. C.; Becker, A. E., Atherosclerosis, inflammation, and infection. *J Pathol* **2000**, 190, (3), 237-43.
111. Deatly, A. M.; Haase, A. T.; Fewster, P. H.; Lewis, E.; Ball, M. J., Human herpes virus infections and Alzheimer's disease. *Neuropathol Appl Neurobiol* **1990**, 16, (3), 213-23.
112. Dobson, C. B.; Itzhaki, R. F., Herpes simplex virus type 1 and Alzheimer's disease. *Neurobiol Aging* **1999**, 20, (4), 457-65.
113. Fraser, N. W.; Lawrence, W. C.; Wroblewska, Z.; Gilden, D. H.; Koprowski, H., Herpes simplex type 1 DNA in human brain tissue. *Proc Natl Acad Sci U S A* **1981**, 78, (10), 6461-5.
114. Libikova, H.; Pogady, J.; Wiedermann, V.; Breier, S., Search for herpetic antibodies in the cerebrospinal fluid in senile dementia and mental retardation. *Acta Virol* **1975**, 19, (6), 493-5.
115. Sequiera, L. W.; Jennings, L. C.; Carrasco, L. H.; Lord, M. A.; Curry, A.; Sutton, R. N., Detection of herpes-simplex viral genome in brain tissue. *Lancet* **1979**, 2, (8143), 609-12.

116. Middleton, P. J.; Petric, M.; Kozak, M.; Rewcastle, N. B.; McLachlan, D. R., Herpes-simplex viral genome and senile and presenile dementias of Alzheimer and Pick. *Lancet* **1980**, 1, (8176), 1038.
117. Pogo, B. G.; Casals, J.; Elizan, T. S., A study of viral genomes and antigens in brains of patients with Alzheimer's disease. *Brain* **1987**, 110 (Pt 4), 907-15.
118. Renvoize, E. B.; Awad, I. O.; Hambling, M. H., A sero-epidemiological study of conventional infectious agents in Alzheimer's disease. *Age Ageing* **1987**, 16, (5), 311-4.
119. Taylor, G. R.; Crow, T. J.; Markakis, D. A.; Lofthouse, R.; Neeley, S.; Carter, G. I., Herpes simplex virus and Alzheimer's disease: a search for virus DNA by spot hybridisation. *J Neurol Neurosurg Psychiatry* **1984**, 47, (10), 1061-5.
120. Little, C. S.; Hammond, C. J.; MacIntyre, A.; Balin, B. J.; Appelt, D. M., Chlamydia pneumoniae induces Alzheimer-like amyloid plaques in brains of BALB/c mice. *Neurobiol Aging* **2004**, 25, (4), 419-29.
121. Grant, W. B., Dietary links to Alzheimer's disease: 1999 update. *J Alzheimers Dis* **1999**, 1, (4,5), 197-201.
122. Levin-Allerhand, J. A.; Lominska, C. E.; Smith, J. D., Increased amyloid- levels in APPSWE transgenic mice treated chronically with a physiological high-fat high-cholesterol diet. *J Nutr Health Aging* **2002**, 6, (5), 315-9.
123. Shie, F.-S.; LeBouef, R. C.; Jin, L.-W., Early intraneuronal Ab deposition in the hippocampus of APP transgenic mice. *NeuroReport* **2003**, 14, (1), 123-129.
124. Oksman, M.; Iivonen, H.; Högges, E.; Amtul, Z.; Penke, B.; Leenders, I.; Broersen, L.; Luetjohann, D.; Hartmann, T.; Tanila, H., Impact of different saturated fatty acid, polyunsaturated fatty acid and cholesterol containing diets on beta-amyloid accumulation in APP/PS1 transgenic mice. *Neurobiol Dis* **2006**, 23, (3), 563-572.
125. Wang, S.-W.; Wang, M.; Grossman, B. M.; Martin, R. J., Effects of dietary fat on food intake and brain uptake and oxidation of fatty acids. *Physiol Behavior* **1994**, 56, (3), 517-22.
126. Dhopeswarkar, G. A.; Mead, J. F., Uptake and transport of fatty acids into the brain and role of the blood-brain barrier system. *Adv Lipid Res* **1973**, 11, 109-42.

127. Arvanitakis, Z.; Wilson Robert, S.; Bienias Julia, L.; Evans Denis, A.; Bennett David, A., Diabetes mellitus and risk of Alzheimer disease and decline in cognitive function. *Arch Neurol* **2004**, 61, (5), 661-6.
128. Monti, L. D.; Landoni, C.; Setola, E.; Galluccio, E.; Lucotti, P.; Sandoli, E. P.; Origgi, A.; Lucignani, G.; Piatti, P.; Fazio, F., Myocardial insulin resistance associated with chronic hypertriglyceridemia and increased FFA levels in Type 2 diabetic patients. *Am J Physiol* **2004**, 287, (3, Pt. 2), H1225-H1231.
129. Smith, Q. R.; Nagura, H., Fatty acid uptake and incorporation in brain: studies with the perfusion model. *J Mol Neurosci* **2001**, 16, (2/3), 167-172.
130. Guo, Z.; Cupples, L. A.; Kurz, A.; Auerbach, S. H.; Volicer, L.; Chui, H.; Green, R. C.; Sadovnick, A. D.; Duara, R.; DeCarli, C.; Johnson, K.; Go, R. C.; Growdon, J. H.; Haines, J. L.; Kukull, W. A.; Farrer, L. A., Head injury and the risk of AD in the MIRAGE study. *Neurology* **2000**, 54, (6), 1316-23.
131. Homayoun, P.; De Turco, E. B. R.; Parkins, N. E.; Lane, D. C.; Soblosky, J.; Carey, M. E.; Bazan, N. G., Delayed phospholipid degradation in rat brain after traumatic brain injury. *J Neurochem* **1997**, 69, (1), 199-205.
132. Lipton, P., Ischemic cell death in brain neurons. *Physiol Rev* **1999**, 79, (4), 1431-568.
133. Goux, W. J.; Rodriguez, S.; Sparkman, D. R., Analysis of the core components of Alzheimer paired helical filaments. A gas chromatography/mass spectrometry characterization of fatty acids, carbohydrates and long-chain bases. *FEBS Letters* **1995**, 366, (1), 81-5.
134. Roher, A. E.; Weiss, N.; Kokjohn, T. A.; Kuo, Y.-M.; Kalback, W.; Anthony, J.; Watson, D.; Luehrs, D. C.; Sue, L.; Walker, D.; Emmerling, M.; Goux, W.; Beach, T., Increased Ab Peptides and Reduced Cholesterol and Myelin Proteins Characterize White Matter Degeneration in Alzheimer's Disease. *Biochemistry* **2002**, 41, (37), 11080-11090.
135. Petot, G. J.; Traore, F.; Debanne, S. M.; Lerner, A. J.; Smyth, K. A.; Friedland, R. P., Interactions of apolipoprotein E genotype and dietary fat intake of healthy older persons during mid-adult life. *Metabolism Clin Exp* **2003**, 52, (3), 279-281.
136. Braak, H.; Braak, E., Neuropathological staging of Alzheimer-related changes. *Acta Neuropathol* **1991**, 82, (4), 239-59.

137. Arriagada, P. V.; Growdon, J. H.; Hedley-Whyte, E. T.; Hyman, B. T., Neurofibrillary tangles but not senile plaques parallel duration and severity of Alzheimer's disease. *Neurology* **1992**, 42, (3 Pt 1), 631-9.
138. Bierer, L. M.; Hof, P. R.; Purohit, D. P.; Carlin, L.; Schmeidler, J.; Davis, K. L.; Perl, D. P., Neocortical neurofibrillary tangles correlate with dementia severity in Alzheimer's disease. *Arch Neurol* **1995**, 52, (1), 81-8.
139. Lee, M. S.; Kwon, Y. T.; Li, M.; Peng, J.; Friedlander, R. M.; Tsai, L. H., Neurotoxicity induces cleavage of p35 to p25 by calpain. *Nature* **2000**, 405, (6784), 360-4.
140. Hwang, S. C.; Jhon, D. Y.; Bae, Y. S.; Kim, J. H.; Rhee, S. G., Activation of phospholipase C-gamma by the concerted action of tau proteins and arachidonic acid. *J Biol Chem* **1996**, 271, (31), 18342-9.
141. Flanagan, L. A.; Cunningham, C. C.; Chen, J.; Prestwich, G. D.; Kosik, K. S.; Janmey, P. A., The structure of divalent cation-induced aggregates of PIP2 and their alteration by gelsolin and tau. *Biophys J* **1997**, 73, (3), 1440-7.
142. Reszka, A. A.; Seger, R.; Diltz, C. D.; Krebs, E. G.; Fischer, E. H., Association of mitogen-activated protein kinase with the microtubule cytoskeleton. *Proc Natl Acad Sci U S A* **1995**, 92, (19), 8881-5.
143. Liao, H.; Li, Y.; Brautigan, D. L.; Gundersen, G. G., Protein phosphatase 1 is targeted to microtubules by the microtubule-associated protein Tau. *J Biol Chem* **1998**, 273, (34), 21901-8.
144. Cunningham, C. C.; Leclerc, N.; Flanagan, L. A.; Lu, M.; Janmey, P. A.; Kosik, K. S., Microtubule-associated protein 2c reorganizes both microtubules and microfilaments into distinct cytological structures in an actin-binding protein-280-deficient melanoma cell line. *J Cell Biol* **1997**, 136, (4), 845-57.
145. Billingsley, M. L.; Kincaid, R. L., Regulated phosphorylation and dephosphorylation of tau protein: effects on microtubule interaction, intracellular trafficking and neurodegeneration. *Biochem J* **1997**, 323 (Pt 3), 577-91.
146. Morita-Fujimura, Y.; Kurachi, M.; Tashiro, H.; Komiya, Y.; Tashiro, T., Reduced microtubule-nucleation activity of tau after dephosphorylation. *Biochem Biophys Res Commun* **1996**, 225, (2), 462-8.

147. Geschwind, D. H., Tau phosphorylation, tangles, and neurodegeneration: the chicken or the egg? *Neuron* **2003**, 40, (3), 457-60.
148. Lee, H. G.; Perry, G.; Moreira, P. I.; Garrett, M. R.; Liu, Q.; Zhu, X.; Takeda, A.; Nunomura, A.; Smith, M. A., Tau phosphorylation in Alzheimer's disease: pathogen or protector? *Trends Mol Med* **2005**, 11, (4), 164-9.
149. Grundke-Iqbal, I.; Iqbal, K.; Tung, Y. C.; Quinlan, M.; Wisniewski, H. M.; Binder, L. I., Abnormal phosphorylation of the microtubule-associated protein tau (tau) in Alzheimer cytoskeletal pathology. *Proc Natl Acad Sci U S A* **1986**, 83, (13), 4913-7.
150. Bancher, C.; Brunner, C.; Lassmann, H.; Budka, H.; Jellinger, K.; Wiche, G.; Seitelberger, F.; Grundke-Iqbal, I.; Iqbal, K.; Wisniewski, H. M., Accumulation of abnormally phosphorylated tau precedes the formation of neurofibrillary tangles in Alzheimer's disease. *Brain Res* **1989**, 477, (1-2), 90-9.
151. Braak, E.; Braak, H.; Mandelkow, E. M., A sequence of cytoskeleton changes related to the formation of neurofibrillary tangles and neuropil threads. *Acta Neuropathol* **1994**, 87, (6), 554-67.
152. Alonso, A.; Zaidi, T.; Novak, M.; Grundke-Iqbal, I.; Iqbal, K., Hyperphosphorylation induces self-assembly of tau into tangles of paired helical filaments/straight filaments. *Proc Natl Acad Sci U S A* **2001**, 98, (12), 6923-8.
153. Perez, M.; Cuadros, R.; Smith, M. A.; Perry, G.; Avila, J., Phosphorylated, but not native, tau protein assembles following reaction with the lipid peroxidation product, 4-hydroxy-2-nonenal. *FEBS Lett* **2000**, 486, (3), 270-4.
154. Morishima-Kawashima, M.; Hasegawa, M.; Takio, K.; Suzuki, M.; Yoshida, H.; Titani, K.; Ihara, Y., Proline-directed and non-proline-directed phosphorylation of PHF-tau. *J Biol Chem* **1995**, 270, (2), 823-9.
155. Gong, C. X.; Grundke-Iqbal, I.; Damuni, Z.; Iqbal, K., Dephosphorylation of microtubule-associated protein tau by protein phosphatase-1 and -2C and its implication in Alzheimer disease. *FEBS Lett* **1994**, 341, (1), 94-8.
156. Gong, C. X.; Singh, T. J.; Grundke-Iqbal, I.; Iqbal, K., Alzheimer's disease abnormally phosphorylated tau is dephosphorylated by protein phosphatase-2B (calcineurin). *J Neurochem* **1994**, 62, (2), 803-6.

157. Gong, C. X.; Lidsky, T.; Wegiel, J.; Zuck, L.; Grundke-Iqbal, I.; Iqbal, K., Phosphorylation of microtubule-associated protein tau is regulated by protein phosphatase 2A in mammalian brain. Implications for neurofibrillary degeneration in Alzheimer's disease. *J Biol Chem* **2000**, 275, (8), 5535-44.
158. Gong, C. X.; Singh, T. J.; Grundke-Iqbal, I.; Iqbal, K., Phosphoprotein phosphatase activities in Alzheimer disease brain. *J Neurochem* **1993**, 61, (3), 921-7.
159. Gomez-Ramos, A.; Diaz-Nido, J.; Smith, M. A.; Perry, G.; Avila, J., Effect of the lipid peroxidation product acrolein on tau phosphorylation in neural cells. *J Neurosci Res* **2003**, 71, (6), 863-70.
160. Lovell, M. A.; Xiong, S.; Xie, C.; Davies, P.; Markesbery, W. R., Induction of hyperphosphorylated tau in primary rat cortical neuron cultures mediated by oxidative stress and glycogen synthase kinase-3. *J Alzheimers Dis* **2004**, 6, (6), 659-71; discussion 673-81.
161. Nakashima, H.; Ishihara, T.; Yokota, O.; Terada, S.; Trojanowski, J. Q.; Lee, V. M.; Kuroda, S., Effects of alpha-tocopherol on an animal model of tauopathies. *Free Radic Biol Med* **2004**, 37, (2), 176-86.
162. Zhu, X.; Rottkamp, C. A.; Boux, H.; Takeda, A.; Perry, G.; Smith, M. A., Activation of p38 kinase links tau phosphorylation, oxidative stress, and cell cycle-related events in Alzheimer disease. *J Neuropathol Exp Neurol* **2000**, 59, (10), 880-8.
163. Butterfield, D. A.; Drake, J.; Pocernich, C.; Castegna, A., Evidence of oxidative damage in Alzheimer's disease brain: central role for amyloid beta-peptide. *Trends Mol Med* **2001**, 7, (12), 548-54.
164. Butterfield, D. A.; Lauderback, C. M., Lipid peroxidation and protein oxidation in Alzheimer's disease brain: potential causes and consequences involving amyloid beta-peptide-associated free radical oxidative stress. *Free Radic Biol Med* **2002**, 32, (11), 1050-60.
165. Nunomura, A.; Perry, G.; Aliev, G.; Hirai, K.; Takeda, A.; Balraj, E. K.; Jones, P. K.; Ghanbari, H.; Wataya, T.; Shimohama, S.; Chiba, S.; Atwood, C. S.; Petersen, R. B.; Smith, M. A., Oxidative damage is the earliest event in Alzheimer disease. *J Neuropathol Exp Neurol* **2001**, 60, (8), 759-67.

166. Lovell, M. A.; Ehmann, W. D.; Butler, S. M.; Markesbery, W. R., Elevated thiobarbituric acid-reactive substances and antioxidant enzyme activity in the brain in Alzheimer's disease. *Neurology* **1995**, 45, (8), 1594-601.
167. Marcus, D. L.; Thomas, C.; Rodriguez, C.; Simberkoff, K.; Tsai, J. S.; Strafaci, J. A.; Freedman, M. L., Increased peroxidation and reduced antioxidant enzyme activity in Alzheimer's disease. *Exp Neurol* **1998**, 150, (1), 40-4.
168. Mark, R. J.; Lovell, M. A.; Markesbery, W. R.; Uchida, K.; Mattson, M. P., A role for 4-hydroxynonenal, an aldehydic product of lipid peroxidation, in disruption of ion homeostasis and neuronal death induced by amyloid beta-peptide. *J Neurochem* **1997**, 68, (1), 255-64.
169. Lovell, M. A.; Xie, C.; Markesbery, W. R., Acrolein is increased in Alzheimer's disease brain and is toxic to primary hippocampal cultures. *Neurobiol Aging* **2001**, 22, (2), 187-94.
170. Berlett, B. S.; Stadtman, E. R., Protein oxidation in aging, disease, and oxidative stress. *J Biol Chem* **1997**, 272, (33), 20313-6.
171. Smith, C. D.; Carney, J. M.; Starke-Reed, P. E.; Oliver, C. N.; Stadtman, E. R.; Floyd, R. A.; Markesbery, W. R., Excess brain protein oxidation and enzyme dysfunction in normal aging and in Alzheimer disease. *Proc Natl Acad Sci U S A* **1991**, 88, (23), 10540-3.
172. Lyras, L.; Cairns, N. J.; Jenner, A.; Jenner, P.; Halliwell, B., An assessment of oxidative damage to proteins, lipids, and DNA in brain from patients with Alzheimer's disease. *J Neurochem* **1997**, 68, (5), 2061-9.
173. Wille, H.; Drewes, G.; Biernat, J.; Mandelkow, E. M.; Mandelkow, E., Alzheimer-like paired helical filaments and antiparallel dimers formed from microtubule-associated protein tau in vitro. *J Cell Biol* **1992**, 118, (3), 573-84.
174. Schweers, O.; Mandelkow, E. M.; Biernat, J.; Mandelkow, E., Oxidation of cysteine-322 in the repeat domain of microtubule-associated protein tau controls the in vitro assembly of paired helical filaments. *Proc Natl Acad Sci U S A* **1995**, 92, (18), 8463-7.
175. Smith, M. A.; Perry, G.; Richey, P. L.; Sayre, L. M.; Anderson, V. E.; Beal, M. F.; Kowall, N., Oxidative damage in Alzheimer's. *Nature* **1996**, 382, (6587), 120-1.

176. Chandler, L. J.; Newsom, H.; Sumners, C.; Crews, F., Chronic ethanol exposure potentiates NMDA excitotoxicity in cerebral cortical neurons. *J Neurochem* **1993**, 60, (4), 1578-81.
177. Pshenichkin, S. P.; Wise, B. C., Okadaic acid increases nerve growth factor secretion, mRNA stability, and gene transcription in primary cultures of cortical astrocytes. *J Biol Chem* **1995**, 270, (11), 5994-9.
178. Williamson, R.; Scales, T.; Clark, B. R.; Gibb, G.; Reynolds, C. H.; Kellie, S.; Bird, L. N.; Varndell, L. M.; Sheppard, P. W.; Everall, I.; Anderton, B. H., Rapid tyrosine phosphorylation of neuronal proteins including tau and focal adhesion kinase in response to amyloid- $\beta$  peptide exposure: involvement of src family protein kinases. *J Neurosci* **2002**, 22, (1), 10-20.
179. Sauer, H.; Klimm, B.; Hescheler, J.; Wartenberg, M., Activation of p90RSK and growth stimulation of multicellular tumor spheroids are dependent on reactive oxygen species generated after purinergic receptor stimulation by ATP. *FASEB J* **2001**, 15, (13), 2539-2541, 10 1096/fj 01-0360fje.
180. Kosik, K. S.; Crandall, J. E.; Mufson, E. J.; Neve, R. L., Tau in situ hybridization in normal and Alzheimer brain: localization in the somatodendritic compartment. *Ann Neurol* **1989**, 26, (3), 352-61.
181. Papasozomenos, S. C., Tau protein immunoreactivity in dementia of the Alzheimer type: II. Electron microscopy and pathogenetic implications. Effects of fixation on the morphology of the Alzheimer's abnormal filaments. *Lab Invest* **1989**, 60, (3), 375-89.
182. Blazquez, C.; Galve-Roperh, I.; Guzman, M., De novo-synthesized ceramide signals apoptosis in astrocytes via extracellular signal-regulated kinase. *FASEB J* **2000**, 14, (14), 2315-2322.
183. Gorina, R.; Petegnief, V.; Chamorro, A.; Planas, A. M., AG490 prevents cell death after exposure of rat astrocytes to hydrogen peroxide or proinflammatory cytokines: involvement of the Jak2/STAT pathway. *J Neurochem* **2005**, 92, (3), 505-518.
184. Goedert, M.; Jakes, R.; Vanmechelen, E., Monoclonal antibody AT8 recognizes tau protein phosphorylated at both serine 202 and threonine 205. *Neurosci Lett* **1995**, 189, (3), 167-70.



185. Otvos, L., Jr.; Feiner, L.; Lang, E.; Szendrei, G. I.; Goedert, M.; Lee, V. M. Y., Monoclonal antibody PHF-1 recognizes Tau protein phosphorylated at serine residues 396 and 404. *J Neurosci Res* **1994**, 39, (6), 669-73.
186. Gong, C. X.; Singh, T. J.; Grundke-Iqbal, I.; Iqbal, K., Alzheimer's disease abnormally phosphorylated  $\tau$  is dephosphorylated by protein phosphatase-2B (calcineurin). *J Neurochem* **1994**, 62, (2), 803-6.
187. Davis, D. R.; Anderton, B. H.; Brion, J.-P.; Reynolds, C. H.; Hanger, D. P., Oxidative stress induces dephosphorylation of  $\tau$  in rat brain primary neuronal cultures. *J Neurochem* **1997**, 68, (4), 1590-1597.
188. Glenner, G. G.; Wong, C. W., Alzheimer's disease: initial report of the purification and characterization of a novel cerebrovascular amyloid protein. *Biochem Biophys Res Commun* **1984**, 120, (3), 885-90.
189. Price, D. L.; Sisodia, S. S., Mutant genes in familial Alzheimer's disease and transgenic models. *Annu Rev Neurosci* **1998**, 21, 479-505.
190. Hardy, J.; Selkoe, D. J., The amyloid hypothesis of Alzheimer's disease: progress and problems on the road to therapeutics. *Science* **2002**, 297, (5580), 353-6.
191. St George-Hyslop, P. H.; Petit, A., Molecular biology and genetics of Alzheimer's disease. *C R Biol* **2005**, 328, (2), 119-30.
192. Tanzi, R. E.; Bertram, L., Twenty years of the Alzheimer's disease amyloid hypothesis: a genetic perspective. *Cell* **2005**, 120, (4), 545-55.
193. Desai, P. P.; Ikonomic, M. D.; Abrahamson, E. E.; Hamilton, R. L.; Isanski, B. A.; Hope, C. E.; Klunk, W. E.; DeKosky, S. T.; Kamboh, M. I., Apolipoprotein D is a component of compact but not diffuse amyloid-beta plaques in Alzheimer's disease temporal cortex. *Neurobiol Dis* **2005**, 20, (2), 574-82.
194. Frey, H. J.; Mattila, K. M.; Korolainen, M. A.; Pirttila, T., Problems associated with biological markers of Alzheimer's disease. *Neurochem Res* **2005**, 30, (12), 1501-10.
195. Selkoe, D. J., Translating cell biology into therapeutic advances in Alzheimer's disease. *Nature* **1999**, 399, (6738 Suppl), A23-31.

196. Klein, W. L., Abeta toxicity in Alzheimer's disease: globular oligomers (ADDLs) as new vaccine and drug targets. *Neurochem Int* **2002**, 41, (5), 345-52.
197. Golde, T. E., Alzheimer disease therapy: can the amyloid cascade be halted? *J Clin Invest* **2003**, 111, (1), 11-8.
198. Pereira, C.; Agostinho, P.; Moreira, P. I.; Cardoso, S. M.; Oliveira, C. R., Alzheimer's disease-associated neurotoxic mechanisms and neuroprotective strategies. *Curr Drug Targets CNS Neurol Disord* **2005**, 4, (4), 383-403.
199. De Strooper, B.; Annaert, W., Proteolytic processing and cell biological functions of the amyloid precursor protein. *J Cell Sci* **2000**, 113 (Pt 11), 1857-70.
200. Nunan, J.; Small, D. H., Regulation of APP cleavage by alpha-, beta- and gamma-secretases. *FEBS Lett* **2000**, 483, (1), 6-10.
201. LeBlanc, A. C.; Chen, H. Y.; Autilio-Gambetti, L.; Gambetti, P., Differential APP gene expression in rat cerebral cortex, meninges, and primary astroglial, microglial and neuronal cultures. *FEBS Lett* **1991**, 292, (1-2), 171-8.
202. Beyreuther, K.; Masters, C. L., Alzheimer's disease. The ins and outs of amyloid-beta. *Nature* **1997**, 389, (6652), 677-8.
203. Allinson, T. M.; Parkin, E. T.; Turner, A. J.; Hooper, N. M., ADAMs family members as amyloid precursor protein alpha-secretases. *J Neurosci Res* **2003**, 74, (3), 342-52.
204. Sinha, S.; Lieberburg, I., Cellular mechanisms of beta-amyloid production and secretion. *Proc Natl Acad Sci U S A* **1999**, 96, (20), 11049-53.
205. Kojro, E.; Gimpl, G.; Lammich, S.; Marz, W.; Fahrenholz, F., Low cholesterol stimulates the nonamyloidogenic pathway by its effect on the alpha -secretase ADAM 10. *Proc Natl Acad Sci U S A* **2001**, 98, (10), 5815-20.
206. Ehehalt, R.; Keller, P.; Haass, C.; Thiele, C.; Simons, K., Amyloidogenic processing of the Alzheimer beta-amyloid precursor protein depends on lipid rafts. *J Cell Biol* **2003**, 160, (1), 113-23.

207. Weidemann, A.; Konig, G.; Bunke, D.; Fischer, P.; Salbaum, J. M.; Masters, C. L.; Beyreuther, K., Identification, biogenesis, and localization of precursors of Alzheimer's disease A4 amyloid protein. *Cell* **1989**, 57, (1), 115-26.
208. Hussain, I.; Powell, D.; Howlett, D. R.; Tew, D. G.; Meek, T. D.; Chapman, C.; Gloger, I. S.; Murphy, K. E.; Southan, C. D.; Ryan, D. M.; Smith, T. S.; Simmons, D. L.; Walsh, F. S.; Dingwall, C.; Christie, G., Identification of a novel aspartic protease (Asp 2) as beta-secretase. *Mol Cell Neurosci* **1999**, 14, (6), 419-27.
209. Vassar, R.; Bennett, B. D.; Babu-Khan, S.; Kahn, S.; Mendiaz, E. A.; Denis, P.; Teplow, D. B.; Ross, S.; Amarante, P.; Loeloff, R.; Luo, Y.; Fisher, S.; Fuller, J.; Edenson, S.; Lile, J.; Jarosinski, M. A.; Biere, A. L.; Curran, E.; Burgess, T.; Louis, J. C.; Collins, F.; Treanor, J.; Rogers, G.; Citron, M., Beta-secretase cleavage of Alzheimer's amyloid precursor protein by the transmembrane aspartic protease BACE. *Science* **1999**, 286, (5440), 735-41.
210. Yan, R.; Bienkowski, M. J.; Shuck, M. E.; Miao, H.; Tory, M. C.; Pauley, A. M.; Brashier, J. R.; Stratman, N. C.; Mathews, W. R.; Buhl, A. E.; Carter, D. B.; Tomasselli, A. G.; Parodi, L. A.; Heinrikson, R. L.; Gurney, M. E., Membrane-anchored aspartyl protease with Alzheimer's disease beta-secretase activity. *Nature* **1999**, 402, (6761), 533-7.
211. Cai, H.; Wang, Y.; McCarthy, D.; Wen, H.; Borchelt, D. R.; Price, D. L.; Wong, P. C., BACE1 is the major beta-secretase for generation of Abeta peptides by neurons. *Nat Neurosci* **2001**, 4, (3), 233-4.
212. Koo, E. H.; Squazzo, S. L., Evidence that production and release of amyloid beta-protein involves the endocytic pathway. *J Biol Chem* **1994**, 269, (26), 17386-9.
213. Haass, C.; Lemere, C. A.; Capell, A.; Citron, M.; Seubert, P.; Schenk, D.; Lannfelt, L.; Selkoe, D. J., The Swedish mutation causes early-onset Alzheimer's disease by beta-secretase cleavage within the secretory pathway. *Nat Med* **1995**, 1, (12), 1291-6.
214. Walter, J.; Fluhner, R.; Hartung, B.; Willem, M.; Kaether, C.; Capell, A.; Lammich, S.; Multhaup, G.; Haass, C., Phosphorylation regulates intracellular trafficking of beta-secretase. *J Biol Chem* **2001**, 276, (18), 14634-41.
215. Haass, C.; Hung, A. Y.; Schlossmacher, M. G.; Teplow, D. B.; Selkoe, D. J., beta-Amyloid peptide and a 3-kDa fragment are derived by distinct cellular mechanisms. *J Biol Chem* **1993**, 268, (5), 3021-4.

216. Cordy, J. M.; Hussain, I.; Dingwall, C.; Hooper, N. M.; Turner, A. J., Exclusively targeting beta-secretase to lipid rafts by GPI-anchor addition up-regulates beta-site processing of the amyloid precursor protein. *Proc Natl Acad Sci U S A* **2003**, 100, (20), 11735-40.
217. Abad-Rodriguez, J.; Ledesma, M. D.; Craessaerts, K.; Perga, S.; Medina, M.; Delacourte, A.; Dingwall, C.; De Strooper, B.; Dotti, C. G., Neuronal membrane cholesterol loss enhances amyloid peptide generation. *J Cell Biol* **2004**, 167, (5), 953-60.
218. Shiraishi, H.; Marutani, T.; Wang, H.-Q.; Maeda, Y.; Kurono, Y.; Takashima, A.; Araki, W.; Nishimura, M.; Yanagisawa, K.; Komano, H., Reconstitution of g-secretase by truncated presenilin (PS) fragments revealed that PS C-terminal transmembrane domain is critical for formation of g-secretase complex. *Genes to Cells* **2006**, 11, (1), 83-93.
219. Thinakaran, G.; Borchelt, D. R.; Lee, M. K.; Slunt, H. H.; Spitzer, L.; Kim, G.; Ratovitsky, T.; Davenport, F.; Nordstedt, C.; Seeger, M.; Hardy, J.; Levey, A. I.; Gandy, S. E.; Jenkins, N. A.; Copeland, N. G.; Price, D. L.; Sisodia, S. S., Endoproteolysis of presenilin 1 and accumulation of processed derivatives in vivo. *Neuron* **1996**, 17, (1), 181-90.
220. Ratovitski, T.; Slunt, H. H.; Thinakaran, G.; Price, D. L.; Sisodia, S. S.; Borchelt, D. R., Endoproteolytic processing and stabilization of wild-type and mutant presenilin. *J Biol Chem* **1997**, 272, (39), 24536-41.
221. Xu, H.; Sweeney, D.; Wang, R.; Thinakaran, G.; Lo, A. C.; Sisodia, S. S.; Greengard, P.; Gandy, S., Generation of Alzheimer beta-amyloid protein in the trans-Golgi network in the apparent absence of vesicle formation. *Proc Natl Acad Sci U S A* **1997**, 94, (8), 3748-52.
222. Cook, D. G.; Forman, M. S.; Sung, J. C.; Leight, S.; Kolson, D. L.; Iwatsubo, T.; Lee, V. M.; Doms, R. W., Alzheimer's A beta(1-42) is generated in the endoplasmic reticulum/intermediate compartment of NT2N cells. *Nat Med* **1997**, 3, (9), 1021-3.
223. Greenfield, J. P.; Tsai, J.; Gouras, G. K.; Hai, B.; Thinakaran, G.; Checler, F.; Sisodia, S. S.; Greengard, P.; Xu, H., Endoplasmic reticulum and trans-Golgi network generate distinct populations of Alzheimer beta-amyloid peptides. *Proc Natl Acad Sci U S A* **1999**, 96, (2), 742-7.
224. Takahashi, R. H.; Milner, T. A.; Li, F.; Nam, E. E.; Edgar, M. A.; Yamaguchi, H.; Beal, M. F.; Xu, H.; Greengard, P.; Gouras, G. K., Intraneuronal Alzheimer abeta42

accumulates in multivesicular bodies and is associated with synaptic pathology. *Am J Pathol* **2002**, 161, (5), 1869-79.

225. Vetrivel, K. S.; Cheng, H.; Lin, W.; Sakurai, T.; Li, T.; Nukina, N.; Wong, P. C.; Xu, H.; Thinakaran, G., Association of gamma-secretase with lipid rafts in post-Golgi and endosome membranes. *J Biol Chem* **2004**, 279, (43), 44945-54.

226. Haass, C.; Schlossmacher, M. G.; Hung, A. Y.; Vigo-Pelfrey, C.; Mellon, A.; Ostaszewski, B. L.; Lieberburg, I.; Koo, E. H.; Schenk, D.; Teplow, D. B.; et al., Amyloid beta-peptide is produced by cultured cells during normal metabolism. *Nature* **1992**, 359, (6393), 322-5.

227. Younkin, S. G., Evidence that A beta 42 is the real culprit in Alzheimer's disease. *Ann Neurol* **1995**, 37, (3), 287-8.

228. Burdick, D.; Soreghan, B.; Kwon, M.; Kosmoski, J.; Knauer, M.; Henschen, A.; Yates, J.; Cotman, C.; Glabe, C., Assembly and aggregation properties of synthetic Alzheimer's A4/beta amyloid peptide analogs. *J Biol Chem* **1992**, 267, (1), 546-54.

229. Irie, K.; Murakami, K.; Masuda, Y.; Morimoto, A.; Ohigashi, H.; Ohashi, R.; Takegoshi, K.; Nagao, M.; Shimizu, T.; Shirasawa, T., Structure of beta-amyloid fibrils and its relevance to their neurotoxicity: implications for the pathogenesis of Alzheimer's disease. *J Biosci Bioeng* **2005**, 99, (5), 437-47.

230. Chartier-Harlin, M. C.; Crawford, F.; Hamandi, K.; Mullan, M.; Goate, A.; Hardy, J.; Backhovens, H.; Martin, J. J.; Broeckhoven, C. V., Screening for the beta-amyloid precursor protein mutation (APP717: Val----Ile) in extended pedigrees with early onset Alzheimer's disease. *Neurosci Lett* **1991**, 129, (1), 134-5.

231. Murrell, J.; Farlow, M.; Ghetti, B.; Benson, M. D., A mutation in the amyloid precursor protein associated with hereditary Alzheimer's disease. *Science* **1991**, 254, (5028), 97-9.

232. Eckman, C. B.; Mehta, N. D.; Crook, R.; Perez-tur, J.; Prihar, G.; Pfeiffer, E.; Graff-Radford, N.; Hinder, P.; Yager, D.; Zenk, B.; Refolo, L. M.; Prada, C. M.; Younkin, S. G.; Hutton, M.; Hardy, J., A new pathogenic mutation in the APP gene (I716V) increases the relative proportion of A beta 42(43). *Hum Mol Genet* **1997**, 6, (12), 2087-9.

233. Sherrington, R.; Rogaev, E. I.; Liang, Y.; Rogaeva, E. A.; Levesque, G.; Ikeda, M.; Chi, H.; Lin, C.; Li, G.; Holman, K.; et al., Cloning of a gene bearing missense mutations in early-onset familial Alzheimer's disease. *Nature* **1995**, 375, (6534), 754-60.
234. Rogaev, E. I.; Sherrington, R.; Rogaeva, E. A.; Levesque, G.; Ikeda, M.; Liang, Y.; Chi, H.; Lin, C.; Holman, K.; Tsuda, T.; et al., Familial Alzheimer's disease in kindreds with missense mutations in a gene on chromosome 1 related to the Alzheimer's disease type 3 gene. *Nature* **1995**, 376, (6543), 775-8.
235. Sisodia, S. S.; St George-Hyslop, P. H., gamma-Secretase, Notch, Abeta and Alzheimer's disease: where do the presenilins fit in? *Nat Rev Neurosci* **2002**, 3, (4), 281-90.
236. Iwatsubo, T., The gamma-secretase complex: machinery for intramembrane proteolysis. *Curr Opin Neurobiol* **2004**, 14, (3), 379-83.
237. Roses, A. D., Apolipoprotein E and Alzheimer's disease. The tip of the susceptibility iceberg. *Ann N Y Acad Sci* **1998**, 855, 738-43.
238. Wen, Y.; Onyewuchi, O.; Yang, S.; Liu, R.; Simpkins James, W., Increased beta-secretase activity and expression in rats following transient cerebral ischemia. *Brain Res* **2004**, 1009, (1-2), 1-8.
239. Rossner, S.; Lange-Dohna, C.; Zeitschel, U.; Perez-Polo, J. R., Alzheimer's disease beta-secretase BACE1 is not a neuron-specific enzyme. *J Neurochem* **2005**, 92, (2), 226-34.
240. Zhao, J.; Fu, Y.; Yasvoina, M.; Shao, P.; Hitt, B.; O'Connor, T.; Logan, S.; Maus, E.; Citron, M.; Berry, R.; Binder, L.; Vassar, R., Beta-site amyloid precursor protein cleaving enzyme 1 levels become elevated in neurons around amyloid plaques: implications for Alzheimer's disease pathogenesis. *J Neurosci* **2007**, 27, (14), 3639-49.
241. Gupta, S. V.; Khosla, P., Palmitic and stearic acids similarly affect plasma lipoprotein metabolism in cynomolgus monkeys fed diets with adequate levels of linoleic acid. *J Nutr* **2001**, 131, (8), 2115-20.
242. Chang, K.-A.; Suh, Y.-H., Pathophysiological roles of amyloidogenic carboxy-terminal fragments of the b-amyloid precursor protein in Alzheimer's disease. *J Pharmacol Sci* **2005**, 97, (4), 461-471.

243. Li, Y.; Zhou, W.; Tong, Y.; He, G.; Song, W., Control of APP processing and Ab generation level by BACE1 enzymatic activity and transcription. *FASEB J* **2006**, 20, (2), 285-292.
244. Yan, S. D.; Yan, S. F.; Chen, X.; Fu, J.; Chen, M.; Kuppusamy, P.; Smith, M. A.; Perry, G.; Godman, G. C.; et al., Non-enzymatically glycated tau in Alzheimer's disease induces neuronal oxidant stress resulting in cytokine gene expression and release of amyloid b-peptide. *Nat Med* **1995**, 1, (7), 693-9.
245. Hoyer, S., Abnormalities of glucose metabolism in Alzheimer's disease. *Ann N Y Acad Sci* **1991**, 640, 53-8.
246. Munch, G.; Schinzel, R.; Loske, C.; Wong, A.; Durany, N.; Li, J. J.; Vlassara, H.; Smith, M. A.; Perry, G.; Riederer, P., Alzheimer's disease--synergistic effects of glucose deficit, oxidative stress and advanced glycation endproducts. *J Neural Transm* **1998**, 105, (4-5), 439-61.
247. Sorbi, S.; Piacentini, S.; Latorraca, S.; Piersanti, P.; Amaducci, L., Alterations in metabolic properties in fibroblasts in Alzheimer disease. *Alzheimer Dis Assoc Disord* **1995**, 9, (2), 73-7.
248. Sheu, K. F.; Cooper, A. J.; Koike, K.; Koike, M.; Lindsay, J. G.; Blass, J. P., Abnormality of the alpha-ketoglutarate dehydrogenase complex in fibroblasts from familial Alzheimer's disease. *Ann Neurol* **1994**, 35, (3), 312-8.
249. Sorbi, S.; Bird, E. D.; Blass, J. P., Decreased pyruvate dehydrogenase complex activity in Huntington and Alzheimer brain. *Ann Neurol* **1983**, 13, (1), 72-8.
250. Kish, S. J., Brain energy metabolizing enzymes in Alzheimer's disease: alpha-ketoglutarate dehydrogenase complex and cytochrome oxidase. *Ann N Y Acad Sci* **1997**, 826, 218-28.
251. Gibson, G. E.; Park, L. C.; Sheu, K. F.; Blass, J. P.; Calingasan, N. Y., The alpha-ketoglutarate dehydrogenase complex in neurodegeneration. *Neurochem Int* **2000**, 36, (2), 97-112.
252. Parker, W. D., Jr.; Mahr, N. J.; Filley, C. M.; Parks, J. K.; Hughes, D.; Young, D. A.; Cullum, C. M., Reduced platelet cytochrome c oxidase activity in Alzheimer's disease. *Neurology* **1994**, 44, (6), 1086-90.

253. Cardoso, S. M.; Proenca, M. T.; Santos, S.; Santana, I.; Oliveira, C. R., Cytochrome c oxidase is decreased in Alzheimer's disease platelets. *Neurobiol Aging* **2004**, 25, (1), 105-10.
254. Kish, S. J.; Bergeron, C.; Rajput, A.; Dozic, S.; Mastrogiacono, F.; Chang, L. J.; Wilson, J. M.; DiStefano, L. M.; Nobrega, J. N., Brain cytochrome oxidase in Alzheimer's disease. *J Neurochem* **1992**, 59, (2), 776-9.
255. Mutisya, E. M.; Bowling, A. C.; Beal, M. F., Cortical cytochrome oxidase activity is reduced in Alzheimer's disease. *J Neurochem* **1994**, 63, (6), 2179-84.
256. Tretter, L.; Adam-Vizi, V., Inhibition of Krebs cycle enzymes by hydrogen peroxide: A key role of [alpha]-ketoglutarate dehydrogenase in limiting NADH production under oxidative stress. *J Neurosci* **2000**, 20, (24), 8972-9.
257. Drzezga, A.; Grimmer, T.; Riemenschneider, M.; Lautenschlager, N.; Siebner, H.; Alexopoulos, P.; Minoshima, S.; Schwaiger, M.; Kurz, A., Prediction of individual clinical outcome in MCI by means of genetic assessment and 18F-FDG PET. *J Nucl Med* **2005**, 46, (10), 1625-1632.
258. Gibson, G. E., Interactions of oxidative stress with cellular calcium dynamics and glucose metabolism in Alzheimer's disease. *Free Radic Biol Med* **2002**, 32, (11), 1061-1070.
259. Gibson, G. E.; Jope, R.; Blass, J. P., Decreased synthesis of acetylcholine accompanying impaired oxidation of pyruvic acid in rat brain minces. *Biochem J* **1975**, 148, (1), 17-23.
260. Rupprecht, R.; Holsboer, F., Neuroactive steroids: mechanisms of action and neuropsychopharmacological perspectives. *Trends Neurosci* **1999**, 22, (9), 410-6.
261. Ehrenstein, G.; Galdzicki, Z.; Lange, G. D., The choline-leakage hypothesis for the loss of acetylcholine in Alzheimer's disease. *Biophys J* **1997**, 73, (3), 1276-80.
262. Sims, N. R.; Bowen, D. M.; Allen, S. J.; Smith, C. C.; Neary, D.; Thomas, D. J.; Davison, A. N., Presynaptic cholinergic dysfunction in patients with dementia. *J Neurochem* **1983**, 40, (2), 503-9.



263. Nitsch, R. M.; Slack, B. E.; Wurtman, R. J.; Growdon, J. H., Release of Alzheimer amyloid precursor derivatives stimulated by activation of muscarinic acetylcholine receptors. *Science* **1992**, 258, (5080), 304-7.
264. Baskin, D. S.; Browning, J. L.; Pirozzolo, F. J.; Korporaal, S.; Baskin, J. A.; Appel, S. H., Brain choline acetyltransferase and mental function in Alzheimer disease. *Arch Neurol* **1999**, 56, (9), 1121-3.
265. Hoyer, S., Oxidative metabolism deficiencies in brains of patients with Alzheimer's disease. *Acta Neurol Scand Suppl* **1996**, 165, 18-24.
266. Hoyer, A.; Bardenheuer, H. J.; Martin, E.; Plaschke, K., Amyloid precursor protein (APP) and its derivatives change after cellular energy depletion. An in vitro-study. *J Neural Transm* **2005**, 112, (2), 239-253.
267. Planel, E.; Miyasaka, T.; Launey, T.; Chui, D.-H.; Tanemura, K.; Sato, S.; Murayama, O.; Ishiguro, K.; Tatebayashi, Y.; Takashima, A., Alterations in glucose metabolism induce hypothermia leading to tau hyperphosphorylation through differential inhibition of kinase and phosphatase activities: implications for Alzheimer's disease. *J Neurosci* **2004**, 24, (10), 2401-2411.
268. Velliquette, R. A.; O'Connor, T.; Vassar, R., Energy inhibition elevates b-secretase levels and activity and is potentially amyloidogenic in APP transgenic mice: Possible early events in Alzheimer's disease pathogenesis. *J Neurosci* **2005**, 25, (47), 10874-10883.
269. Gong, C.-X.; Liu, F.; Grundke-Iqbal and, I.; Iqbal, K., Impaired brain glucose metabolism leads to Alzheimer neurofibrillary degeneration through a decrease in tau O-GlcNAcylation. *J Alzheimers Dis* **2006**, 9, (1), 1-12.
270. Liu, F.; Iqbal, K.; Grundke-Iqbal, I.; Hart, G. W.; Gong, C.-X., O-GlcNAcylation regulates phosphorylation of tau: A mechanism involved in Alzheimer's disease. *Proc Natl Acad Sci U S A* **2004**, 101, (29), 10804-10809.
271. Chih, C. P.; Lipton, P.; Roberts, E. L., Do active cerebral neurons really use lactate rather than glucose? *Trends Neurosci* **2001**, 24, (10), 573-578.
272. Pellerin, L.; Magistretti, P. J., Glutamate uptake into astrocytes stimulates aerobic glycolysis: a mechanism coupling neuronal activity to glucose utilization. *Proc Natl Acad Sci U S A* **1994**, 91, (22), 10625-9.

273. Kasischke, K. A.; Vishwasrao, H. D.; Fisher, P. J.; Zipfel, W. R.; Webb, W. W., Neural Activity Triggers Neuronal Oxidative Metabolism Followed by Astrocytic Glycolysis. *Science* **2004**, 305, (5680), 99-103.
274. Patil, S.; Li, Z.; Chan, C., Cellular to tissue informatics: approaches to optimizing cellular function of engineered tissue. *Adv Biochem Eng Biotechnol* **2006**, 102, 139-59.
275. Srivastava, S.; Chan, C., Application of metabolic flux analysis to identify the mechanisms of free fatty acid toxicity to human hepatoma cell line. *Biotechnol Bioeng* **2007**.
276. Chan, C.; Berthiaume, F.; Lee, K.; Yarmush, M. L., Metabolic flux analysis of cultured hepatocytes exposed to plasma. *Biotechnol Bioeng* **2003**, 81, (1), 33-49.
277. Rose, C.; Felipo, V., Limited capacity for ammonia removal by brain in chronic liver failure: potential role of nitric oxide. *Metab Brain Dis* **2005**, 20, (4), 275-83.
278. McGinnis, J. F.; de Vellis, J., Cell surface modulation of gene expression in brain cells by down regulation of glucocorticoid receptors. *Proc Natl Acad Sci U S A* **1981**, 78, (2), 1288-92.
279. Bligh, E. G.; Dyer, W. J., A rapid method of total lipide extraction and purification. *Can J Biochem Physiol* **1959**, 37, 911-17.
280. Merrill, A. H., Jr.; Wang, E.; Mullins, R. E.; Jamison, W. C. L.; Nimkar, S.; Liotta, D. C., Quantitation of free sphingosine in liver by high-performance liquid chromatography. *Anal Biochem* **1988**, 171, (2), 373-81.
281. Berry, M. N.; Phillips, J. W.; Henly, D. C.; Clark, D. G., Effects of fatty acid oxidation on glucose utilization by isolated hepatocytes. *FEBS Lett* **1993**, 319, (1-2), 26-30.
282. Hue, L.; Maisin, L.; Rider, M. H., Palmitate inhibits liver glycolysis. Involvement of fructose 2,6-bisphosphate in the glucose/fatty acid cycle. *Biochem J* **1988**, 251, (2), 541-5.
283. Ji, H.; Graczyk-Milbrandt, G.; Osbakken, M. D.; Friedman, M. I., Interactions of dietary fat and 2,5-anhydro-D-mannitol on energy metabolism in isolated rat hepatocytes. *Am J Physiol* **2002**, 282, (3, Pt. 2), R715-R720.

284. Lovell, M. A.; Xie, C.; Markesbery, W. R., Acrolein, a product of lipid peroxidation, inhibits glucose and glutamate uptake in primary neuronal cultures. *Free Radic Biol Med* **2000**, 29, (8), 714-720.
285. Mark, R. J.; Pang, Z.; Geddes, J. W.; Uchida, K.; Mattson, M. P., Amyloid  $\beta$ -peptide impairs glucose transport in hippocampal and cortical neurons: involvement of membrane lipid peroxidation. *J Neurosci* **1997**, 17, (3), 1046-1054.
286. Miwa, I.; Adachi, K.; Murase, S.; Hamada, Y.; Sugiura, M., 4-Hydroxy-2-nonenal hardly affects glycolysis. *Free Radic Biol Med* **1997**, 23, (4), 610-615.
287. Smith, J. M.; Solar, S. M.; Paulson, D. J.; Hill, N. M.; Broderick, T. L., Effect of palmitate on carbohydrate utilization and Na/K-ATPase activity in aortic vascular smooth muscle from diabetic rats. *Mol Cell Biochem* **1999**, 194, (1-2), 125-32.
288. King, L. M.; Sidell, R. J.; Wilding, J. R.; Radda, G. K.; Clarke, K., Free fatty acids, but not ketone bodies, protect diabetic rat hearts during low-flow ischemia. *Am J Physiol Heart Circ Physiol* **2001**, 280, (3), H1173-81.
289. Fukuyama, H.; Ogawa, M.; Yamauchi, H.; Yamaguchi, S.; Kimura, J.; Yonekura, Y.; Konishi, J., Altered cerebral energy metabolism in Alzheimer's disease: a PET study. *J Nucl Med* **1994**, 35, (1), 1-6.
290. Hoyer, S., Risk factors for Alzheimer's disease during aging. Impacts of glucose/energy metabolism. *J Neural Transm Suppl* **1998**, 54, 187-94.
291. Pettegrew, J. W.; Klunk, W. E.; Kanal, E.; Panchalingam, K.; McClure, R. J., Changes in brain membrane phospholipid and high-energy phosphate metabolism precede dementia. *Neurobiol Aging* **1995**, 16, (6), 973-5.
292. Pifferi, F.; Roux, F.; Langelier, B.; Alessandri, J.-M.; Vancassel, S.; Jouin, M.; Lavialle, M.; Guesnet, P., (n-3) polyunsaturated fatty acid deficiency reduces the expression of both isoforms of the brain glucose transporter GLUT1 in rats. *J Nutr* **2005**, 135, (9), 2241-2246.
293. Li, J.; Hu, X.; Selvakumar, P.; Russell, R. R., III; Cushman, S. W.; Holman, G. D.; Young, L. H., Role of the nitric oxide pathway in AMPK-mediated glucose uptake and GLUT4 translocation in heart muscle. *Am J Physiol* **2004**, 287, (5, Pt.1), E834-E841.

294. Turnley, A. M.; Stapleton, D.; Mann, R. J.; Witters, L. A.; Kemp, B. E.; Bartlett, P. F., Cellular distribution and developmental expression of AMP-activated protein kinase isoforms in mouse central nervous system. *J Neurochem* **1999**, 72, (4), 1707-16.
295. Blazquez, C.; Woods, A.; de Ceballos, M. L.; Carling, D.; Guzman, M., The AMP-activated protein kinase is involved in the regulation of ketone body production by astrocytes. *J Neurochem* **1999**, 73, (4), 1674-82.
296. Giri, S.; Nath, N.; Smith, B.; Viollet, B.; Singh Avtar, K.; Singh, I., 5-aminimidazole-4-carboxamide-1-beta-4-ribofuranoside inhibits proinflammatory response in glial cells: a possible role of AMP-activated protein kinase. *J Neurosci* **2004**, 24, (2), 479-87.
297. McCullough Louise, D.; Zeng, Z.; Li, H.; Landree Leslie, E.; McFadden, J.; Ronnett Gabriele, V., Pharmacological inhibition of AMP-activated protein kinase provides neuroprotection in stroke. *J Biol Chem* **2005**, 280, (21), 20493-502.
298. Simpson, I. A.; Chundu, K. R.; Davies-Hill, T.; Honer, W. G.; Davies, P., Decreased concentrations of GLUT1 and GLUT3 glucose transporters in the brains of patients with Alzheimer's disease. *Ann Neurol* **1994**, 35, (5), 546-51.
299. Mandelin, A. M., 2000. Alzheimer's disease severity is associated with a progressive decline in glut1 gene expression: role of posttranscriptional regulation. 193 pp. From: Diss. Abstr. Int., B 2002, 62(11), 4951.
300. Listenberger, L. L.; Ory, D. S.; Schaffer, J. E., Palmitate-induced apoptosis can occur through a ceramide-independent pathway. *J Biol Chem* **2001**, 276, (18), 14890-5.
301. Palicz, A.; Foubert, T. R.; Jesaitis, A. J.; Marodi, L.; McPhail, L. C., Phosphatidic acid and diacylglycerol directly activate NADPH oxidase by interacting with enzyme components. *J Biol Chem* **2001**, 276, (5), 3090-7.
302. Lu, Z. H.; Mu, Y. M.; Wang, B. A.; Li, X. L.; Lu, J. M.; Li, J. Y.; Pan, C. Y.; Yanase, T.; Nawata, H., Saturated free fatty acids, palmitic acid and stearic acid, induce apoptosis by stimulation of ceramide generation in rat testicular Leydig cell. *Biochem Biophys Res Commun* **2003**, 303, (4), 1002-7.
303. Yi, F.; Zhang, A. Y.; Jansch, J. L.; Li, P.-L.; Zou, A.-P., Homocysteine activates NADH/NADPH oxidase through ceramide-stimulated Rac GTPase activity in rat mesangial cells. *Kidney Int* **2004**, 66, (5), 1977-1987.

304. Borg, J.; London, J., Copper/zinc superoxide dismutase overexpression promotes survival of cortical neurons exposed to neurotoxins in vitro. *J Neurosci Res* **2002**, 70, (2), 180-9.
305. Lieb, K.; Fiebich, B. L.; Hull, M.; Berger, M.; Bauer, J., Potent inhibition of interleukin-6 expression in a human astrocytoma cell line by tenidap. *Cell Tissue Res* **1997**, 288, (2), 251-257.
306. Pahan, K.; Sheikh, F. G.; Khan, M.; Namboodiri, A. M. S.; Singh, I., Sphingomyelinase and ceramide stimulate the expression of inducible nitric-oxide synthase in rat primary astrocytes. *J Biol Chem* **1998**, 273, (5), 2591-2600.
307. Floyd, R. A.; Hensley, K.; Jaffery, F.; Maidt, L.; Robinson, K.; Pye, Q.; Stewart, C., Increased oxidative stress brought on by pro-inflammatory cytokines in neurodegenerative processes and the protective role of nitron-based free radical traps. *Life Sci* **1999**, 65, (18/19), 1893-1899.
308. Wei, T.; Chen, C.; Hou, J.; Xin, W.; Mori, A., Nitric oxide induces oxidative stress and apoptosis in neuronal cells. *Biochim Biophys Acta* **2000**, 1498, (1), 72-79.
309. Zwingmann, C.; Richter-Landsberg, C.; Brand, A.; Leibfritz, D., NMR spectroscopic study on the metabolic fate of [3-(13)C]alanine in astrocytes, neurons, and cocultures: implications for glia-neuron interactions in neurotransmitter metabolism. *Glia* **2000**, 32, (3), 286-303.
310. Sykes, J. E.; Lopes-Cardozo, M., Effect of exogenous fatty acids on lipid synthesis, marker-enzymes, and development of glial cells maintained in serum-free culture. *Glia* **1990**, 3, (6), 495-501.
311. Sharma, K.; Shi, Y., The yins and yangs of ceramide. *Cell Res* **1999**, 9, (1), 1-10.
312. Perry, D. K.; Hannun, Y. A., The role of ceramide in cell signaling. *Biochim Biophys Acta* **1998**, 1436, (1-2), 233-43.
313. Holland, W. L.; Brozinick, J. T.; Wang, L. P.; Hawkins, E. D.; Sargent, K. M.; Liu, Y.; Narra, K.; Hoehn, K. L.; Knotts, T. A.; Siesky, A.; Nelson, D. H.; Karathanasis, S. K.; Fontenot, G. K.; Birnbaum, M. J.; Summers, S. A., Inhibition of ceramide synthesis ameliorates glucocorticoid-, saturated-fat-, and obesity-induced insulin resistance. *Cell Metab* **2007**, 5, (3), 167-79.

314. Haughey, N. J.; Cutler, R. G.; Tamara, A.; McArthur, J. C.; Vargas, D. L.; Pardo, C. A.; Turchan, J.; Nath, A.; Mattson, M. P., Perturbation of sphingolipid metabolism and ceramide production in HIV-dementia. *Ann Neurol* **2004**, 55, (2), 257-67.
315. Han, X.; Holtzman, D. M.; McKeel, D. W., Jr.; Kelley, J.; Morris, J. C., Substantial sulfatide deficiency and ceramide elevation in very early Alzheimer's disease: potential role in disease pathogenesis. *J Neurochem* **2002**, 82, (4), 809-818.
316. Cutler, R. G.; Kelly, J.; Storie, K.; Pedersen, W. A.; Tammara, A.; Hatanpaa, K.; Troncoso, J. C.; Mattson, M. P., Involvement of oxidative stress-induced abnormalities in ceramide and cholesterol metabolism in brain aging and Alzheimer's disease. *Proc Natl Acad Sci U S A* **2004**, 101, (7), 2070-2075.
317. Satoi, H.; Tomimoto, H.; Ohtani, R.; Kitano, T.; Kondo, T.; Watanabe, M.; Oka, N.; Akiguchi, I.; Furuya, S.; Hirabayashi, Y.; Okazaki, T., Astroglial expression of ceramide in Alzheimer's disease brains: a role during neuronal apoptosis. *Neuroscience* **2005**, 130, (3), 657-666.
318. Han, X.; D, M. H.; McKeel, D. W., Jr.; Kelley, J.; Morris, J. C., Substantial sulfatide deficiency and ceramide elevation in very early Alzheimer's disease: potential role in disease pathogenesis. *J Neurochem* **2002**, 82, (4), 809-18.
319. Katsel, P.; Li, C.; Haroutunian, V., Gene expression alterations in the sphingolipid metabolism pathways during progression of dementia and Alzheimer's disease: a shift toward ceramide accumulation at the earliest recognizable stages of Alzheimer's disease? *Neurochem Res* **2007**, 32, (4-5), 845-56.
320. Malaplate-Armand, C.; Florent-Bechard, S.; Youssef, I.; Koziel, V.; Sponne, I.; Kriem, B.; Leininger-Muller, B.; Olivier, J. L.; Oster, T.; Pillot, T., Soluble oligomers of amyloid-beta peptide induce neuronal apoptosis by activating a cPLA2-dependent sphingomyelinase-ceramide pathway. *Neurobiol Dis* **2006**, 23, (1), 178-89.
321. Jana, A.; Pahan, K., Fibrillar amyloid-beta peptides kill human primary neurons via NADPH oxidase-mediated activation of neutral sphingomyelinase. Implications for Alzheimer's disease. *J Biol Chem* **2004**, 279, (49), 51451-9.
322. Lee, J. T.; Xu, J.; Lee, J. M.; Ku, G.; Han, X.; Yang, D. I.; Chen, S.; Hsu, C. Y., Amyloid-beta peptide induces oligodendrocyte death by activating the neutral sphingomyelinase-ceramide pathway. *J Cell Biol* **2004**, 164, (1), 123-31.

323. Marty, M. S.; Atchison, W. D., Pathways mediating  $\text{Ca}^{2+}$  entry in rat cerebellar granule cells following in vitro exposure to methyl mercury. *Toxicol Appl Pharmacol* **1997**, 147, (2), 319-30.
324. Puglielli, L.; Ellis, B. C.; Saunders, A. J.; Kovacs, D. M., Ceramide stabilizes b-site amyloid precursor protein-cleaving enzyme 1 and promotes amyloid b-peptide biogenesis. *J Biol Chem* **2003**, 278, (22), 19777-19783.
325. Fan, Q. W.; Yu, W.; Gong, J. S.; Zou, K.; Sawamura, N.; Senda, T.; Yanagisawa, K.; Michikawa, M., Cholesterol-dependent modulation of dendrite outgrowth and microtubule stability in cultured neurons. *J Neurochem* **2002**, 80, (1), 178-90.
326. Emamian, E. S.; Hall, D.; Birnbaum, M. J.; Karayiorgou, M.; Gogos, J. A., Convergent evidence for impaired AKT1-GSK3b signaling in schizophrenia. *Nat Genet* **2004**, 36, (2), 131-137.
327. de la Monte, S. M.; Ganju, N.; Feroz, N.; Luong, T.; Banerjee, K.; Cannon, J.; Wands, J. R., Oxygen free radical injury is sufficient to cause some Alzheimer-type molecular abnormalities in human CNS neuronal cells. *J Alzheimers Dis* **2000**, 2, (3-4), 261-281.
328. Lee, M.-s.; Kwon, Y. T.; Li, M.; Peng, J.; Friedlander, R. M.; Tsai, L.-H., Neurotoxicity induces cleavage of p35 to p25 by calpain. *Nature* **2000**, 405, (6784), 360-364.
329. Kerokoski, P.; Suuronen, T.; Salminen, A.; Soininen, H.; Pirttila, T., Cleavage of the cyclin-dependent kinase 5 activator p35 to p25 does not induce tau hyperphosphorylation. *Biochem Biophys Res Commun* **2002**, 298, (5), 693-698.
330. Takashima, A., GSK-3 is essential in the pathogenesis of Alzheimer's disease. *J Alzheimers Dis* **2006**, 9, 309-317.
331. Phiel, C. J.; Wilson, C. A.; Lee, V. M. Y.; Klein, P. S., GSK-3a regulates production of Alzheimer's disease amyloid-b peptides. *Nature* **2003**, 423, (6938), 435-439.
332. Beffert, U.; Cohn, J. S.; Petit-Turcotte, C.; Tremblay, M.; Aumont, N.; Ramassamy, C.; Davignon, J.; Poirier, J., Apolipoprotein E and b-amyloid levels in the hippocampus and frontal cortex of Alzheimer's disease subjects are disease-related and apolipoprotein E genotype dependent. *Brain Res* **1999**, 843, (1-2), 87-94.

333. Szutowicz, A.; Bielarczyk, H.; Gul, S.; Ronowska, A.; Pawelczyk, T.; Jankowska-Kulawy, A., Phenotype-dependent susceptibility of cholinergic neuroblastoma cells to neurotoxic inputs. *Metabol Brain Dis* **2006**, 21, (2/3), 149-161.
334. Szutowicz, A.; Lysiak, W., Regional and subcellular distribution of ATP-citrate lyase and other enzymes of acetyl-CoA metabolism in rat brain. *J Neurochem* **1980**, 35, (4), 775-85.
335. Pei, Z.; Oey, N. A.; Zuidervaart, M. M.; Jia, Z.; Li, Y.; Steinberg, S. J.; Smith, K. D.; Watkins, P. A., The Acyl-CoA Synthetase "Bubblegum" (Lipidosin): Further Characterization and Role in Neuronal Fatty Acid  $\beta$ -Oxidation. *J Biol Chem* **2003**, 278, (47), 47070-47078.
336. Alessenko, A. V.; Bugrova, A. E.; Dudnik, L. B., Connection of lipid peroxide oxidation with the sphingomyelin pathway in the development of Alzheimer's disease. *Biochem Soc Trans* **2004**, 32, (Pt 1), 144-6.
337. Patil, S.; Chan, C., Palmitic and stearic fatty acids induce Alzheimer-like hyperphosphorylation of tau in primary rat cortical neurons. *Neurosci Lett* **2005**, 384, (3), 288-293.
338. Patil, S.; Sheng, L.; Masserang, A.; Chan, C., Palmitic acid-treated astrocytes induce BACE1 upregulation and accumulation of C-terminal fragment of APP in primary cortical neurons. *Neurosci Lett* **2006**, 406, (1-2), 55-9.
339. Sultana, R.; Boyd-Kimball, D.; Poon, H. F.; Cai, J.; Pierce, W. M.; Klein, J. B.; Merchant, M.; Markesbery, W. R.; Butterfield, D. A., Redox proteomics identification of oxidized proteins in Alzheimer's disease hippocampus and cerebellum: an approach to understand pathological and biochemical alterations in AD. *Neurobiol Aging* **2006**, 27, (11), 1564-1576.
340. Sultana, R.; Poon, H. F.; Cai, J.; Pierce, W. M.; Merchant, M.; Klein, J. B.; Markesbery, W. R.; Butterfield, D. A., Identification of nitrated proteins in Alzheimer's disease brain using a redox proteomics approach. *Neurobiol Dis* **2006**, 22, (1), 76-87.
341. Trepanier, G.; Furling, D.; Puymirat, J.; Mirault, M. E., Immunocytochemical localization of seleno-glutathione peroxidase in the adult mouse brain. *Neuroscience* **1996**, 75, (1), 231-243.



342. Wu, C.-K.; Thal, L.; Pizzo, D.; Hansen, L.; Masliah, E.; Geula, C., Apoptotic signals within the basal forebrain cholinergic neurons in Alzheimer's disease. *Exp Neurol* **2005**, 195, (2), 484-496.
343. McKinney, M.; Coyle, J. T.; Hedreen, J. C., Topographic analysis of the innervation of the rat neocortex and hippocampus by the basal forebrain cholinergic system. *J Comp Neurol* **1983**, 217, (1), 103-21.
344. Ransmayr, G.; Cervera, P.; Hirsch, E.; Ruberg, M.; Hersh, L. B.; Duyckaerts, C.; Hauw, J. J.; Delumeau, C.; Agid, Y., Choline acetyltransferase-like immunoreactivity in the hippocampal formation of control subjects and patients with Alzheimer's disease. *Neuroscience* **1989**, 32, (3), 701-14.
345. Arendt, T.; Bigl, V.; Tennstedt, A.; Arendt, A., Neuronal loss in different parts of the nucleus basalis is related to neuritic plaque formation in cortical target areas in Alzheimer's disease. *Neurosci* **1985**, 14, (1), 1-14.
346. Kashiwaya, Y.; Takeshima, T.; Mori, N.; Nakashima, K.; Clarke, K.; Veech, R. L., D-beta-hydroxybutyrate protects neurons in models of Alzheimer's and Parkinson's disease. *Proc Natl Acad Sci U S A* **2000**, 97, (10), 5440-4.
347. Wu, M. M.; Chiou, H. Y.; Wang, T. W.; Hsueh, Y. M.; Wang, I. H.; Chen, C. J.; Lee, T. C., Association of blood arsenic levels with increased reactive oxidants and decreased antioxidant capacity in a human population of northeastern Taiwan. *Environ Health Perspect* **2001**, 109, (10), 1011-7.
348. Mudher, A.; Lovestone, S., Alzheimer's disease-do tauists and baptists finally shake hands? *Trends Neurosci* **2002**, 25, (1), 22-6.
349. Yuan, H.; Zheng, J. C.; Liu, P.; Zhang, S. F.; Xu, J. Y.; Bai, L. M., Pathogenesis of Parkinson's disease: oxidative stress, environmental impact factors and inflammatory processes. *Neurosci Bull* **2007**, 23, (2), 125-30.
350. Pereira, A. C.; Wu, W.; Small, S. A., Imaging-guided microarray: isolating molecular profiles that dissociate Alzheimer's disease from normal aging. *Ann N Y Acad Sci* **2007**, 1097, 225-38.
351. Blanchard, B. J.; Hiniker, A. E.; Lu, C. C.; Margolin, Y.; Yu, A. S.; Ingram, V. M., Elimination of Amyloid beta Neurotoxicity. *J Alzheimers Dis* **2000**, 2, (2), 137-149.

352. Cheng, I. H.; Searce-Levie, K.; Legleiter, J.; Palop, J. J.; Gerstein, H.; Bien-Ly, N.; Puolivali, J.; Lesne, S.; Ashe, K. H.; Muchowski, P. J.; Mucke, L., Accelerating Amyloid-beta Fibrillization Reduces Oligomer Levels and Functional Deficits in Alzheimer Disease Mouse Models. *J Biol Chem* **2007**, 282, (33), 23818-28.
353. Azad, N. A.; Al Bugami, M.; Loy-English, I., Gender differences in dementia risk factors. *Gend Med* **2007**, 4, (2), 120-9.
354. Bonomo, S. M.; Rigamonti, A. E.; Giunta, M.; Galimberti, D.; Guaita, A.; Gagliano, M. G.; Muller, E. E.; Cella, S. G., Menopausal transition: A possible risk factor for brain pathologic events. *Neurobiol Aging* **2007**.
355. Saez, T. E.; Pehar, M.; Vargas, M.; Barbeito, L.; Maccioni, R. B., Astrocytic nitric oxide triggers tau hyperphosphorylation in hippocampal neurons. *In Vivo* **2004**, 18, (3), 275-80.
356. Ayasolla, K.; Khan, M.; Singh, A. K.; Singh, I., Inflammatory mediator and beta-amyloid (25-35)-induced ceramide generation and iNOS expression are inhibited by vitamin E. *Free Radic Biol Med* **2004**, 37, (3), 325-38.
357. Vesce, S.; Rossi, D.; Brambilla, L.; Volterra, A., Glutamate release from astrocytes in physiological conditions and in neurodegenerative disorders characterized by neuroinflammation. *Int Rev Neurobiol* **2007**, 82, 57-71.
358. Tilleux, S.; Hermans, E., Neuroinflammation and regulation of glial glutamate uptake in neurological disorders. *J Neurosci Res* **2007**, 85, (10), 2059-70.
359. Takuma, K.; Baba, A.; Matsuda, T., Astrocyte apoptosis: implications for neuroprotection. *Prog Neurobiol* **2004**, 72, (2), 111-27.
360. Assis-Nascimento, P.; Jarvis, K. M.; Montague, J. R.; Mudd, L. M., Beta-amyloid toxicity in embryonic rat astrocytes. *Neurochem Res* **2007**, 32, (9), 1476-82.
361. Pardridge, W. M., The blood-brain barrier and neurotherapeutics. *NeuroRx* **2005**, 2, (1), 1-2.
362. Bennett, J. W.; Klich, M., Mycotoxins. *Clin Microbiol Rev* **2003**, 16, (3), 497-516.

363. Sundaram, K. S.; Lev, M., Inhibition of cerebroside synthesis in the brains of mice treated with L-cycloserine. *J Lipid Res* **1985**, 26, (4), 473-7.

MICHIGAN STATE UNIVERSITY LIBRARIES



3 1293 02956 3545